UNIVERSITE SULTAN MOULAY SLIMANE
Faculté des Sciences et Techniques
Béni-Mellal

Centre d'Études Doctorales : Sciences et Techniques
Formation Doctorale : ***Ressources Naturelles, Environnement et Santé (RNES)***

THÈSE

Présentée par

Asmaa HRIOUA

Pour l'obtention du grade de

DOCTEUR

Discipline : Chimie Physique
Spécialité : Electrochimie Analytique

Complexation de l'amoxicilline par les métaux de transition : Analyse électrochimique et activité antibactérienne

---

Soutenue le Samedi 24 Septembre 2022 à 10h devant la commission d'examen :

M. Bakasse	Faculté des Sciences, El jadida	Présidente
S. Touhtouh	Ecole Nationale des Sciences Appliquées, El jadida	Rapporteur
B. Bencharki	Faculté des Sciences et Techniques, Settat	Rapporteur
S. El Houssame	Faculté Polydisciplinaire, Khouribga	Rapporteur
A. Ouasri	Centre Régional des Métiers de L'éducation et de la Formation, Rabat	Examinateur
S. Lahrich	Faculté Polydisciplinaire, Khouribga	Examinateur
A. Farahi	Faculté Polydisciplinaire, Khouribga	Examinateur
S. Saqrane	Faculté Polydisciplinaire, Khouribga	Co-directrice de thèse
M. A. El Mhammedi	Faculté Polydisciplinaire, Khouribga	Directeur de thèse

SULTAN MOULAY SLIMANE UNIVERSITY

Faculty of Science and Techniques

Beni-Mellal

Center for Doctoral Studies: Sciences and Techniques
Doctoral Training: Natural Resources, Environment and Health (NREH)

THESIS

Presented by

Asmaa HRIOUA

To obtain the degree of

DOCTOR

Discipline: Physical Chemistry

Speciality: Analytical Electrochemistry

Complexation of amoxicillin by transition metals: Electrochemical analysis and antibacterial activity

---

Defended on Saturday, September 24, 2022, at 10:00 a.m. in front of the examining committee:

M. Bakasse	Faculty of Sciences, El jadida	President
S. Touhtouh	National School of Applied Sciences, El jadida	Reviewer
B. Bencharki	Faculty of Science and Technology, Settat	Reviewer
S. El Houssame	Polydisciplinary Faculty, Khouribga	Reviewer
A. Ouasri	Center Régional des Métiers de L'éducation et de la Formation, Rabat	Examiner
S. Lahrich	Polydisciplinary Faculty, Khouribga	Examiner
A. Farahi	Polydisciplinary Faculty, Khouribga	Examiner
S. Saqrane	Polydisciplinary Faculty, Khouribga	Co-supervisor
M. A. El Mhammedi	Polydisciplinary Faculty, Khouribga	Supervisor

Acknowledgements

The present work was carried out in the laboratory of chemistry and mathematical modeling at the polydisciplinary faculty of Khouribga, under the direction of Professor **Moulay Abderrahim EL MHAMMEDI**.

First and foremost, I would like to pay sincere gratitude to my thesis director **Moulay Abderrahim EL MHAMMEDI** for accepting me in his group, continuous support, patience, vast knowledge and guidance during my PhD thesis. I can now tell him what a joy it was to prepare a thesis under his direction. His availability throughout these years of research, his judicious criticisms, his untiring attention, his human qualities, his moral support and his enthusiasm as a researcher have created an atmosphere conducive to work. The freedom he gave me and the responsibilities he entrusted to me contributed a lot to the formation of my personality and to my autonomy of work.

Special thanks to co-director of my thesis, **Sanaa SAQRANE** for having faith in me during the realization of the biological part of my thesis. I am also grateful to her, not only for her human and warm qualities, but also for her rigor and her analytical mind which allowed me to acquire skills in several other fields of science.

My thanks also go to professors **Abdelfattah FARAHI** and **Sara LAHRICH**, for having followed this work from beginning to end and also for the scientific qualities that they are able to transmit to me during my initiation to research. I would also like to thank them for their availability and for all the attention they have given to this work.

I express all my gratitude to Doctor **Mohammed CHERFAOUI** to have welcomed me in his laboratory of medical analysis and to all the staff of his laboratory and especially **Aziza FALAAH** for her help, her patience, and her kindness.

Would also like to thank members of jury for the thesis defence Professors: **M. Bakasse**, **S. Touhtouh**, **B. Bencharki**, **S. El Houssame**, **A. Ouasri, S. Lahrich** and **A. Farahi** for taking time out of their busy schedules to evaluate this research work. Their suggestions and critical opinions will help to improve quality of this work.

I would also like to extend my gratitude to all members of the LCMM research group (past and present), without whom this experience would not have been as enjoyable, and I would not have developed such strong and lasting relationships. I would like to thank those particularly whom

I have had the pleasure of supervising during my studies, especially **Noureddine AJERMOUN, Sara AGHRISS, Hasna HAMMANI, Fath-ellah LAGHRIB and Abdlouahed LOUDIKI**.

Obviously, I did not do this work alone; the research is indeed the result of teamwork. I would therefore like to thank most sincerely all the people who made it possible for me to carry out this work.

My apologies to all those that I would have forgotten

DEDICATION

To the person who is the source of success in my life, with her prayers, encouragement and tenderness, my dearest mother ***Safia BRAKSA****.*

To the one who was always close to me, who brought me up, taught me perseverance and have been endlessly supportive since, my dear father ***Abderrahim HRIOUA****.*

To my brother ***Adnane****, my sisters* ***Niserine and Assia****, and their little families.*

To my colleagues.

To my honorable professors.

To all those who are dear to me

I dedicate this work

Asmaa HRIOUA

Abstract

β-Lactam antibiotics are among the extensively used classes of antibiotics. One important compound of this class is amoxicillin (AMX). Besides its use in human medicine, amoxicillin is also used in veterinary medicine for treating and preventing animal diseases as well as it is used as growth promoter for many domestic and food animals. This practice, however, carries many disadvantages, such as the stimulation of microbial resistance to amoxicillin, with the possible transfer of resistant pathogens from animal and animal products to human, which may pose a major health risk to the public. The use of amoxicillin in food-producing animals may leave residues in foodstuffs of animal origin. Antibiotic residues in foods of animal origin may be the cause of numerous health concerns in humans. So, the highly sensitive and selective sensors for rapid and effective detection of amoxicillin are an extremely urgent issue concerning homeland security, environmental protection, and humanitarian concerns. Several electrochemical techniques have been explored for the quantitative determination of amoxicillin via either electrode surface modification or indirect methods based on derivatization or complexation of amoxicillin with metal ions. In terms of the complexation of drugs with metal ions, the redox properties of a drug can give insights into its metabolic fate or pharmaceutical activity. The medicinal applications of these metal complexes range from anticancer to antibacterial. This concept, which allows to have a synergistic effect of metal/ligand on the same molecular entity, has been demonstrated for its efficiency and represents a new alternative for the control of antimicrobial resistance. In this context, the present research work describes the study of a novel metal-amoxicillin complexes for analytical, biological, and pharmaceutical applications using electrochemical techniques.

In this context, the work of this thesis aims to study new metal-amoxicillin complexes based on Cu (II), Fe(III) and Zn(II) for electroanalytical and antibacterial applications using electrochemical and spectroscopic techniques.

Initially, the focus was on the indirect determination of amoxicillin via copper (II) ions. The method is based on the complexation of β-lactam antibiotic with copper (II) ions. This newly developed analytical method has been applied for the determination of amoxicillin in human blood and pharmaceutical products containing amoxicillin.

In a second step, the work was devoted to the study of the ability of transition metals, in particular copper (II), zinc (II) and iron (III) ions, to inhibit the reaction of amoxicillin oxidation. The electrochemical and spectroscopic results showed that the minimal overvoltage (delay) of oxidation recorded is due to the complexation of amoxicillin by metal ions.

The oxidation delay, observed after amoxicillin complexation, was evaluated by testing the antibacterial activity of the synthesized complexes (Metal-AMX) against the bacterium *Escherichia coli*. The results showed that amoxicillin, in the complexed state, has a relatively interesting antibacterial activity than that of amoxicillin in the free state. This activity depends on the nature of the central atom of the complex. Thus, the maximum inhibitory activity, evaluated by the antibiogram method, was obtained by the Iron-AMX complex in comparison with the other complexes (Metal-AMX) studied. These complexes could be used for the fight against bacterial resistance to amoxicillin and the improvement of its antibacterial activity.

Keywords: β-Lactam antibiotics; amoxicillin, transition metals; transition metals; electrochemical techniques; antibacterial activity; *Escherichia coli*.

Résumé

Les β-lactamines font partie des classes d'antibiotiques les plus utilisées. L'amoxicilline (AMX) est l'un des composés importants de cette classe. Outre son utilisation en médecine humaine, l'amoxicilline est également utilisée en médecine vétérinaire, il est également utilisé comme stimulateur de croissance pour de nombreux animaux domestiques et de consommation. Cette pratique comporte toutefois de nombreux inconvénients, tels que la stimulation de la résistance microbienne à l'AMX, avec le transfert possible d'agents pathogènes résistants de l'animal et des produits d'origine animale à l'homme, ce qui peut constituer un risque majeur pour la santé publique. L'utilisation d'AMX chez les animaux destinés à l'alimentation peut laisser des résidus dans les denrées alimentaires d'origine animale. Ces résidus peuvent être à l'origine de nombreux problèmes de santé humaine. Par conséquent, les capteurs hautement sensibles et sélectifs permettant une détection rapide et efficace d'AMX constituent une question extrêmement urgente concernant la sécurité intérieure, la protection de l'environnement et les préoccupations humanitaires. Plusieurs techniques électrochimiques ont été explorées pour la détermination quantitative de l'amoxicilline, soit par modification de la surface de l'électrode, soit par des méthodes indirectes basées sur la dérivation ou la complexation de l'AMX avec des ions métalliques. En ce qui concerne la complexation des médicaments avec des ions métalliques, les propriétés redox d'un médicament peuvent donner un aperçu de son devenir métabolique ou de son activité pharmaceutique. Les applications médicinales de ces complexes métalliques vont des anticancéreux aux antibactériens. Ce concept, qui permet d'avoir un effet synergique métal/ligand sur la même entité moléculaire, a été démontré pour son efficacité et représente une nouvelle alternative pour le contrôle de la résistance antimicrobienne. Dans ce contexte, le présent travail de recherche décrit l'étude des nouveaux complexes métallo-amoxicilline pour des applications analytiques, biologiques et pharmaceutiques en utilisant des techniques électrochimiques.

Le travail de cette thèse a pour objectifs l'étude de nouveaux complexes métal-amoxicilline à base de Cu, Fe et Zn pour des applications électroanalytiques et antibactériennes en utilisant des techniques électrochimiques et spectroscopiques.

Dans un premier temps, l'accent a été mis sur la détermination indirecte de l'amoxicilline par l'intermédiaire des ions de cuivre (II). La méthode s'est basée sur la complexation d'antibiotique β-lactam par les ions de cuivre (II). Cette méthode analytique, nouvellement développée, a été appliquée pour la détermination de l'amoxicilline dans le sang humain et dans des produits pharmaceutiques contenant l'amoxicilline.

Dans un deuxième temps, le travail a été consacré à l'étude de l'aptitude des métaux de transition, en particulier les ions de cuivre (II), zinc (II) et de fer (III), à inhiber la réaction d'oxydation d'amoxicilline. Les résultats électrochimiques et spectroscopiques ont montré que la surtension minimale (retard) d'oxydation enregistrée est due à la complexation d'amoxicilline par les ions métalliques.

Le retard d'oxydation, observé après la complexation de l'amoxicilline, a été évaluée par des tests de l'activité antibactérienne des complexes synthétisés (Métal-AMX) contre la bactérie *Escherichia coli*. Les résultats ont montré que l'amoxicilline à l'état complexé, présente une activité antibactérienne relativement intéressante que celle de l'amoxicilline à l'état libre. Cette activité dépend de la nature de l'atome central du complexe. Ainsi, l'activité inhibitrice maximale, évaluée par la méthode d'antibiogramme, a été obtenue par le complexe Fer-AMX en comparaison avec les autres complexes (Métal-AMX) étudiés. Ces complexes pourraient être utilisés pour la lutte contre la résistance bactérienne vis-à-vis de l'amoxicilline et l'amélioration de son activité antibactérienne.

Mots clés : β-Lactam antibiotiques ; amoxicilline ; métaux de transition ; techniques électrochimiques ; activité antibactérienne ; *Escherichia coli*.

– List of abbreviations –

NAG	N-acetylglucosamine
NAM	N-acetylmuramic acid
PBP	Penicillin binding protein
RNA	Ribonucleic acid
AMX	Amoxicillin
CPE	Carbon paste eletrode
GC	Glassy carbon
CNP	Carbon nanotube paste
CG	Carbon-graphite
CT	Carbon Toray
CF	Carbon felt
SP	Screen-printed
CV	Cyclic voltammetric
CMEs	Chemically modified electrodes
NP	Nanoparticle
CILE	Carbon ionic liquid electrode
CNTs	Carbon nanotubes
SWCNTs	Single-walled carbon nanotubes

MWNTs	Multi-walled carbon nanotube
CB	carbon black
RGO	reduced graphene oxide
AdSV	The adsorptive stripping cyclic voltammetry
CA	Chronoamperometry
CV	Cyclic voltammetry
DPV	Differential pulse voltammetry
SWV	Square wavevoltammetry
NPV	Normal pulse voltammetry
RPV	Reverse pulse voltammetry
FTIR	Fourier-transform infrared spectroscopy
LOD	Limit of detection
LSV	Linear scanning voltammetry
EAPs	Electroactive polymers
MIP	Molecularly imprinted polymer
HR	Enzyme horseradish peroxidase
NMR	Nuclear magnetic resonance
ESR	Electron spin resonance

WHO	World Health Organization
CNS	Central nervous system
ESI-MS	Electrospray ionization mass spectrometry
LDR	linear dynamic range.
LC-MS/MS	Liquid Chromatography coupled with tandem Mass Spectrometry
AR	Antibiotic-resistant
MHB	Mueller Hinton broth
CFU	Colony-forming unit
SD	Standard deviation
IZD	Inhibition zone diameter
E. coli	Escherichia. coli
MIC	Minimum inhibitory concentration
CLSI	Clinical and Laboratory Standards Institute
CV	Crystal violet
RSD	Relative standard deviation

– List of figures –

–Chapter 1–

–Chapter 2–

–Chapter 3–

–Chapter 4–

–Chapter 5–

– List of tables –

–Chapter 1–

–Chapter 3–

–Chapter 4–

–Chapter 5–

Content

– Chapter I –
Literature review

– Chapter II –
Experimental techniques

– Chapter III –
Chronoamperometric detection of amoxicillin

– Chapter VI –
Electrochemical investigation of amoxicillin interaction with some metal ions related to complexation process

– Chapter V–
Complexation of amoxicillin by transition metals: physico-chemical and antibacterial activity evaluation

Introduction

The antibiotic penicillin has been used to cure a wide range of microbial infections since its discovery in 1928 by Alexander Fleming [1]. Nowadays, the name "penicillin" is generically used to refer to different molecules that have a beta lactam-based structure. The classification of penicillins relies on chemical substitutions on the residue attached to the beta-lactam ring. The latter confers an antibacterial activity, and the side chain determines the agent's antibacterial spectrum and pharmacologic properties [2−5]. In 1960s, another broad-spectrum penicillins sometimes referred to a third generation (semisynthetic modifications of natural penicillin) were introduced. This generation proved to be more effective against a wider group of gram-positive and gram-negative bacteria [6], where amoxicillin (AMX) is the most frequently prescribed drug in this category against a wide range of infections such as ear, nose, throat, skin and lower respiratory tract caused by susceptible microorganisms [7−9]. It may be administered by injection, orally in food and water, topically, and by intramammary or intrauterine infusions [10], usually chosen because it has higher absorption ability, following oral administration, than other β-lactam antibiotics [11]. Besides, its use in human medicine, amoxicillin is also used in veterinary medicine for treating and preventing animal diseases [12−13]. In addition, subtherapeutic concentrations of antimicrobial are commonly added to animal feed and/or drinking water sources as growth promoters and have been a regular part of swine (Sus scrofa) production since the early 1950s [14]. However, the use of large quantities of antibiotic during an animal's growth cycle leaves a certain amount of compound residues. Also, when used in this manner, antibiotic can select for resistant bacteria in the gastrointestinal tract of production animals, providing a potential reservoir for dissemination of drug resistant bacteria into other animals, humans, and the environment [15]. Bacteria have been shown to readily exchange genetic information in nature, permitting the transfer of different resistance mechanisms already present in the environment from one bacterium to another. Transfer of resistance genes from fecal organisms to indigenous soil and water bacteria may occur, and because native populations are generally better adapted for survival in aquatic or terrestrial ecosystems, persistence of resistance traits may be likely in natural environments once they are acquired. Antibiotic resistance has received considerable attention due to the problem of emergence and rapid expansion of antibiotic resistant pathogenic bacteria [16]. Therefore, quantitative measurements of antibiotic in different types of matrices and the development of new strategies to combat bacterial resistance are needed.

Several works have explored the quantitative determination of amoxicillin in different types of matrices such as drug substances, formulation products, biological fluids, environmental water samples and food animal products, using voltammetric methods that exhibit low cost per

analysis, possibility of multi-analyte detection, easy miniaturization, and high sensitivity when compared to other methods of determination, such as, e.g., chromatographic and fluorescence methods. Electrochemical techniques have been an active research topic due to their great practical potential, merits of high selectivity and sensitivity, less time consumption, simple pre-treatment procedure and low cost, even received remarkable attention as for amoxicillin detection [17−23]. Some reports indicated that it is possible to perform an electrochemical determination of AMX by electrode surface modification and indirect methods based on AMX derivatization [24] or complexation with metal ions [25−26].

In terms of the complexation of drugs with metal ions, the Redox properties of a drug can give insights into its metabolic fate or pharmaceutical activity [27-28]. In addition, intrinsic nature of metal centers, characteristic coordination modes, accessible redox states and tuneable thermodynamic and kinetic properties allow metal complexes to offer potential advantages over organic agents alone [29]. Metal complexes are well known to play important roles in various biological processes [30,31]. The medicinal applications of these metal complexes range from anticancer to antimalaria over to neurodegenerative diseases. Strangely, antibacterial applications are remarkably sparse in this list and the number of literature reports on metal-based antimicrobials is dwarfed by the much more frequent publications on metal-based anticancer compounds. Nevertheless, the systematic evaluation of the antimicrobial properties of metal complexes has increased in pace over the last decade, with several reports highlighting the activity and potential modes of action of metal-based antibiotics [31]. In this context, the development, and the characterization of new metal-based antibiotics with the possibility of associating a metal with organic antibiotic molecules. This concept, which allows to have a synergistic effect of metal/ligand on the same molecular entity, has been demonstrated for its efficiency and represents a new alternative for the control of antimicrobial resistance.

The aim of this thesis is to study a novel metal-based amoxicillin for electroanalytical, biological and pharmaceutical applications using electrochemical techniques. The electrochemical and spectroscopic behaviour of amoxicillin was visualized in the presence of three transition metal ions namely Fe, Cu and Zn. No doubt, interest in iron, copper and zinc (so called late first row transition elements) was borne out of their biological relevance as they are associated with various biomolecules related to essential physiological activities. Moreover, from a biological point of view, some metal ions, such as copper, function as a key cofactor in a diverse array of biological redox reactions. These ions may affect amoxicillin via the formation of coordination bonds and/or redox reactions. Herein, we analyzed the interactions

of amoxicillin with metal ions and the formation of Metal-AMX complexes using UV-Visible spectrophotometry, infrared spectroscopy and electrochemical methods.

The interaction of amoxicillin with copper ions was exploited for the indirect analysis of amoxicillin on graphite electrode, based on the fact that the chronoamperometric current intensity of the Cu (II)/Cu(I) redox system were proportional to the AMX concentrations. The method has been applied to the AMX determination in blood and pharmaceuticals.

For biological application, the organometallic complexes synthesized, were screened for them in-vitro antibacterial activity against *Escherichia coli* with a view of finding alternative to bacteria resistance to antibiotic.

This thesis is presented in five chapters; the first chapter presents the general antibiotic mechanisms of both action and resistance, special attention is paid for β-lactam antibiotics, and focuses on the different strategies that are used to fight against their resistance. Then, the focus is on the development and the use of recent electrochemical sensors for β-lactam antibiotics analysis in biological media.

The second chapter aims to present the principles of the different techniques which were used to carry out the present work.

The third chapter is devoted to the chronoamperometric determination of amoxicillin in the presence of copper ions Cu (II) at carbon paste electrode (CPE). This study is followed by an application on the analysis of the AMX in human blood and pharmaceutical tablets.

In the fourth chapter, our approach is the electrochemical study of the reaction of amoxicillin with transition metals such as Cu(II), Zn(II) and Fe(III) at graphite electrode. The formation of Metal-AMX complexes was examined by square wave voltammetry, UV–visible and infrared spectroscopy.

The fifth chapter presents our work relating to the synthesis and characterization of new antimicrobial complexes. Also, in order to evaluate the synergistic effect of these complexes, we studied the antibacterial activity by determining the minimum inhibitory concentration against bacterial strains *Escherichia. coli*.

References

[1] J. P. Swann, The search for synthetic penicillin during world war II. Br. J. Hist. Sci. 16 (1983) 154–190.

[2] T. Dörr, B.M. Davis, M. K. Waldor, Endopeptidase-mediated beta lactam tolerance. PLoS Pathog. 11 (2015) 1004850.

[3] F. Baquero, B. R. Levin, Proximate and ultimate causes of the bactericidal action of antibiotics, Nat. Rev. Microbiol. 19 (2021) 123-132.

[4] G. Kumar, C. Galanis, H. R. Batchelder, C. A. Townsend, G. Lamichhane, Penicillin Binding Proteins, and β-Lactamases of Mycobacterium tuberculosis: Reexamination of the Historical Paradigm, Msphere. 7 (2022) 00039-22.

[5] S. Sharifzadeh, F. Dempwolff, D. B. Kearns, E. E. Carlson, Harnessing β-lactam antibiotics for illumination of the activity of penicillin-binding proteins in Bacillus subtilis. ACS Chem. Biol. 15 (2020) 1242-1251.

[6] K. Kubelkova, A. Macela, Putting the Jigsaw Together-A Brief Insight into the Tularemia, Open. Life. Sci. 10 (2015).

[7] R. Rao, P.S. Kaur, S. Nanda, Amoxicillin: a broad-spectrum antibiotic. J. Inter. Pharm. And Pharm. Sci. 3 (2011) 30–37.

[8] M. G. A. El-Sayed, A. A. A. El-Komy, A. M. El-barawy, M. E. A. Gehan, Pharmacokinetical Interactions of Amoxicillin and Amprolium in Broiler Chickens, J. Phys. Pharm. Adv. 4 (2014) 515-524

[9] R. G. Finch, D. Greenwood, S. R. Norrby, R.J. Whitley, Antibiotic and Chemotherapy: Anti-infective agents and their use in therapy Antibiotic and Chemotherapy, Eighth Edition, J. Antimicrob. Chemother. 52 (2003) 740–741.

[10] K. Brown, M. Mugoh, D. R. Call, S. Omulo, Antibiotic residues and antibiotic-resistant bacteria detected in milk marketed for human consumption in Kibera Nairobi, Plos one. 15 (2020) 0233413.

[11] A. Ashnagar, N.G. Naseri, Analysis of three penicillin antibiotics (ampicillin, amoxicillin and cloxacillin) of several Iranian pharmaceutical companies by HPLC, E-J. Chem. 4 (2007) 536–545.

[12] K. Kümmerer, Antibiotics in the aquatic environment–a review–part I, Chemosphere. 75 (2009) 417-434.

[13] A. Hrioua, A. Loudiki, A. Farahi, M. Bakasse, S. Lahrich, S. Saqrane, M. A. El Mhammedi, Recent advances in electrochemical sensors for amoxicillin detection in biological and environmental samples; Bioelectrochemistry. 137 (2021) 107687.
[14] G. L. Cromwell, Antimicrobial and promicrobial agents, In A. Lewis and L. Southern (ed.) Swine nutrition. 2nd ed. CRC Press, Boca Raton, FL (2001) 401–426.
[15] A. Andremont, Commensal flora may play key role in spreading antibiotic resistance, ASM News. 69 (2003) 601–607.
[16] J. C. Chee-Sanford, R. I. Mackie, S. Koike, I. G. Krapac, Y. F. Lin, A. C. Yannarell, S. Maxwell, R. I. Aminov, Fate and transport of antibiotic residues and antibiotic resistance genes following land application of manure waste, J. Environ. Qual. 38 (2009) 1086-1108.
[17] H. Karimi-Maleh, O. A. Arotiba, Simultaneous determination of cholesterol, ascorbic acid and uric acid as three essential biological compounds at a carbon paste electrode modified with copper oxide decorated reduced graphene oxide nanocomposite and ionic liquid, J. Colloid. Interf. Sci. 560 (2020) 208-212.
[18] Z. Shamsadin-Azad, M. A. Taher, S. Cheraghi, H. Karimi-Maleh, A nanostructure voltammetric platform amplified with ionic liquid for determination of tert-butylhydroxyanisole in the presence kojic acid, J. Food. Meas. Charact. 13 (2019) 1781-1787.
[19] M. Miraki, H. Karimi-Maleh, M. A.Taher, S. Cheraghi, F. Karimi, S. Agarwal, V. K. Gupta, Voltammetric amplified platform based on ionic liquid/NiO nanocomposite for determination of benserazide and levodopa, J. Mol. Liq.278 (2019) 672-676.
[20] H. Karimi-Maleh, M. Sheikhshoaie, I. Sheikhshoaie, M. Ranjbar, J. Alizadeh, N. W. Maxakato, A. Abbaspourrad, A novel electrochemical epinine sensor using amplified CuO nanoparticles and an-hexyl-3-methylimidazolium hexafluorophosphate electrode, New. J. Chem. 43 (2019) 2362-2367.
[21] G. Absalan, M. Akhond, H. Ershadifar, highly sensitive determination and selective immobilization of amoxicillin using carbon ionic liquid electrode, J. Solid. State. Electrochem. 19 (2015) 2491-2499.
[22] C. Chen, X. Lv, W. Lei, Y. Wu, S. Feng, Y.Ding,J.Lv, Q. Hao, S. M. Chen, Amoxicillin on polyglutamic acid composite three-dimensional graphene modified electrode: Reaction mechanism of amoxicillin insights by computational simulations, Analytica. Chimica. Acta. 1073 (2019) 22-29.
[23] M. Aliyu, A. Y. Nor, H. Reza, A. Jaafar, Construction of an Electrochemical Sensor Based on Carbon Nanotubes/Gold Nanoparticles for Trace Determination of Amoxicillin in Bovine Milk, Sensors16 (2016) 56.

[24] M. H. Chiu, J. L. Chang, J. M. Zen, An Analyte Derivatization Approach for Improved Electrochemical Detection of Amoxicillin, Electroanalysis. 21 (2009) 1562-1567.
[25] A. Hrioua, A. Farahi, S. Lahrich, M. Bakasse, S. Saqrane, M. A. El Mhammedi, Chronoamperometric Detection of Amoxicillin at Graphite Electrode using Chelate Effect of Copper (II) Ions: Application in Human Blood and Pharmaceutical Tablets, J. Chem. Select. 4 (2019) 8350 –8357.
[26] S. A. Ozkan, J. M. Kauffmann, P. Zuman, Electroanalysis in biomedical and pharmaceutical sciences (2019).
[27] E. D. S. Gil, G. R. D. Melo, Electrochemical biosensors in pharmaceutical analysis, Braz. J. Pharm. Sci. 46 (2010) 375-391.
[28] P.T. Kissinger, W.R. Heineman, Laboratory Techniques in Electroanalytical Chemistry, revised and expanded. CRC press. (2018).
[29] S. H. Rijt, P. J. Sadler, Current applications, and future potential for bioinorganic chemistry in the development of anticancer drugs. Drug. Discov. Today. 14 (2009) 1089-1097.
[30] S. Tabassum, Synthesis of new piperazine derived Cu (II)/Zn (II) metal complexes, their DNA binding studies, electrochemistry and anti-microbial activity: Validation for specific recognition of Zn (II) complex to DNA helix by interaction with thymine base, Spectrochim. Acta. A. Mol. Biomol. Spectrosc. 72 (2009) 1026-1033.
[31] Frei, Angelo, Metal complexes, an untapped source of antibiotic potential?, Antibiotics. 9 (2020) 90.

Chapter I

Literature Review

I. Bacterial infections/bacterial pathogens

I.1. Bacteria

Bacteria are self-sufficient packets of life, the smallest independently living creatures on Earth. Most bacteria are between 0.5 and 1.5 μm in diameter and 1 to 2 μm long, bacterial volumes ranging, thus, from 0.02 to 400 μm [1]. In a microscope, bacteria exhibit several different shapes: spheres (coccus), rods (bacillus), spirals (spirillum), corkscrews (spirochaete), and boomerangs (vibrio) [2-3]. Bacteria can be classified into two major groups according to differential Gram staining (Fig. 1). The staining effect depends on the components of the cell walls. Gram-positive bacteria consist of a cytoplasmic membrane surrounded by a cell wall. In contrast, Gram-negative bacteria are composed of a thin cell wall surrounded by a second lipid membrane called the outer membrane. Gram-negative cells contain very little peptidoglycan and are normally less sensitive to penicillin than Gram-positive organisms that have a peptidoglycan-rich cell wall with multiple layers of meshwork. However, Gram-negative bacteria acquire supplemental protection through the presence of an outer membrane known as the lipopolysaccharide layer, which consists of lipids, proteins, and polysaccharides instead of standard phospholipid molecules. The outer membrane contains specialized proteins called porins.

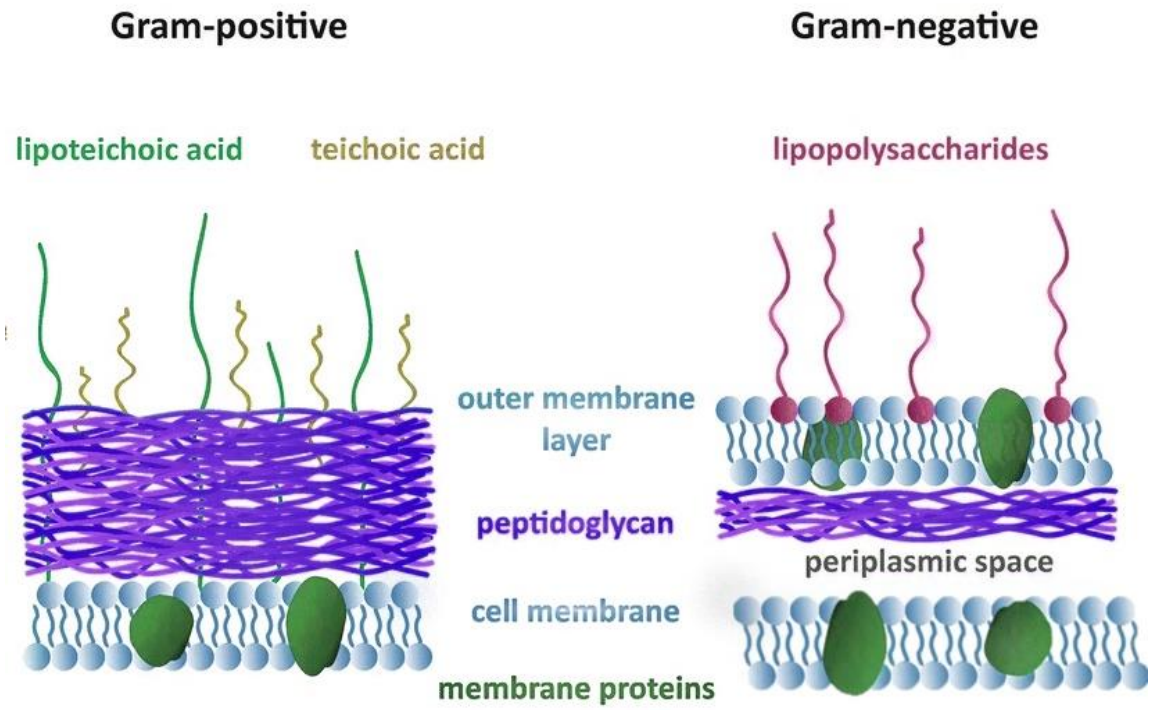

Figure 1: *Schematic diagram showing cell wall structures of Gram-positive and Gram-negative bacteria.*

I.2. Bacterial infections /bacterial pathogens

There are numerous strains of bacteria that are harmless, and some are even beneficial, for example those found in the human gastrointestinal tract to aid digestion and produce vitamins. Less than 1% of all types of bacteria cause disease in humans. They cause disease by secreting or excreting toxins, by producing internal toxins that are released when the bacterium breaks down (such as typhoid), or by causing sensitivity to antigenic properties (tuberculosis). The severity of the infection and where it occurs varies according to the type of bacteria a person has contracted.

As noted above, a minority of bacterial species can cause disease in humans. Bacteria that cause disease can only replicate within the cells of the human body and are called obligate pathogens. Others replicate in an environmental reservoir such as water or soil and only cause disease if they encounter a susceptible host; these are called facultative pathogens.

Many bacteria are normally benign but have a latent ability to cause disease in an injured or immunocompromised host; these are called opportunistic pathogens. All human organs are susceptible to bacterial infection. Each species of bacteria prefers infecting certain organ and not anothers.

For example, Neisseria meningitidis normally infects the meninges of the central nervous system, causing meningitis, and can even infect the lungs, causing pneumonia.

Staphylococcus aureus, which people usually carry on their skin or mucous membranes, often causes skin and soft tissue infections, but it also spreads easily throughout the body via the bloodstream and can cause infection of the lungs, abdomen, heart valves and almost any other site [4-8].

I.3. Treatment

Often, bacterial infections resolve quickly, even without treatment. However, many bacterial infections need to be treated with prescription antibiotics. Untreated bacterial infections can spread or linger, causing major health problems.

Bacterial infections are most often treated with antibiotics, antibiotic selection is based on the type of bacteria involved. Most antibiotics work against more than one type of bacteria, not against all of them.

In Table 1, [9-33] we present the most common bacterial infections and the commonly used antimicrobial therapy.

Table 1: *The most common bacterial infections and the commonly used antimicrobial therapy.*

Bacterial species	Infections/ Diseases	Symptoms	Antibiotic treatment	Ref
Borrelia burgdorferi	Lyme disease	Fever, malaise, headache, stiff neck, myalgia, or arthralgia	Doxycycline Amoxicillin Cephalosporin	[9]
Chlamydia trachomatis	Sexually transmitted infections (lymphogranuloma venereum, cervicitis, urethritis)	Men : dysuria urethral discharge women : vaginal discharge or postcoital bleeding	Rifampin, Tetracyclines Macrolides Fluoroquinolones (ofloxacin).	[10]
Clostridium difficile	Colitis	Diarrhea, intestinal disorders	Metronidazole oral Vancomycin	[11]
Escherichia coli	Urinary tract infections: hemorrhagic colitis, hemolytic uremic, syndrome, bloodstream prostate	Diarrhea	Doxycycline Trimethoprim-sulfamethoxazole Erythromycin Norfloxacin Ciprofloxacin Ofloxacin Azithromycin Rifamycin.	[12]
Helicobacter pylori	Gastric ulcers	Anemia, gastrointestinal bleeding, or weight loss	Amoxicillin Clarithromycin Metronidazole Tetracycline Bismuth	[13]
Legionella pneumophila	Lung infection	Eadache, myalgia, asthenia, and anorexia.	Azithromycin Quinolones	[14]
Listeria monocytogenes	Listeriosis	Septicaemia, meningitis or encephalitis	Trimethoprim-sulphamethoxazole Ampicillin Erythromycin Meropenem Penicillin	[15]
Mycobacterium tuberculosis	Tuberculosis	Weight loss fever jaundice	Rifampin Isoniazid Pyrazinamide	[16-17]
Neisseria gonorrhoeae	Genital tract infection	Urulent urethral cervical discharge discomfort	Flumequine Sulfathiazole Penicillin	[18]

Neisseria meningitidis	Meningitis	Fever, headache neck stiffness, abdominal pain, nausea and vomiting	cephalosporins	[19-20]
Pseudomonas aeruginosa	Respiratory tract infections, urinary tract infections, skin and soft tissue infections bacterial keratitis, 'swimmers ear' infections	-	Colistin and polymyxin B Multidrug therapy due to resistance	[21-22]
Staphylococcus aureus	Toxic shock syndrome	Ever, rash formation, and hypotension	Vancomycin + Clindamycin	[23-24]
Campylobacter spp.	Diarrhea	Diarrhea	Unnecessary in most cases (macrolides, quinolones)	[25]
Streptococcus bovis group	Endocarditis	Fever, abdominal pain, jaundice	Penicillin, Ceftriaxone and Vancomycin Clindamycin and Levofloxacin	[26]
Capnocytophaga canimorsus	Sepsis	Fever with leukocytosis)	β-Lactam–β-lactamase combinations Cephalosporin Carbapenem	[27]
Chlamydia pneumoniae	Pneumonia, bronchitis, sinusitis, and pharyngitis	No set of symptoms or signs is unique to pulmonary infec-tions with C. pneumoniae	Macrolides Doxycycline Tetracycline Erythromycin	[28]
Rhodococcus equi	Pneumonia in immunosuppressed	dyspnea, cough (which may be nonproductive), pleuritic chest pain, and fever.	Multidrug therapy due to resistance	[29]
Ehrlichia chaffeensis	Human ehrlichiosis	Fever, chills, headache, malaise, myalgia, and nausea	Doxycycline	[30]

Non-diphtheria Corynebacterium spp	Endocarditis in immunosuppressed, patients with underlying valve disease or prosthetic valve; other invasive infections	symptoms of respiratory infections.	β-Lactam + Glycopeptides; if resistant, Vancomycin	[31-32]
Bartonella henselae	Cat-scratch disease, bacillary angiomatosis	Fever, vertebral osteomyelitis	Trimethoprim-sulfamethoxazole Rifampin Erythromycin Clarithromycin Azithromycin Doxycycline	[33]

II. Antibiotics

II.1. The action mechanisms of antibiotics

The mechanism of action describes the biochemical process specifically at the molecular level. The modes of action of different antibiotics differ, due to the nature of their structure and their degree of affinity for certain target sites within bacterial cells. The most common targets of antibiotics are shown in Fig. 2.

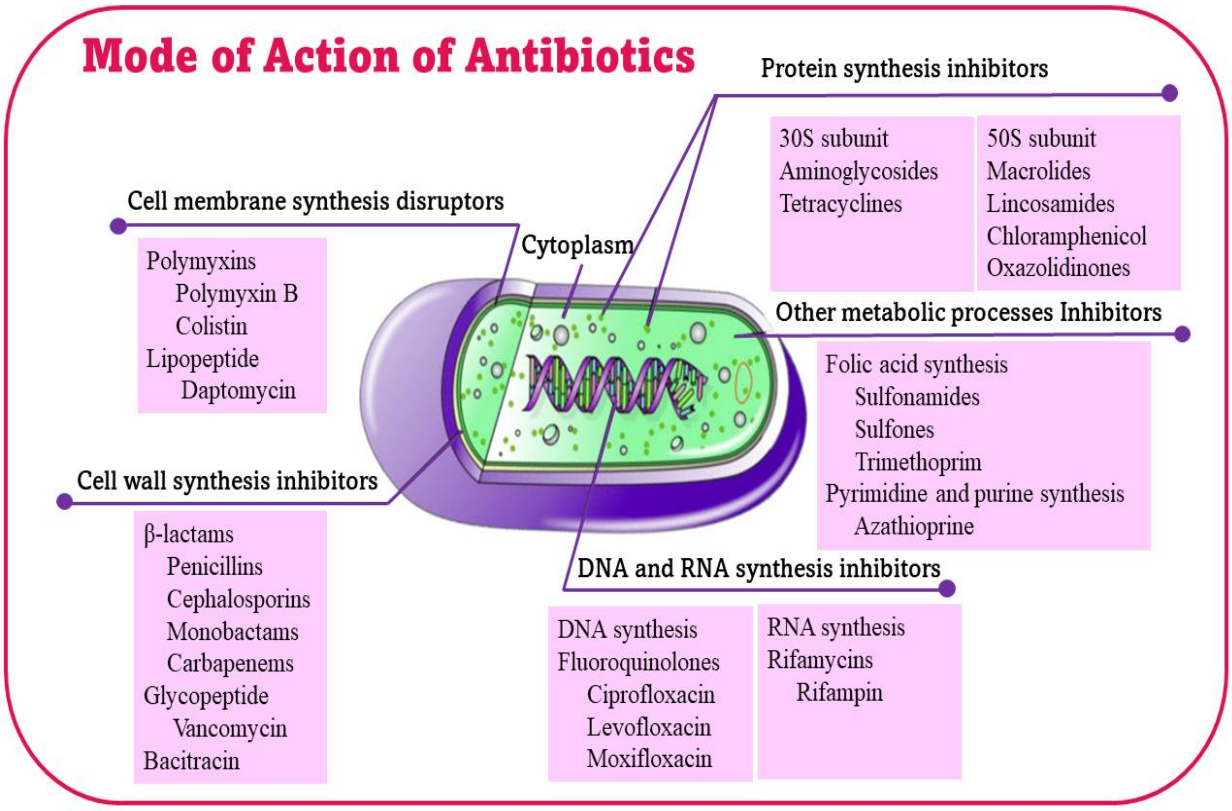

Figure 2: *Mechanism of action of antibiotics.*

The mechanisms of action of antibiotics are as follows:

- Inhibition of cell wall biosynthesis
- Breakdown of the cell membrane structure or function
- Inhibition of protein synthesis
- Inhibition of the structure and function of nucleic acids
- Inhibition of other metabolic processes

II.1.1. Inhibition of cell wall biosynthesis

Cell walls of microorganisms are constructed by peptidoglycan. The peptidoglycan is a polymer that provides tensile strength and maintains intracellular osmotic pressure. This polymer is composed of monomers that synthesized in the cytoplasm from amino acid and sugar building blocks and then transported across the cytoplasmic membrane. A peptidoglycan monomer consists of two joined amino sugars, N-acetylglucosamine (NAG) and N-acetylmuramic acid (NAM), with a pentapeptide (L-Ala-D-Glu-L-Lys-Ala-D-Ala) coming off of the NAM. The monomers are first associated with each other by transglycosidation reactions catalyzed by transglycosylase enzymes that join these monomers together to form chains. Then, transpeptidation reactions cross-link the peptidoglycan by establishing a covalent bond between two neighboring peptide chains. This reaction is catalyzed by a transpeptidase, the PBP (penicillin binding protein) which recognizes the D-Ala-D-Ala motif of the glycan chain. Some antibiotics can inhibit peptidoglycan synthesis by inhibiting these two enzymes (transglycosylase and transpeptidase) [34-35].

II.1.2. Inhibition of cell membrane structure or function

The cell membrane, also called the plasma membrane, is a membrane that surrounds each living cell and separates the cell from the surrounding environment. The cell membrane wraps the components of the cell, usually large water-soluble high-charge molecules, such as proteins, nucleic acids, carbohydrates and substances involved in cell metabolism. Outside the cell, in the surrounding water-based environment, there are ions, acids and alkalis that are toxic to the cell, as well as nutrients that the cell must absorb to survive and grow. The cell membrane, therefore, has two functions: first, to be a barrier keeping the constituents of the cell in and unwanted substances out and, Second, it is a gate that can transport essential nutrients into the cell and the movement of waste products out of the cell. The plasma membrane is composed of

phospholipids and proteins that provide a barrier between the external environment and the cell, regulate the transportation of molecules across the membrane, and communicate with other cells via protein receptors. There are several types of antimicrobial drugs that function by disrupting or injuring the plasma membrane, either by acting as detergents that disrupt lipids or by forming a pore in the membrane that will allow cell Plasma membranes of bacteria are constructed by fatty acids that can be synthesized in cell or taken from environment as building blocks [36].

II.1.3. Inhibition of protein synthesis

Bacteria, as mammalian cells, need protein synthesis for self-replication and maintenance. DNA acts as an "instruction manual," containing all of the information needed for protein synthesis. The first step in this process is transcription, which involves RNA polymerase catalyzing the synthesis of a single-stranded ribonucleic acid (RNA) from a DNA template. Translation is the function of newly synthesized RNA. RNA has three roles in the translation process: (1) it informs ribosomes which proteins to synthesize as messenger RNA (mRNA); (2) it transfers unique amino acids called for by mRNA codons from the cytoplasm to ribosomes as transfer RNA (tRNA); and (3) it ensures that the amino acid carried by the charged tRNA is the one called for by the corresponding mRNA codon as ribosomal RNA (rRNA) [37]. Protein biosynthesis is catalyzed by ribosomes and cytoplasmic factors. The bacterial 70S ribosome is formed by two ribonucleoprotein subunits, the 30S and 50S subunits. Antimicrobials target the 30S or 50S subunit of the bacterial ribosome to inhibit protein biosynthesis.

II.1.4. Inhibition of the structure and function of nucleic acids

Antimicrobial drugs can inhibit nucleic acid synthesis through the inhibition of replication, transcription, and folate synthesis of microorganisms.

DNA replication is the biological process that occurs in all living organisms that copies their DNA and is the basis of biological inheritance. DNA replication, like all biological polymerization processes, occurs in three coordinated, enzyme-catalyzed steps: initiation, elongation, and termination. Each of the steps in the DNA replication process can be targeted by antimicrobial drugs. For example, quinolones including nalidixic acid and ciprofloxacin, inhibit DNA gyrase by binding to the gyrA subunit, thereby preventing the formation of the replication fork. By binding to the gyrB subunit, novobiocin and coumermycin prevent the formation of replication forks by inhibiting DNA gyrase.

Transcription is the process by which messenger RNA transcripts of genetic material are produced and then translated into proteins. The transcription process consists of the following steps: initiation, elongation, and termination. Antimicrobial drugs have been created to target each of these steps. For example, Rifampin, that is a derivative of rifamycine family of antibiotics, binds to DNA-dependent RNA polymerase, hence blocking the initiation of RNA transcription [38].

II.1.5. Inhibition of other metabolic processes

Antibiotic that prevents metabolite synthesis is a chemical that inhibits the use of a metabolite, a chemical that is part of normal metabolism. Such Antibiotics are often similar in structure to the metabolite that they interfere with, such as antifolates that alter the function of folic acid, resulting in disruption of DNA and RNA production. For example, methotrexate is an analogue of folic acid. Because of its structural similarity to folic acid, methotrexate binds and inhibits the enzyme dihydrofolate reductase, thereby preventing the formation of tetrahydrofolate. Since tetrahydrofolate is essential for the synthesis of purines and pyrimidines, its deficiency can lead to inhibition of DNA, RNA and protein production.

II.2. Antibiotics resistance

II.2.1. Resistance Intrinsic, Acquired, and Adaptive

Antibiotic resistance is the ability of a microorganism to withstand the effects of an antibiotic. Antibiotic resistance in bacteria can be intrinsic, acquired, or adaptive [39-40].

Intrinsic or natural resistance occurs when all strains of a given bacterial species are resistant to a given antibiotic. In fact, these bacteria are insensitive to the mode of action of the antibiotic; It is its genetic heritage. Resistance is inscribed in the genetics of these bacteria, and resistance genes are found on their chromosomes [41-42]. Some bacteria are naturally resistant to many antibiotics, an example of this type of resistance is the biocide triclosan, which has widespread performance against gram-positive bacteria and many gram-negative bacteria, but it is incapable of inhibiting the growth of members of the gram-negative genus Pseudomonas. This is because there is no susceptible target for triclosan in this bacterium [43].

Acquired resistance occurs when a particular microorganism obtains the ability to resist the activity of an antimicrobial agent to which it was previously susceptible. Acquired resistance is therefore characterized by the sudden appearance of resistance to one or more antibiotics in certain bacteria that were previously sensitive [44-45]. Acquired resistance results from

mechanisms that are linked to the DNA of the bacteria and are therefore characterized by mutations or transfers of resistant genes from a resistant bacterium to a susceptible bacterium, via a plasmid. Aminoglycosides, β-Lactam, Chloramphenicol, Glycopeptide, Macrolide–Lincosamide–Streptogramin B, Quinolone, Streptothricin, Sulfonamide, Tetracycline, and Trimethoprim can develop resistance to these forms [46].

Adaptive resistance is defined as resistance to one or more antibiotics induced by a specific environmental signal. Bacteria can rapidly modify their transcription in response to changes in the environment to increase their chances of survival [47-48]. Some of these changes give the bacteria a greater ability to resist the challenges posed by antimicrobial drugs. There are many indications of the environment that can show the acquisition of temporary resistance by a given antimicrobial compound, including ion densities, temperature, and, very importantly, exposure to non-lethal doses of antibiotics [49].

II.2.2. Mechanisms of resistance

Resistance to antibiotics is typically the result of enzymatic inactivation, modification, or replacement of the drug target, and reduced antibiotic accumulation due to either decreased permeability and/or increased efflux. Fig. 3 shows an illustration of these different resistance mechanisms in Gram-negative bacteria.

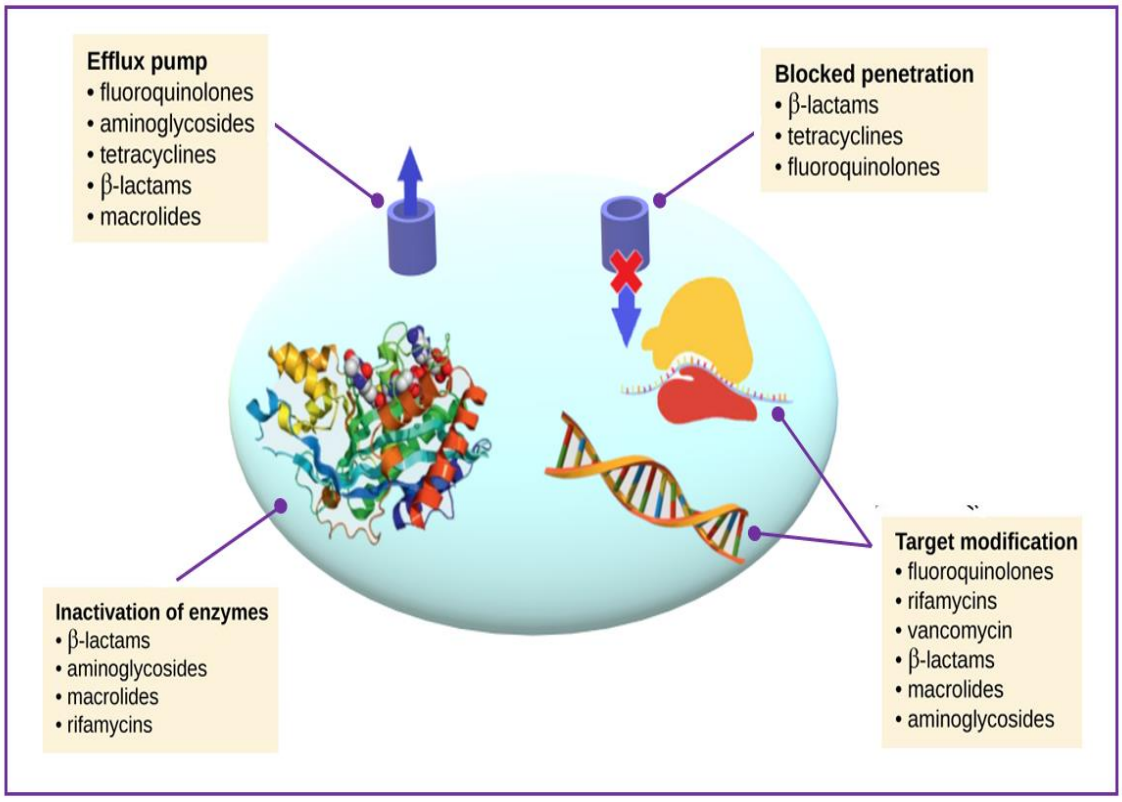

Figure 3: *Mechanism of resistance of antibiotics.*

II.2.2.1. Modification or replacement of the drug target

A common strategy for bacteria to develop antimicrobial resistance is to avoid the effects of antibiotics by interfering with their target sites. To achieve this goal, bacteria have evolved different strategies, including protecting the target (preventing the antibiotic from reaching its binding site) and modifying the target site, thereby reducing the affinity for the antibiotic molecule.

Antibiotics exert their antibacterial effect through specific binding to their target. To prevent this binding, bacteria can communicate and share genetic information with each other, resulting in the spread of resistance genes in bacterial populations. These resistance genes can lead to chemical modification of antibiotics or their targets, inhibiting their mechanism of action and providing protection. Tetracycline, fluoroquinolones and fusidic acid can affect by this mechanism [55-56].

II.2.2.2. Decreased permeability

Many antibiotics have bacterial targets that are intracellular or, in the case of gram-negative bacteria, located in the cytoplasmic membrane. Therefore, the compound must penetrate the outer and/or cytoplasmic membrane to exert its antimicrobial effect. There are essentially two pathways that allow penetration through the outer membrane, either according to a lipid-mediated pathway for antibiotics with hydrophobic molecules or via porins which allow the general diffusion of hydrophilic antibiotics.

Drug resistance therefore involves changes in specific lipid and protein compositions of the outer membrane [57]. for instance, E. coli and S. typhimurium contain enzymes that can modify lipid A. Changes to the acylation pattern of lipid A can provide resistance to some cationic antimicrobial peptides due to charge neutralization [58].

II.2.2.3. Efflux pumps

Efflux pumps or the production of complex bacterial systems on the cytoplasmic membrane to pump toxic compounds out of the cell can also lead to antimicrobial resistance by the transport of antimicrobial agents outside bacterial cells [59].

Resistance results from the reduction of antimicrobial concentration in the cytoplasm of the bacteria, efflux is effective at reducing the intracellular concentration of the antibiotic to far below the minimum inhibitory concentration for that antibiotic, even though the external

concentration might be quite high, which prevents and limits the access of the antibiotic to its target [60].

II.2.3. The β-lactams antibiotics

II.2.3.1. Structure

β-lactam antibiotics are the largest and most used group of antimicrobial agents in world-wide. The group is distinguished by a chemical structure known as the β-lactam ring (Fig. 4). Overall, side chain modifications within groups alter the pharmacokinetic and antibacterial properties of different β-lactam antibiotics. Although there are several classification schemes for antibiotics based on bacterial spectrum (broad versus narrow) or type of activity (bactericidal vs. bacteriostatic), the most useful is based on chemical structure [61].

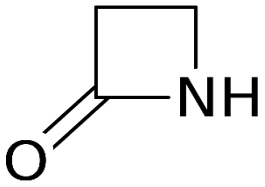

Figure 4: The structure of the β-lactam ring.

Based on their chemical structure they can be divided in four different groups, depending on the ring structure fused to the beta-lactam ring, but are often divided in the following groups: penicillins, cephalosporins, carbapenems and monobactam [62]. β-Lactam antibiotics are indicated for the prophylaxis and treatment of bacterial infections caused by susceptible organisms. β-Lactams can range from very narrow spectrum to very broad spectrum depending on the subgroups.

II.2.3.2. Mechanism of action

The ß-lactams include penicillins, ciclosporins, monobactams, and carbapenems, which are structural analogs of acyl-D-alanyl-D-alanine group in the peptidoglycan structure (Fig. 5), react with Penicillin binding proteins (PBPs) having high affinity to β-lactams by binding to PBPs as a substrate during transpeptidation reaction.

Transpeptidation reaction is blocked by these antibiotics inactivating transpeptidase domain of PBPs and prevent the assembly of the peptidoglycan layer in both Gram-positive and Gram negative bacteria [63]. The β-lactams acts as pseudo substrates of the PBP's and the β-lactam ring acylates their active site serine and forms a stable covalent acyl-enzyme complex (Fig. 6).

II.2.3.3. Mechanism of resistance

Resistance to β-lactam drugs occurs through three general mechanisms: (i) target modification. of the PBPs resulting in a lack of β-lactam binding, (ii) regulation of β-lactam entry and efflux, and (iii) enzymatic degradation by β- lactamases [64-65].

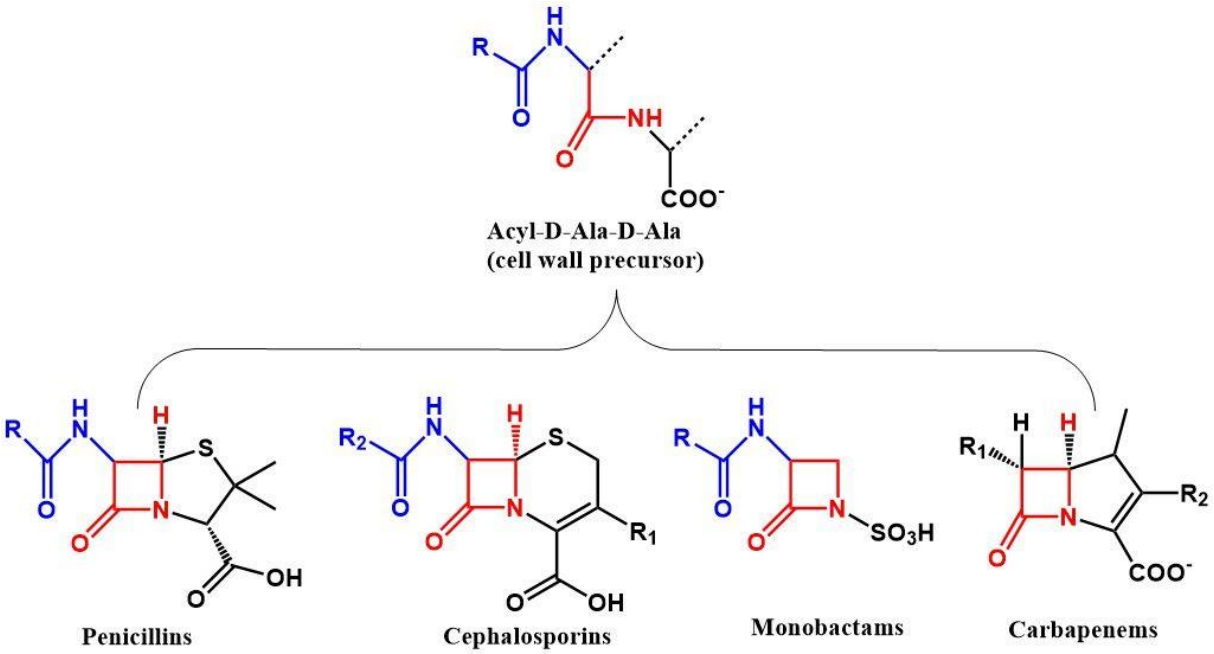

Figure 5: *Core structures of major classes of β-lactam compounds and the structure of acyl-D-alanyl-D-alanine group.*

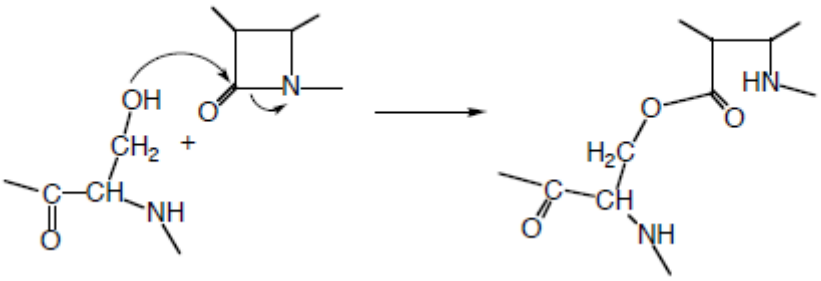

Figure 6: *Interaction between the β-lactam antibiotics and the active site serine of the PBP, resulting in a stable acyl-enzyme complex.*

II.2.3.3.1. Target modification

A common mechanism by which Gram-positive bacteria evade the onslaught of β-lactams is through the acquisition of modified PBP targets with reduced susceptibility. Modified PBPs typically arise via resistance mutations that occur in the presence of β-lactam induced selective pressure, or by acquisition of resistant PBPs by horizontal gene transfer. The modified PBP

must have reduced susceptibility to β-lactams, yet still retain cellular function [66]. Today, some of the most prominent nosocomial multi-drug resistant Gram-positive bacterial infections owe their resistance to modified low-affinity PBPs [67-68].

II.2.3.3.2. Regulation of β-lactam entry and efflux

β-Lactams are among the few antibacterial that are effective against both Gram-positive and Gram-negative bacteria, facilitated by the accessibility of the PBP targets that reside on the outer leaflet of the cytoplasmic membrane. Nevertheless, some Gram-negatives such as Pseudomonas aeruginosa have developed sophisticated mechanisms for restricting access of the β-lactams to their target PBPs.

The two most common mechanisms that regulate this phenomenon at the Gram-negative outer membrane are the restricted entry of drugs via the alteration or loss of porins and their active expulsion via multi-drug efflux pumps [69-70].

II.2.3.3.3. Enzymatic degradation

β-Lactamases are the best example of antibiotic resistance mediated by the destruction of the antibiotic molecule, these enzymes destroy the amide bond of the β-lactam ring essentially rendering the antimicrobial ineffective [71]. The β-lactamases inactivate β-lactam drugs by hydrolyzing a specific site in the β-lactam ring structure, causing the ring to open (Fig. 7).

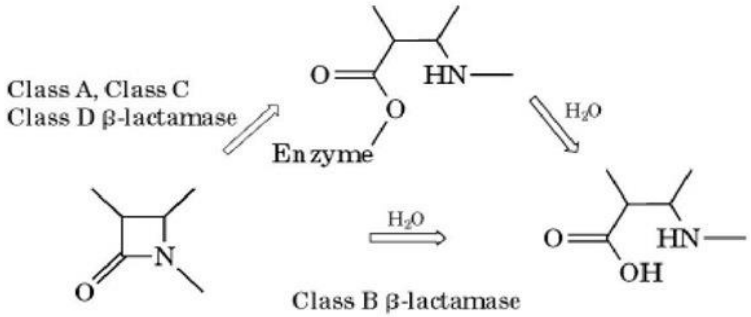

Figure 7: *The hydrolysis of the β-lactam ring by β-lactamases.*

The open-ring drugs are not able to bind to their target PBP proteins, there are 4 groups (A, B, C, D) of beta-lactamase enzymes [53]. Beta-lactamases A, C, and D that deferent from B-class that function cool ester enzymes mediated, while the latest was need zinc ion as metalloenzyme [72]. The class A, C and D beta-lactamases share structural similarities with the target of beta-lactam antibiotics, the DD-peptidases, and therefore are thought to have emerged from the same ancestral enzyme [73].

The Beta-lactamases Class A occur in both Gram-positive and Gram-negative bacteria and mostly mediated by plasmid or transposon. Capable usually of being inducible [74]. These enzymes may exist on the bacterial chromosomes congenitally, or they may be obtained through plasmids. Many members of Gram-negative bacteria of the Enterobacteriaceae family have chromosomal β-lactamase genes. Other Gram-negative bacteria with these characteristics include Aeromonas, Acinetobacter and Pseudomonas. The β-lactamase gene carrying the plasmid is most commonly found in Enterobacteriaceae, but may also be present in certain Gram-positive bacteria, such as Staphylococcus aureus, Enterococcus faecalis, and Enterococcus faecium [75-76].

The Beta-lactamases Class B or Metallo-beta-lactamases, based on functional characteristics, are classified as group 3 enzymes because they hydrolyze penicillins, cephalosporins and carbapenems, but are resistant to almost all conventional beta-lactam inhibitors. In addition, metallo-beta-lactamases do not hydrolyze aztreonam, a monobactam, at significant rates. These enzymes also require divalent cation(s), primarily zinc, for activity and are thus inhibited by metal chelators such as EDTA and EGTA [77]**.** More recently (2008), a new carbapenemase was identified in a K. pneumoniae isolate recovered from a Swedish patient who had been previously admitted to a hospital in New Delhi, India. The enzyme was designated NDM-1, in reference to its origin (New Delhi Metallo β-lactamase) [78].

The Beta-lactamases Class C often known as Inducibleo Beta-Lactamaseso (IBL), are defined as group 1 beta-lactamases. Generally seen in Gram-negative bacteria and chromosomelocalized (Group I, AmpC, etc.). they found in Enterobacterocloacae, Citrobacterofreundii, Serratiaomarce scens, and P. aeruginosa [77,79-80]. Although class C enzymes were originally referred to as cephalosporinases, they confer resistance to a variety of beta-lactam antibiotics such as ampicillin, cephamycins, third generation cephalosporins and now, combined with an outer membrane protein deficiency, confer resistance to carbapenems [81]. This resistance mechanism is not inhibited by clavulanic acid and has an inducible characteristic so produced in high levels the presence of beta-lactam antibiotics [82].

The Class D β-lactamases include OXA enzymes. The name OXA comes from the ability of these enzymes to effectively hydrolyze oxacillin. These enzymes are induced by β-lactamase antibiotics and are produced in Gram-positive cocci (such as Staphylococcus aureus). In addition to oxacillin, OXA variants can also hydrolyze amoxicillin, which poses a problem for the treatment of infectious diseases. Another clinical problem caused by class D β-lactamases is the lack of inhibitors of these enzymes [83].

II.2.3.4. Novel Strategies to fight Antimicrobial Resistance of β-lactam antibiotic

II.2.3.4.1. The revival of old antibiotics:

The reintroduction of previously used antibiotics that are active against multidrug-resistant (MDR) bacteria represents a new alternative to control antimicrobial resistance [84]. Since old antibiotics rarely undergo contemporary drug development procedures or are compared with commonly used antibiotics, they are less considered in practice guidelines. Therefore, its safety and effectiveness must be reassessed to optimize treatment [85]. *Temocillin*: The β-lactam antibiotic introduced in the UK in the 1980s, temocillin was quickly abandoned because its lack of activity against Gram-positive organisms, is also characterized by its resistance to most beta-lactamases and some carbapenemases. Currently, temocillin can be used as a microbiologically directed therapy, particularly for urinary-tract infections (UTIs) caused by confirmed ESBL (Extended-spectrum beta-lactamases) producers [86].

II.2.3.4.2. Discovery and development of novel antibiotics

As of December 2018, there are 45 new candidate antibiotics in clinical trials in the US market [87]. Among them, 28 belong to the known natural products (NP) classes, while 17 are synthetic, including 12 classes, of which 7 are new. The NP category includes 13 based on β-lactams. Five of them are variant β-lactams, two are hybrids (in combination with glycopeptides and siderophores), and seven are combinations with β-lactamase inhibitors. There are five new tetracyclines, one aminoglycoside, one destamycin, one fusitine, one macrolide, one pleuromutilin and two polymyxins. There are two new synthetic categories in phase III clinical trials: ridinilazole, which specifically blocks cell division in Clostridium difficile through an undisclosed mechanism; and murepavedin, which has a new mechanism of action that can inhibit LptD prevents the transport of lipopolysaccharides to the outer membrane [88-89].

II.2.3.4.3. Combinations of antibiotics and nonantibiotic drugs

Combinations of antibiotics and of antibiotics with non- antibiotic activity- enhancing compounds offer a productive strategy to address the widespread emergence of antibiotic-resistant strains. Currently, the combination of individual antibiotics is intended to achieve several goals: 1), increase the antimicrobial spectrum; 2), achieve synergistic effects and thus improve efficacy; 3), suppress the emergence of resistance; and 4), to minimize toxicity [90]. For example, the β- lactam-β- lactamase inhibitor pairs are the best examples of syncretic combinations in current clinical use. Several β-lactamase inhibitors have been synthesized and

used in combination with sensitive antibiotics such as clavulanic acid, Sulbactam, Tazobactam, Avibactam and Relebactam [91]. Clavulanic acid is a β-lactam compound with weak antibacterial activity but potent inhibition of serine-β-lactamases, in its first clinical use, it was associated with amoxicillin, this β-lactam-β-lactamase inhibitor combination is called augmentin. augmentin was a clinical and financial success, followed by the discovery of penicillin sulfones inhibitors of serine-β-lactamase tazobactam and sulbactam [92-93].

II.2.3.4.4. Metal complex-based antibiotic compounds

The medical applications of metal complexes range from anti-cancer to anti-malaria over to neurodegenerative diseases. Strangely, the antibacterial applications on this list are very rare, and the number of literature reports on metal-based antimicrobial agents pales in comparison to the more frequent publications on metal-based anticancer compounds. However, in the last decade, systematic evaluations of the antibacterial properties of metal complexes have increased, and some reports have emphasized their activity and potential mode of action of metal antibiotics [94]. Recently, gold has been shown to be effective against a range of drug-resistant Gram-positive species including Staphylococcus aureus, methicillin-resistant S. aureus, Enterococcus faecium and faecalis, as well as against M. tuberculosis [95]. Gold-containing auranofin is an approved drug for the treatment of rheumatoid arthritis and is currently being investigated for its anticancer and antimicrobial properties [96-97]. Another metal known for its beneficial medicinal properties for a long time is bismuth. Bismuth and its complexes have reportedly been used in the treatment of syphilis, colitis wound infection, and quaternary malaria. However, its most common use to date is for gastrointestinal disorders [98]. Encouraged by these successes, the field has expanded to many other elements in recent decades, with complexes of iron, palladium, silver, and copper entering clinical trials [99-102].

II.2.3.4.5. Nanomaterial-based therapeutics for antibiotic

Nanomaterials provide access to antimicrobial modalities that are novel to bacteria and therefore not part of their natural defensive arsenal. The physicochemical properties of nanomaterials, such as size, shape, and surface chemistry, influence their therapeutic activity and provide unique capabilities to target bacteria, particularly through multivalent interactions with bacterial cells including Van der Waals forces, receptor-ligand interactions, hydrophobic interactions, and electrostatic attractions [103-104]. For example, ampicillin chelates with AgNPs to form an AgNP-ampicillin complex. Ampicillin molecules target the bacterial

membrane, allowing better penetration of the AgNPs, which in turn bind to DNA, leading to cell death [105].

III. Electrochemical detection of β-lactam antibiotic: Amoxicillin

III.1. Voltammetric behaviour of amoxicillin at unmodified electrodes

The electrochemical behaviour of amoxicillin (AMX) has been studied using unmodified electrodes such as glassy carbon, carbon graphite, carbon felt, carbon nanotubes-based carbon Toray, stainless steel, gold, ruthenium, PbO_2, boron-doped diamond electrode, platinum and screen-printed electrodes [106−116].

Table 2: Cyclic voltammetric performances of several unmodified electrodes towards AMX

Electrode [a]	Medium [b]	Anodic peak potential (V)	Ref.
CPE	Acetate buffer	0.5	[114]
	PBS	0.7	[118]
CNP	PBS	0.58, 0.78	[115]
GCE	Na_2SO_4	0.6	[112]
	Acetate buffer	0.7	[116]
CGE	Na_2SO_4	0.68	[112]
CTE	NaCl	Between 0.5 and 1	[111]
CFE	Na_2SO_4	0.65	[112]
SPE	PBS	0.25	[107]
SPCE	H_3PO_4	0.6	[108]

[a] CPE-carbon paste eletrode, CNP-carbon nanotube paste, GCE- glassy carbon electrode, CGE- carbon-graphite electrode , CTE- carbon toray electrode, CFE- carbon felt electrode, SPE- screen-printed electrode, SPCE- screen-printed carbon electrode. [b] PBS-phosphate buffer solution.

In most of these studies amoxicillin did not present any voltammetric signal of the unmodified electrodes [109−112], but only some of them (glassy carbon (GC), carbon paste (CP), carbon nanotube paste (CNP), carbon-graphite (CG), carbon Toray (CT), carbon felt (CF) and screen-printed (SP) electrodes) were able to display it, often with a not well-defined peak, which reflects their low sensitivity [107,108,112−116], therefore, they were not good enough for analytical purpose. In this context, cyclic voltammetric measurements (CV) were used to study the electrooxidation of amoxicillin at unmodified electrodes (table 2). The electrochemical

response showed an oxidation peak, which is due to the oxidation reaction of the phenolic (Ø-OH) substituent to respective carbonyl group (Ø=O) on the side chain of the molecule [117].

III.2. Chemically modified electrodes for AMX detection

CMEs have attracted considerable interest for the analysis of AMX using electroanalytical techniques, due to their high sensitivity, simplicity and relatively low cost related to the modifier characteristics. The CME is defined as an electrode made of a conductive or semiconductive material, which is coated with a monomolecular, multimolecular, ionic or polymeric film of a chemical modifier devoted for a particular application, in order to overcome the limitations of the unmodified electrodes. The general types of CMEs have been classified according to the chemical modifier or the modification method, as covalent bonding, irreversible adsorption, self-assembled layers, electropolymerization, chemisorption, polymer film coating and many others [119−120]. In this review, we have broadly classified them as carbon based modified electrodes (carbon paste, graphene, carbon nanotubes and carbon black), nanoparticles, polymers materials and biosensors.

III.2.1. Carbon based modified electrodes

Carbon is one of the most "multipurpose" elements due to its capability to form multiple stable covalent bonds with different atoms, by dint of its electronic configuration ($1s^2$ $2s^2$ $2p^2$) and hybridization. It is naturally present in different pure forms (graphite, diamond, ...), the family of carbon-based materials now includes graphite, glassy carbon, diamond, graphene, nanofibers, fullerenes (C_{60}) and nanotubes [121−122], which have been applied widely in the fabrication of new sensors and biosensors, owing to their interesting advantages including a chemically inert nature, low cost and good conductivity. In addition, carbon-based electrodes also have the benefit of a large potential window, low background signal, low electrical resistance, good conductivity and suitability for modification with various modifiers with high compatibility [123].

III.2.1.1. Carbon paste electrode

The first known application of carbon-based electrodes was the carbon paste electrode (CPE) in 1958 by the Professor Ralph Norman Adams [124]. The CPE has all the carbon's advantages included (cost, conductivity…). It is prepared generally by thoroughly mixing graphite powder with a binder such as paraffin oil, mineral oil or ionic liquids (Carbon ionic liquid electrode (CILE)) [125]. Therefore, carbon paste electrode has attracted much attention as being easily

modifiable. CPE may be advantageously modified to improve its selectivity and sensitivity to match or even surpass other solid electrodes [126]. The modifiers were employed in order to increase the number of electroactive sites and/or to facilitate the extraction and accumulation of analyte at electrode, mainly used for two purposes: electroanalysis or electrocatalysis. In both cases, the analytical performance of the electrode is considerably improved by obtaining a lower detection limit of the analyte [127−129]. For these reasons, modified carbon paste electrodes have found wide application in the amoxicillin determination [130−132]. CPEs modified with [N,N-ethylenebis(salicylideneaminato)] oxovanadium (IV) complex were used for the voltammetric determination of AMX in 0.1 mol L^{-1} H_2SO_4 medium. In this case, two concentration ranges were considered: 1.0×10^{-6}–1.0×10^{-5} and 1.0×10^{-5}– 2.0×10^{-4} mol L^{-1}, and the detection limit was calculated to be of 8.12×10^{-7} mol L^{-1}. The modified electrode was applied successfully in the determination of AMX in pharmaceutical formulations [131].

Ionic liquid of N-octylpyridinium hexafluorophosphate was also employed as binder, instead of paraffin oil which is widely used in the conventional carbon paste electrode, to construct carbon ionic liquid electrode (CILE), then was tested for the detection of amoxicillin in phosphate buffer solution. The carbon ionic liquid electrode (CILE) showed good selectivity as well as high sensitivity toward AMX in pharmaceuticals and urine samples [132]. However, their toxicity due to possible release into soil or watercourses, CILE could become persistent pollutants and pose environmental hazards [133] and their high cost, sensitivity to the moisture and reactivity under certain conditions restrict utilizing of ionic liquids in electrochemical sensing [134-135].

III.2.1.2. Carbon-based nanomaterials

Several carbon-based nanomaterials as graphene, carbon nanotubes and carbon black have recently gained increasing attention due to their unique properties and wide application range in some of the major industries such as for drug delivery, energy storage and sensing devices. Graphene is considered as elite of carbon based two-dimensional (2-D) materials, composed of single thin layers with sp2 hybrid orbitals of carbon atoms bound together in a hexagonal configuration which promoted it to be an ideal material in the field of electrochemistry [134], it was used as a modifier for electrode surfaces and tested to obtain sensors with improved properties.

One relevant example is the deposition of three-dimensional graphene (3D-GE) combined with polyglutamic acid (PGA) on a glassy carbon electrode (GC), a process that generated a sensor (PGA/3D-GE/GCE) for fast and accurate voltammetric determination of amoxicillin by SWV

between 2.0×10^{-6} and 6.0×10^{-5} mol L^{-1} with a detection limit of 0.118×10^{-6} mol L^{-1}. The proposed method was as well applied to detect the concentration of the AMX in human urine samples [135]. Iijima et *al.* [136] were the first to introduce carbon nanotubes (CNTs) that belongs to the family of carbon-based nanomaterial, produced by rolling up a single layer of graphite or graphene along a certain direction into a closed cylinder. The CNTs are classified into two types based on wall's number to give single-walled carbon nanotubes (SWCNTs) or multi-walled carbon nanotubes (MWNTs) [137].

CNTs have usually been electrochemically tested for AMX analysis, for their great potential, closely associated to their chemical stability, low background current, higher active surface area, considerate electrical conductivity. According to the work of Rezaei et *Al.*, the use of multiwalled carbon nanotubes (MWCNTs) for electrode modification has enhanced the determination of AMX in pharmaceuticals and human urine samples, after being purified by metal oxides elimination within the nanotubes. The adsorptive stripping cyclic voltammetry (AdSV) method was utilized in two linear dynamic ranges of 0.6 – 8.0 and 10.0 – 80.0 µM, to give a detection limit of 0.2 µM [110]. Carbon paste electrode (CPE) was used to obtain (SWCNT/CPE) electrode modified with MWCNTs and ferrocene dicarboxylic acid and employed for the determination of amoxicillin in real samples with a detection limit of 8.7 nmol L^{-1} [115].

Among the recently investigated carbonaceous nanostructured materials carbon black (CB), because it is one of the most inexpensive materials with many attractive electrochemical properties. In the work of Patrícia et al., a simple and low-cost electroanalytical sensor for the simultaneous determination of amoxicillin (AMX) and an anti-inflammatory drug (nimesulide–NIM) was developed, based on glassy carbon (GC) substrate modified with carbon black (CB) immobilized within a dihexadecylphosphate (DHP) film electrode. The modified electrode was able to determine AMX and NIM using square-wave voltammetry. The obtained detection limits for AMX and NIM were 0.12 µmol L^{-1} and 0.016 µmol L^{-1} respectively. Moreover, the suggested sensor was successfully applied for the determination of AMX and NIM in biological urine and environmental samples [138].

III.2.2. Nanoparticles (NPs) based modified electrodes

Nanoparticles, as a subset of nanomaterials, are currently defined as single particles with a diameter less than 100 nm. Nanoparticles (NPs) have better optical, magnetic, electronic and chemical properties, which differ greatly from those of the bulk material. The properties of nanoparticles depend considerably on the nature of the material from where they are

synthesized, they are prepared generally by chemical reduction of metal salts precursors in the presence of a stabilizer to synthesis metallic or metal oxides NPs, which affect their charge, solubility and stability [139].

With regards to electroanalysis, the use of nanoparticle-modified electrodes has received increasing attention due to their electrocatalytical properties using metal NPs. The main advantages obtained from nanoparticles in modified electrodes are the facilitation of electron kinetics through the provision of a high surface area, enhanced mass transport, higher signal-to-noise ratio, better control of nanoparticle sizeand distributionand controllable functionalization with a variety of ligands such as small molecules, surfactants, dendrimers, polymers, and biomolecules [140]. In the literature, most of the studies related to the electrochemical detection of amoxicillin, are based metallic nanoparticles which have been used with CNTs and graphene to get different geometries and stacking configurations, resulting in a novel nanohybrids that could potentially present new physico-chemical properties, due to the interaction between CNT/NP and graphene/NP.

Thus, the modification of GCE with $FeCr_2O_4$ nanoparticles decorated multiwall carbon nanotubes (MWCNTs) led to a sensor that was used for electrocatalytic amoxicillin determination. The sensor showed good sensitivity, selectivity, and stability for the determination of AMX in real samples [113].

Noble metal nanoparticles have been widely used to modify the sensing interface in electrochemical sensors because of their significant biocompatibility and catalytic properties (stability and excellent conductivity).

Among them, AuNPs are the most widely used [141], They are used with carbon-based nanomaterials in electrochemical sensors and has been extensively studied for the detection of amoxicillin [107,142]. The construction of the nanocomposite CNT/AuNP nanocomposites are primarily formed by decorating CNT with AuNP, for example, SWCNTs decorated with AuNP were used for the investigation of a novel electrochemical amoxicillin sensor, exhibiting an excellent electro-transfer capacity due to the high surface area of the MWCNTs and a good sensitivity after decoration of MWCNTs with AuNPs [107].

There are some other examples of modified electrodes, where the integration of metal nanoparticles with graphene material is used for the development of hybrid nanostructures for electrochemical amoxicillin sensors. The nanocomposite material of reduced graphene oxide (rGO) and Ruthenium (Ru) nanoparticles (rGO/RuNP) modified glassy carbon electrode (GCE) was used for simultaneous electroanalysis of amoxicillin (AMX) and ethinylestradiol (EE2), this sensor combined the high conductivity of rGO with the capacity of ruthenium oxide

nanoparticles (RuO_2) on the electrode surface to separate the potential anodic current peaks of each drug and quantify each separately in clinical and food samples [143].

Metal nanoparticles are also used in combination with some other nanoparticles and other materials for electrode surface modification, since bimetallic nanoparticles are well known for their greater electrochemical activity compared to monometallic nanoparticles. Benefiting from this property, Kumar et *al.* designed an amoxicillin (AMX) and lomefloxacin (LMF) sensor based on the immobilization of rGO modified with electrochemically deposited AuNP-PdNP. The sensor (AuNP-PdNP-ErGO) displayed high selectivity and sensitivity for the determination of AMX and LMF in the complex matrix such as urine and in synthetic solutions containing excess of interfering organic substances [144]. Some recent studies that examined the use of carbon and nanoparticles (NPs) based electrode for amoxicillin detections are summarized in Table 3 [107, 110, 113, 115, 130-132, 135, 138, 142-148].

By comparing the data given in Table 3 regarding the simplicity of electrode fabrication method, cost of the material used in fabrication, stability and sensitivity, it is easy to suggest that the electrochemical sensor based on mesoporous carbon (MC and MC^{-}) has better results for amoxicillin determination, it is mainly attributed to its high adsorption ability to amoxicillin during preconcentration step. Its welllayered structure, high surface area, and the negatively charged hydrophilic-layered silicate facilitate reaching of polar amoxicillin species to the electrode surface, hence it makes its oxidation easier [147]. Moreover reduced graphene oxide (RGO) decorated with Ruthenium (Ru) nanoparticles (RGO/RuNP) modified glassy carbon electrode is another example of sensitive electrode. The electrode showed good

separation anodic peak currents of AMX in presence of Ethinylestradiol (EE2) due to a synergistic process involving nanoparticles of ruthenium oxide and the reduced graphene. But using tow interfering compounds (ascorbic acid and uric acid) for studying the selectivity of this method is a disadvantage of this modification [143].

Similarly, as can be seen in Table 3, composite nanomaterials constituted of carbon materials in combination with MNPs are of particular interest due to their enhanced of electrocatalytic activities for AMX detection [144]. However, the longer times needed to prepare these nanocomposites may be a major disadvantage of the modification process. In addition, metallic impurities in carbon-based nanomaterials especially CNTs leading to the unpredictable electrochemical behavior (erroneous electrical signal) of such materials as well as toxicity.

Table 3: *Summary of carbon and nanoparticles (NPs) based nanomaterials for amoxicillin detection.*

Sensor [a]	Technique	Medium [b]	Linear range [µM]	LOD [µM]	Real samples/ Recovery (%)	Ref.
Cu(II)-NCL/CPE	SWV	NaCl	0.04–100	0.02	Urine Tablet Capsule	[130]
[VO(Salen)]/ CPE	LSV DPV SWV	KCl	28.5–82.6 18.3–35.5 18.9–91.9	24.8 16.6 8.49	Tablets 95.8-105.3%	[131]
CILE	CV	PBS	5.0–400 15–120	0. 8 6.0	Capsules Urines	[132]
PGA/3D-GE/GCE	SWV	PBS	2 .0– 60	0.118	Urine/98.4-101.85	[135]
MWCNTs/ GCE	AdSV	universal buffer	0.6 – 8.0 10.0– 80.0	0.2	Capsules/97.21-101.45 Urine/101.5-104.9	[110]
FDCCNTPE	SWV	PBS	0.03–0.35 0.50–32.70	0.0087	Tablets- Capsules Urine	[115]
CB/DPH/GCE	SWV	PBS	2–18.8	0.12	Urine/91-106 Lake water/92-106 Tap water/98-107	[138]
$FeCr_2O_4$/MWCNTs /GCE	DPV	PBS	0.1–10.0 10.0–70.0	0.05	Capsules/96.9-98.6 Urine/100.9-102.7 Plasma/10.4-101.4	[113]
AuNPs/MWCNTs/SPE	CV	PBS	0.2–10 10–30	0.015	Bovine milk/91.5-95.5	[107]
TiO_2/CMK-3/AuNPs/ Nafion/GE	CV	PBS	0.5 –2.5 2.5 –133.0	0.3	Mineral water Environmental water-Capsule	[142]
rGO/RuNPs/GCE	DPV	PBS	5.50– 1.20	0.00163	Urine/96.0-101.1	[143]
AuNPs/PdNPs/ErGO/GCE	SWV	PBS	30–350	9	Urine/98.80-101.1	[144]
ZnO NRs/gold/glass electrode	CV	PBS	5.0–2.5	1.9	Capsule/107.5	[145]
DMBQ/ZnO/CNTs/CPE	SWV	PBS	1.0–950	5	Tablet-Urine	[146]
MC/CPE	LS SW-AdASV	HCl	0.02-5 0.005-1	0.006 0.0015	Tablets/99.7-99.6 Serum/98.78-98.24	[147]
QDs-P6LC-PEDOT:PSS/ GCE	SWV	PBS	0.90–69	0.05	Synthetic urine Milk Tablet	[148]

III.2.3. Polymers based modified electrodes

Polymers are macromolecules consisting of a long-chain back bone of smaller repeating units (monomers) and side groups. Electrode modification by polymers has been proved to be one of the most effective methods, as the electrode properties can be largely modified by a variety of

functional groups in polymers. As polymers are numerous and have different behaviours, whether natural or synthetic, they can be classified in different ways. The polymers are classed according to those used for the modification of electrodes such as electroactive, polyelectrolyte, coordination, and biopolymers.

Electroactive polymers (EAPs) are semiconducting polymers that can be doped and converted into an electrically conductive form using oxidation or reduction reactions, because EAPs are rich with groups that could be either oxidized or reduced. Polyelectrolytes are polymers whose repeating units bear an electrolyte group such as polycations and polyanions. The polyelectrolytes can be dissociated in aqueous solutions, as a result they can attract charges towards the surface of the solution through an ion exchange process. A coordination polymer is composed of metal ions linked by organic ligands. Biopolymers are polymers produced from natural sources either chemically synthesized from a biological material or entirely biosynthesized by living organisms, enzymes, DNA, antibodies and aptamers, they are biological polymers that are employed in typical biosensors [149].

Conductive polymers based modified electrodes have been extensively used for electrochemical analysis of amoxicillin [109, 114, 150−153] due to their inherent charge transport properties, electrocatalytic potential, high reproducibility and stability, where the conductive polymers synthesized by electropolymerization maybe used as redox mediators [154].

For example, Ojani et *al.* used nickel–curcumin complex modified carbon paste electrode as voltammetric sensor for amoxicillin detection. In these electropolymerized film of Ni–curcumin on the carbon paste electrode, nickel oxyhydroxide species act as redox mediator centre for electrooxidation processes of AMX. This electrocatalytic oxidation exhibited a good linear response for amoxicillin concentration in the linear range of 8.0×10^{-6}–1.0×10^{-4} mol L^{-1} of amoxicillin, the detection limit was of 5.0×10^{-6} mol L^{-1}. Moreover, the suggested sensor was successfully applied for the amoxicillin determination in pharmaceutical preparations and biological media [109].

In another work, Cu/Poly (o-Toluidine) (Sodium Dodecyl Sulfate) modified carbon paste electrode was tested for the electrocatalytic oxidation of Amoxicillin. The metal–polymer modified carbon paste electrode have been prepared by electropolymerization and act as a redox mediator. Cyclic voltammetry and chronoamperometry have been used for the determination of amoxicillin under the selected conditions. The calibration curves were obtained in the range of 80–200 and 5–150 μM respectively. Moreover, detection limits were also estimated to be 60

and 3 μM. The proposed method was well applied to determine AMX in pharmaceutical preparations [151].

CPEs modified with charged polymer or polyelectrolyte such as poly-N-vinyl imidazole [155] and poly-4-vinyl pyridine [56] were also used for the voltammetric determination of AMX in pharmaceutical formulations.

Recently, biopolymers have attracted considerable attention in the electrocatalysis area, because of their beneficial functional properties while being biodegradable and environmentally friendly nature. In this context, polyglutamic acid (PGA)/glutaraldehyde film was used as a modifier of glassy carbon electrode to investigate the interaction of the anionic polymer (PGA) with amoxicillin (AMX) as a mimicking model of complex molecules. An interesting, proposed method was based on AMX cathodic pre-concentration, prior to its indirect determination by square wave voltammetry at +0.23V. The LOD obtained was 0.92 μmol L^{-1}. The prepared sensor was applied to the assay AMX in human urine without any separation step [116].

Molecularly imprinted polymers (MIPs) have been used to modify electrodes due to their high affinity, selectivity, stability, low cost and easy preparation, based on the formation of molecular recognition sites in a polymer designed for a target template. MIP synthesis involves the complexation of a template molecule with functional monomers in solution, after polymerization, the molecular models are removed by a thorough washing step, finally the polymer mtrix contains complementary cavities for rebinding the template molecules [157]. Since amoxicillin has a variety of functional groups capable to interact with functional monomers with non-covalent bonds, it tends to create recognition cavities that are complementary to the template molecules in the resulting imprinted polymer following template extraction.

Molecularly imprinted polymers (MIPs) proved to be a powerful tool for the selective amoxicillin determination [158−160]. Recently, several electroactive materials supported MIP were suggested for electrode surface modification to enhance amoxicillin detection, like in the case of the magnetic carbon paste electrode (CPE), where MIP was assembled by a permanent magnet to form a highly sensitive film at CPE surface, then AMX was detected in the linear range from 1.0×10^{-9}–1.1×10^{-7} mol L^{-1} with a detection limit of 2.6×10^{-10} mol L^{-1} [158], in another case, the surface of the multiwalled carbon nanotubes (MWCNTs) was grafted with ionic liquid (IL, i.e. 3-propyl-1-vinylimidazolium bromide) by ionic exchange strategy, the formed MWCNTs-IL monomer was further used to synthesize the multiwalled carbon nanotubes-molecularly imprinted polymer (MWCNTs-MIP), then coated on the above glassy

carbon electrode after being modified with SWCNTs and dendritic Pt-Pd bimetallic NPs prepared, in the AMX ranges of 1.0×10^{-9} – 1.0×10^{-6} and 1.0×10^{-6}– 6.0×10^{-6} mol L^{-1}, a detection limit of 8.9×10^{-10} mol L^{-1} was obtained. The applicability of MWCNTs-MIP sensor was additionally tested in real samples [159].

H. Essousi et *al.* have used reduced graphene oxide (RGO) modified glassy carbon electrode (GCE) as supporting materials for surface imprinting, by electropolymerising pyrrole at GCE surface which containing rGO in the presence of AMX (template molecule), then, the extraction of the template from the surface of GCE/rGO/PPy/AMX has been carried out by overoxidation of polypyrrole. The obtained electrode was modified with gold nanoparticles (AuNPs) in order to increase the conductivity. Under the optimized conditions, the limit of detection was of 1.22×10^{-6} mol L^{-1}, and the application of this sensor (MIP- GCE/RGO/ OPPy/AuNPs) was extended for AMX detection to milk and human serum [160]. The preparation process of MIP modified GCE/RGO was shown in Fig. 8.

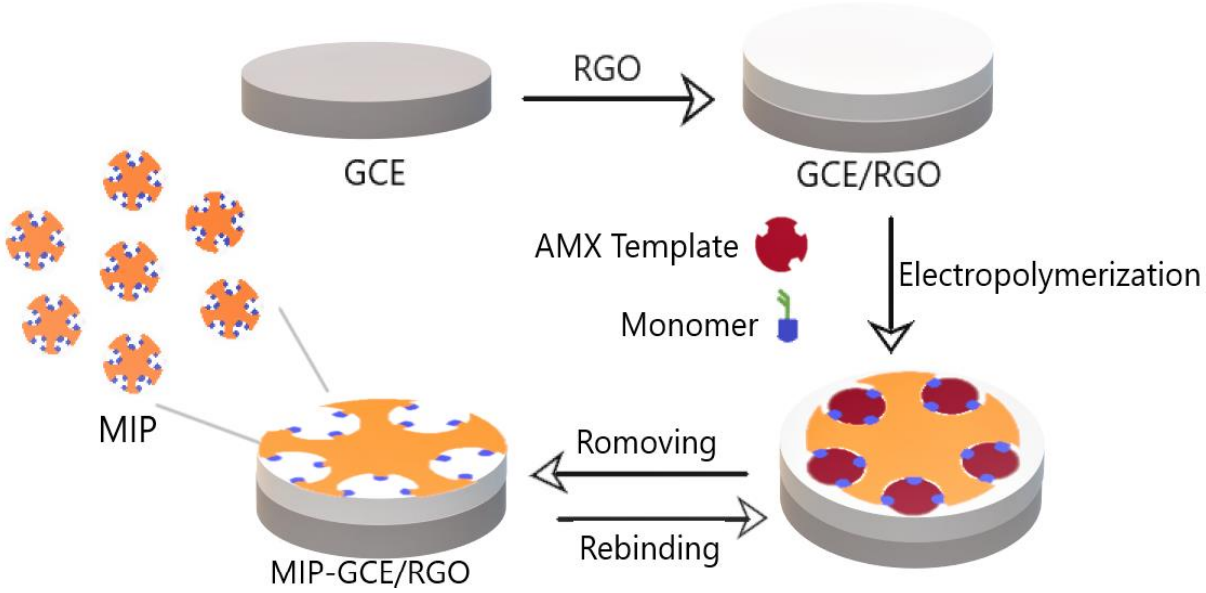

Figure 8: *The preparing process of MIP-GCE/RGO electrode for AMX analysis.*

III.2.4. Electrochemical biosensor

The biosensors are considered as analytical tools with an active biological element combining a bioreceptor or a biorecognition element that is specific to a target analyte with a physical transducer, which converts the recognition event into a measurable signal. Based on typical recognition elements two types can be defined: enzyme-based biosensors and affinity biosensors. The biological recognition compound for the first type is an enzyme, cell or tissue, while for the second type it is a DNA sequence, antibody or membrane receptor [161]. An

electrochemical biosensor is a biosensor with an electrochemical transducer that transforms biochemical information such as analyte concentrations into analytically useful data. The most common recognition elements used in electrochemical biosensors are enzymes, which are widely studied for detecting amoxicillin. In a recent work [162], the enzyme horseradish peroxidase (HRP) modified titanium (TiO_2) based screen-printed electrode (SPE) electrode was used to generate highly reactive intermediate ($^1O_2$) from air under visible light illumination and to oxidize the analytes to electrochemically detectable products, using amperometric measurements, the photocurrent for amoxicillin as a function of its concentration reveals that the detection limit was 2.20×10^{-8} mol L^{-1} [162]. Fig. 9 illustrates the interaction between amoxicillin and enzyme-based screen-printed electrode.

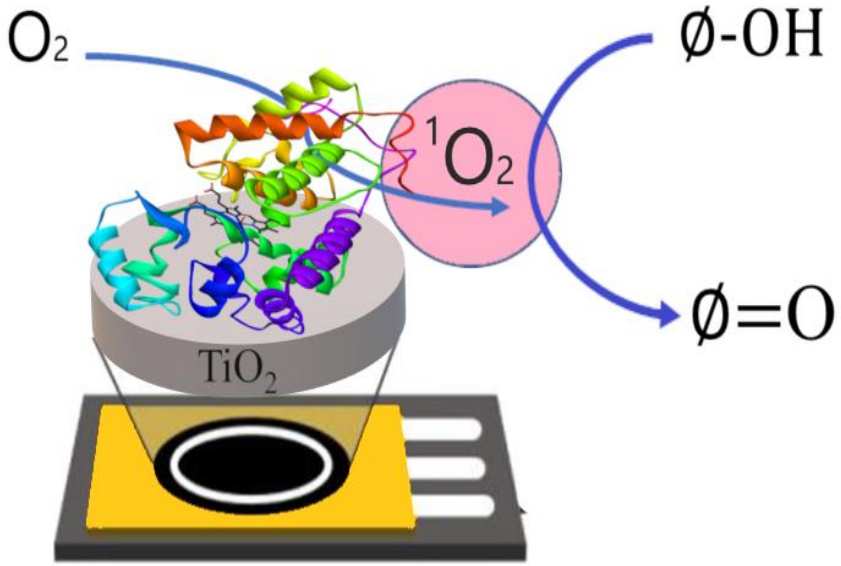

Figure 9: *Schematic illustrating generation of singlet-oxygen for amoxicillin oxidation at enzyme - based screen-printed electrode.*

In a similar example, an amperometric immunosensor was developed for the analysis of pool of β-lactam antibiotics such as AMX and penicillin G in samples of two different river waters. The LOD was of the order of 10^{-10} mol L^{-1}. The immunosensor developed demonstrated low selectivity toward all β -lactam antibiotics, higher selectivity toward other classes of non-β-lactam antibiotics and good recovery in artificially prepared samples [163]. Recently, aptamer-based biosensors have been developed for amoxicillin detection [164]. Aptamers are single-stranded DNA or RNA oligonucleotides, that can selectively bind to a specific target, including proteins, peptides, carbohydrates, small molecules, toxins, and even live cells molecules with high affinity, selectivity and sensitivity [161]. Jialing Song et *al.* [165] used glassy carbon electrode (GCE) modified with graphite phase carbon nitride (g-C_3N4), TiO_2, and AuNPs as

composite materials for the fabrication of aptasensor. This aptasensor TiO_2-g-C_3N_4/GCEwas coated with amoxicillin aptamer solution and bovine serum albumin (BSA). The prepared BSA/Apt/TiO_2-g-C_3N4@AuNPs/GCE electrode was used for the amoxicillin detection in the lineair range of 0.5×10^{-9}–3.0×10^{-9} mol L^{-1} and reached the ultra-very low detection limits (2.0×10^{-10} mol L^{-1}). This sensor was able to detect amoxicillin in wastewater [165]. A detailed comparison between the different polymers modified electrodes and biosensors in terms of analytical figures of merit is reported in Table 4 [109, 114, 116, 150-153, 155-156, 158- 160, 162-163,167].

III.3. Indirect electrochemical detection of AMX (derivatization or complexation)

One of the main reasons for using the indirect method is obtained lower limit detection without any chemical modification of working electrode. Mei-Hsin Chiu et *al.* have developed an analyte derivatization approach based on the reduction of the oxidized product of amoxicillin after its reaction with MnO_2, which can then be easily determined by amperometric method. The proposed amperometric method exhibited an excellent analytical performance for AMX detection with an LOD of 1.7×10^{-8} mol L^{-1}. This process was used for the specific determination of AMX in pond water, river water, and artificial water [107]. In another work [117], a simple electrochemical method was developed for indirect AMX determination on carbon paste electrode using copper ions Cu (II) as coordinatively bounded to AMX. Chronoamperometric current of copper ion was influenced by the addition of AMX. The result showed that the currents intensity of the Cu (II)/Cu(I) redox system were proportional to the AMX concentrations, where the LOD obtained is 8.84×10^{-8} mol L^{-1}. The method has been successfully applied to the AMX determination in blood and pharmaceuticals.

AMX was also detected indirectly by using anodic peak current of Cu after the complexation between the Cu(II) and carboxyl group of AMX [166]. The adsorption of AMX onto gold nanoparticle (GNP)-modified indium tin oxide (ITO) electrode (ITO/GNP) has been performed to prepare ITO/GNP/AMX electrode, which was further modified with Cu(II) by simple dropping of Cu(II) solution. The result showed the amount of Cu (II) at the electrode surface depends on the amount of AMX and the anodic peak of reduced Cu(0) at ITO/GNP/AMX/Cu(II) electrode increased linearly as the concentration of AMX increased. A square wave voltammetric (SWV) method was used, the calibration plot was constructed in the concentration range from 1.0×10^{-8} to 1.0×10^{-6} mol L^{-1}. The detection limit was found to be 5×10^{-10} mol L^{-1} [166]. Polymer-modified electrode was developed for indirect detection of β-lactam antibiotics such as amoxicillin, cefaclor, and ampicillin present in formulated and blood

plasma samples. in this case, the Antibiotics were essentially converted to their electroactive oxazolone analogues after acid treatment (0.1 mol L^{-1} HCl, 85C, 2 h). Then, the Antibiotics in the form of their respective oxazolones were indirectly analyzed by oxazolone entrapment in poly (Nchloranil N,N,N',N'-tetramethylethylene diammonium dichloride) film at hanging mercury drop electrode surface. The detection limit of antibiotics-derived oxazolone was of the order of 1.0×10^{-9} mol L^{-1} [153].

Table 4: *Comparison of analytical figure of merits for electrochemical detection of AMX using polymers modified electrodes and biosensors.*

Sensor [a]	Technique [b]	Medium [c]	Linear range [µM]	LOD [µM]	Real samples	Recovery (%)	Ref.
PVI/CPE	CV	H_2SO_4	1.0–10 10–200	0.812	Tablets Capsules Oral suspension	98.15 101.41 101.41	[155]
Poly-4-vinylpyridine	CV	H_2SO_4	-	8	Pharmaceuticals	-	[156]
Ni/CR/CPE	CA	NaOH	8–100	5	Urine Capsules	105.1 98-103	[109]
Polyaniline film/CPE	SWAdSV DPAdSV	Acetate buffer	0.5-250 7-150	3.5×10^{-4}	Tablet Serum Plasma	99.58-102.1 98.62-99.62 98.28-99.50	[114]
poly(acridine orange)/GCE	DPV SWV	B-R	0.4-20 0.8–80	1.87×10^{-3} 1.55×10^{-2}	Tablet Serum	156-130 99.83-99.81	[150]
POT(SDS)/CPE	CV CA	H_2SO_4	80–200 5–150	60 3	Tablets	102-104	[151]
Copolymer/CPE	DPV	H_2SO_4	20–400	1	-	-	[152]
PCED$(Cl)_2$-HMDE	Polarography	KH_2PO_4-NaOH	-	2.12×10^{-3}	Tablets Suspension	98.6 ± 100.8 97.8 ± 99.5	[153]
PGA/GLU/GCE	SWV	Acetate buffer	2.0–25.0	0.92	Urine	106.7	[116]
MMIP/CPE	DPV	B-R	1.0×10^{-3}–0.11	0.26×10^{-3}	Capsule	98.8-103.2	[158]
MWCNTs@MIP	DPV	PBS	1.0×10^{-3}–1.0 1.0–6.0	8.9×10-4	Milk Honey	90-96 88.95	[159]
MIP-GCE/RGO/OPPy /AuNPs	CV	PBS	1.0×10^{-2}–1.0×10^{3}	1.22	Milk Serum	80.4-99.2 90.5-99.7	[160]
TiO_2-HRP/SPE	CA	KCl+	0.25–15	2.20×10^{-2}	-	-	[162]

		KH_2PO_4	2.0×10^{-2}–5.0×10^{-2}				
Amperometric immunosensor	Amperometry	PBS	5×10^{-4}– 50	$\approx10^{-10}$	Rivers	-	[163]
Penicillinase/flat-bottomed pH electrode	Potentiometry (pH/mV)	PBS	10-30	1	-	-	[167]
BSA/Apt/TiO_2-g-C_3N_4@Au NPs/GCE	EIS	PBS	0.5×10^{-3}–3×10^{-3}	2×10^{-4}	wastewater	91.6-107.4	[165]

References

[1] T. D. Brock, M. T. Madigan, J. M. Martinko, J. Parker, Brock biology of microorganisms, Upper Saddle River (NJ): Prentice-Hall. (2003).

[2] M. T. Cabeen, C. Jacobs-Wagner, Bacterial cell shape, Nat. Rev. Microbiol. 8 (2005) 601-610.

[3] K. D. Young, The selective value of bacterial shape, Microbiol. Mol. Biol. Rev. 70 (2006) 660-703.

[4] B. A. Bannister, N. T. Begg, S. H. Gillespie, Infectious Disease: Structure and classification of pathogens. 2nd edn. Blackwell Science Ltd; Oxford, UK. (1996) 23-34.

[5] P. G. Engelkirk, J. Duben-Engelkirk, C. F. Robert Burton's microbiology for the health sciences; Jones & Bartlett Publishers. (2020).

[6] S. P. Luby, M. Agboatwalla D. R. Feikin, J. Painter, W. Billhimer, A. Altaf, R. M. Hoekstra, Effect of handwashing on child health: A randomised controlled trial. The Lancet. 366 (2005) 225–233.

[7] W. Levinson, Review of medical microbiology and immunology, McGraw-Hill Education (2014).

[8] S. Doron, S. L. Gorbach, Bacterial Infections: Overview. International Encyclopedia of Public Health. (2008) 273–282. https://doi.org/10.1016/B978-012373960-5.00596-7

[9] E. D. Shapiro, Borrelia burgdorferi (Lyme disease). Pediatr Rev . 35 (2014) 500.

[10] C. Bébéar, B. De Barbeyrac, Genital Chlamydia trachomatis infections. Clin. Microbiol. Infect. 15 (2009) 4-10.

[11] D. A. Leffler, J. T. Lamont, Clostridium difficile infection. N. Engl. J. Med. 372 (2015) 1539-1548.

[12] F. Qadri, A. M. Svennerholm, A. S. G. Faruque, R. B. Sack, Enterotoxigenic Escherichia coli in developing countries: epidemiology, microbiology, clinical features, treatment, and prevention. Clin. Microbiol. Rev. 18 (2005) 465-483.

[13] S. Suerbaum, P. Michetti, Helicobacter pylori infection. N. Engl. J. Med. 347 (2002) 1175-1186.

[14] B. A. Cunha, A. Burillo, E. Bouza, Legionnaires' disease, The Lancet. 387 (2016) 376-385.

[15] T. Holmøy, H. von der Lippe, T. M. Leegaard, Listeria monocytogenes infection associated with alemtuzumab–-a case for better preventive strategies. BMC neurol. 17 (2017) 1-4.

[16] N. Panic, H. Maetzel, M. Bulajic, M. Radovanovic, J. M. Löhr, Pancreatic tuberculosis: A systematic review of symptoms, diagnosis and treatment. J. United. Eur. Gastroent. 8 (2020) 396-402.
[17] M. F. Rabahi, J. L. R. D. Silva, A. C. G. Ferreira, D. G. S. Tannus-Silva, M. B. Conde, Tuberculosis treatment. J. Bras Pneumol. 43 (2017) 472-486.
[18] A. Lovett, J. A. Duncan, Human immune responses and the natural history of Neisseria gonorrhoeae infection. Front. immunol. (2019) 3187.
[19] S. N. Ladhani, J. Lucidarme, S. R. Parikh, H. Campbell, R. Borrow, M. E. Ramsay, Meningococcal disease and sexual transmission: urogenital and anorectal infections and invasive disease due to Neisseria meningitidis. The Lancet 395 (2020) 1865-1877.
[20] M. Corr, T. Waterfield, M. Shields, Fifteen-minute consultation: Symptoms and signs of meningococcal disease. Arch. Dis. Child. Educ. Pract. Ed. 105 (2020) 200-203.
[21] J. A. Driscoll, S. L. Brody, M. H. Kollef, The epidemiology, pathogenesis and treatment of Pseudomonas aeruginosa infections, Drugs. 67 (2007) 351-368.
[22] K. Streeter, M. Katouli, Pseudomonas aeruginosa: A review of their Pathogenesis and Prevalence in Clinical Settings and the Environment. Epidemiol. Infect. (2016) 25-32.
[23] P. Pachori, R. Gothalwal, P. Gandhi, Emergence of antibiotic resistance Pseudomonas aeruginosa in intensive care unit; a critical review. Genes Dis. 6 (2019) 109-119.
[24] P. M. Schlievert, K. N. Shands, B. B. Dan, G. P. Schmid, R. D. Nishimura, Identification and characterization of an exotoxin from Staphylococcus aureus associated with toxic-shock syndrome. J. Infect. Dis. 143 (1981) 509-16.
[25] J. K. McCormick, J. M. Yarwood, P. M. Schlievert, Toxic shock syndrome and bacterial superantigens: an update. Annu. Rev. Microbiol. 55 (2001), 77-104.
[26] J. Corredoira, M. P. Alonso, F. García-Garrote, M. J. García-Pais, A. Coira, R. Rabuñal, A. Gonzalez-Ramirez, J. Pita, M. Matesanz, D. Velasco, M. J. López-Álvarez, Streptococcus bovis group and biliary tract infections: an analysis of 51 cases, Clin. Microbiol. Infect. 20 (2014) 405-409.
[27] C. Lion, F. Escande, J. C. Burdin, Capnocytophaga canimorsus infections in human: review of the literature and cases report, Eur. J. Epidemiol. 12 (1996) 521-533.
[28] C. C. Kuo, L. A. J ackson, L. A. Campbell, J. T. Grayston, Chlamydia pneumoniae (TWAR). Clin. Microbiol. Rev. 8 (1995) 451-461.
[29] I. Kedlaya, M. B. Ing, S. S. Wong, Rhodococcus equi infections in immunocompetent hosts: case report and review, Clin. Infect. Dis. 32 (2001) e39-e46.

[30] K. N. Heitman, F. S. Dahlgren, N. A. Drexler, R. F. Massung, C. B. Behravesh, Increasing incidence of ehrlichiosis in the United States: a summary of national surveillance of Ehrlichia chaffeensis and Ehrlichia ewingii infections in the United States, 2008–2012, Am. J. Trop. Med. 94 (2016) 52.

[31] H. Schiffl, C. Mücke, S. M. Lang, Exit-site infections by non-diphtheria corynebacteria in CAPD, Perit. Dial. Int. 24 (2004) 454-459.

[32] N. Rikitomi, T. Nagatake, K. Matsumoto, K. Watanabe, N. Mbaki, Lower respiratory tract infections due to non-diphtheria corynebacteria in 8 patients with underlying lung diseases, Tohoku J. Exp. Med. 153 (1987) 313-325.

[33] G. E. Schutze, Diagnosis and treatment of Bartonella henselae infections, J. Pediatr. Infect. Dis. 19 (2000) 1185-1187.

[34] S. Kırmusaoğlu, The Rise of Virulence and Antibiotic Resistance in Staphylococcus aureus: MRSA and MSSA: The mechanism of methicillin resistance and the influence of meticillin resistance on biofilm phenotype of Staphylococcus aureus, Ed. S. Enany (2016) 25-41.

[35] P. E. Reynolds, Structure, biochemistry and mechanism of action of glycopeptide antibiotics. Eur. J. Clin. Microbiol. Infect. Dis. 8 (1989) 943-950.

[36] G. J. Tortora, B. R. Funke, C. L. Case, Microbiology: an introduction, San Francisco, CA: Pearson Benjamin Cummings (2007) 912.

[37] L. Snyder, W. Champness, W. Champness, Molecular genetics of bacteria, Washington, DC: Asm Press. 19 (1997).

[38] M. K. Bhattacharjee, Antibiotics That Inhibit Nucleic Acid Synthesis. In: Chemistry of Antibiotics and Related Drugs. Springer, Cham. (2016) 109-128. https://doi.org/10.1007/978-3-319-40746-3_5.

[39] J. M. Munita, C. A. Arias, Mechanisms of Antibiotic Resistance. Microbiol. Spectr. 4 (2016) 4-2. https://doi.org/10.1128/microbiolspec.VMBF-0016-2015.

[40] J. H. Lee, Perspectives towards antibiotic resistance: from molecules to population, J. Microbiol. 57 (2019) 181-184

[41] J. L. Martinez, General principles of antibiotic resistance in bacteria. Drug. Discov. Today. 11 (2014) 33-39.

[42] G. Cox, G. D. Wright, Intrinsic antibiotic resistance: mechanisms, origins, challenges and solutions. Int. J. Med. Microbiol. 303 (2013) 287-292.

[43] J. M. Blair, M. A. Webber, A. J. Baylay, D. O. Ogbolu, L. J Piddock, Molecular mechanisms of antibiotic resistance. Nat. Rev. Microbiol. 13 (2015) 42-51.

[44] E. Luna, T. J. Bruce, M. R. Roberts, V. Flors, J. Ton, Next-generation systemic acquired resistance. Plant Physiol. 158 (2012) 844-853.

[45] B. Aslam, W. Wang, M. I. Arshad, M. Khurshid, S. Muzammil, M. H. Rasool, Z. Baloch, Antibiotic resistance: a rundown of a global crisis. Infection and drug resistance, 11 (2018) 1645.

[46] A. H. Van Hoek, D. Mevius, B. Guerra, P. Mullany, A. P. Roberts, H. J. Aarts, Acquired antibiotic resistance genes: an overview. Front. Microbiol. 2 (2011) 203.

[47] L. Fernández, E. B. M. Breidenstein, R. E. W. Hancock Creeping baselines and adaptive resistance to antibiotics. Drug. Resist. Updates. 14 (2011) 1–21. https://doi.org/10.1016/j.drup.2011.01.001.

[48] T. K. Kim, R. S. Herbst, L. Chen, Defining and understanding adaptive resistance in cancer immunotherapy. Trends. Immunol. 39 (2018) 624-631.

[49] C. De la Fuente-Núñez, F.Reffuveille, L. Fernández, R. E. Hancock, Bacterial biofilm development as a multicellular adaptation: antibiotic resistance and new therapeutic strategies, Curr. Opin. Microbiol. 16 (2013) 580-589.

[50] F. J. Pérez-Llarena, G. Bou, Proteomics as a tool for studying bacterial virulence and antimicrobial resistance, Front. Microbiol. 7 (2016) 410.

[51] L. K. Sharkey, A. J. O'Neill, Molecular Mechanisms of Antibiotic Resistance Part II. Bacterial Resistance to Antibiotics From Molecules to Man (2019) 27-50.

[52] L. Guardabassi, P.courvalin, Modes of antimicrobial action and mechanisms of bacterial resistance. In : Aarestrup F.M. (Ed.), Antimicrobial resistance in bacteria of animal origin. ASM Press: Washington, 2006, 1-18

[53] M. N. Alekshun, S. B. Levy, Molecular mechanisms of antibacterial multidrug resistance, Cell. 128 (2007) 1037-1050.

[54] H. Nikaido, Multidrug resistance in bacteria. Annu. Rev. Biochem. 78 (2009) 119-146.

[55] S. R. Connell, D. M Tracz, K. H. Nierhaus, D. E.Taylor, Ribosomal protection proteins and their mechanism of tetracycline resistance, Antimicrob. Agents. Chemother. 47 (2003) 3675–81.

[56] H. Van Acker, P. Van Dijck, T. Coenye, Molecular mechanisms of antimicrobial tolerance and resistance in bacterial and fungal biofilms. Trends. Microbiol. 22 (2014) 326-333.

[57] K. C. VanMeter, R. J. Hubert, W. G. VanMeter, Microbiology for the Healthcare Professional. St. Louis, MO: Mosby Elsevier. (2010) 404-422

[58] L. Guo, K. B. Lim, C. M. Poduje, M. Daniel, J. S Gunn, Lipid A acylation and bacterial resistance against vertebrate antimicrobial peptides, Cell. 95 (1998) 189–98.

[59] L. M. McMurry, R. E Jr Petrucci, S. B. Levy, Active efflux of tetracycline encoded by four genetically different tetracycline resistance determinants in Escherichia coli, Proc. Natl. Acad. Sci. 77 (1980) 3974–7.
[60] A. W. Maresso, Bacterial Virulence: A Conceptual Primer, Springer Nature. (2019)
[61] J. E. Sykes, M. G. Papich, Antibacterial Drugs, Canine and Feline Infectious Diseases, (2014) 66–86. doi:10.1016/b978-1-4377-0795-3.00008-9.
[62] K. Bush, P. A. Bradford, β-Lactams and β-lactamase inhibitors: an overview, Cold. Spring. Harb. Perspect. Med. 6 (2016) a02527.
[63] S. Džidic, J. Šuškovic, B. Kos, Antibiotic resistance mechanisms in bacteria: Biochemical and genetic aspects. Food. Technol. Biotechnol. 46 (2008) 11-21.
[64] Y. Pfeifer, A. Cullik, W. Witte, Resistance to cephalosporins and carbapenems in Gramnegative bacterial pathogens, Int. J. Med. Microbiol. 300 (2010) 371-379.
[65] K. Bush, P. A. Bradford, β-Lactams and β-lactamase inhibitors: an overview, Cold. Spring. Harb. Perspect. Med. 6 (2016) a02527.
[66] P. A. Lambert, Bacterial resistance to antibiotics: modified target sites. Adv Drug Deliv Rev 57. (2005) 1471-1485
[67] H. F. Chambers, F. R. Deleo, Waves of resistance: Staphylococcus aureus in the antibiotic era. Nat. Rev. Microbiol 7 (2009) 629-641.
[68] C. A. Arias, B. E. Murray, The rise of the Enterococcus: beyond vancomycin resistance, Nat. Rev. Microbiol. 10 (2012) 266-278.
[69] Marquez, B. (2005) Bacterial efflux systems and efflux pumps inhibitors. Biochimie 87, 1137-1147
[70] Pagès, J. M., James, C. E., and Winterhalter, M. (2008) The porin and the permeating antibiotic: a selective diffusion barrier in Gram-negative bacteria. Nat Rev Microbiol 6, 893-903
[71] E. Christaki, M. Marcou, A. Tofarides, Antimicrobial resistance in bacteria: mechanisms, evolution, and persistence. J. Mol. Evol. 88 (2020) 26-40.
[72] E. Heinz, H. Ejaz, J. B. Scott, N. Wang, S. Gujaran, D. Pickard, J. Wilksch, H. Cao, I. U. Haq, G. Dougan, R. A. Strugnell, Resistance mechanisms and population structure of highly drug resistant Klebsiella in Pakistan during the introduction of the carbapenemase NDM-1, Sci. Rep. 9 (2019) 1-13.
[73] J. M. Ghuysen, Molecular structures of penicillin-binding proteins and beta-lactamases, Trends. Microbiol. 2 (1994) 372-380.

[74] A. Walkty, J. A. Karlowsky, M. R. Baxter, H. J. Adam, D. Alexander, D. C. Bay, D. Boyd, M. McCracken, M. R. Mulvey, G. G. Zhanel, G. G. Zhanel, Fosfomycin resistance mediated by fos genes remains rare among extended-spectrum betalactamase-producing Escherichia coli clinical isolatesrecovered from the urine of patients evaluated at Canadian hospitals (CANWARD, 2007-2017), Diagn. Microbiol. Infect. 96 (2020) 114962.

[75] S. T. Chancey, D. Zähner, D. S. Stephens, Acquired inducible antimicrobial resistance in Gram-positive bacteria, Future Microbiol. 7 (2012) 959–978

[76] C. Schultsz, S. Geerlings, Plasmid-mediated resistance in Enterobacteriaceae, Drugs. 72 (2012) 1-16.

[77] K. Bush, G. A. Jacoby, A. A. Medeiros, A functional classification scheme for beta-lactamases and its correlation with molecular structure. Antimicrob. Agents. Chemother. 39 (1995) 1211-1233.

[78] K. K. Kumarasamy, M. A. Toleman, T. R. Walsh, J. Bagaria, F. Butt, R. Balakrishnan, U. Chaudhary, M. Doumith, C. G Giske, S. Irfan, P. Krishnan, A. V. Kumar, S. Maharjan, S. Mushtaq, T. Noorie, D. L. Paterson, A. Pearson, C. Perry, R. Pike, B. Rao, U. Ray, J. B. Sarma, M. Sharma, E. Sheridan, M. A. Thirunarayan, J. Turton, S. Upadhyay, M. Warner, W. Welfare, D. M. Livermore, N. Woodford, Emergence of a new antibiotic resistance mechanism in India, Pakistan, and the UK: a molecular, biological, and epidemiological study, Lancet. Infect Dis. 10 (2010) 597–602.

[79] M. R. Jacobs, A. M. Abdelhamed, C. E. Good, D. D. Rhoads, K. M. Hujer, A. M. Hujer, T. N. Domitrovic, S. D. Rudin, S. S.Richter, D. van Duin, B. N. Kreiswirth, ARGONAUT-I: activity of cefiderocol (S-649266), a siderophore cephalosporin, against gram-negative bacteria, including carbapenem-resistant nonfermenters and Enterobacteriaceae with defined extended-spectrum-lactamases and carbapenemases. Antimicrob. Agents Chemother. 63 (2019) e01801-18.

[80] A. Philippon, G. Arlet, G. A. Jacoby, Plasmid-determined AmpC-type betalactamases, Antimicrob. Agents Chemother. 46 (2002) 1-11. https://doi.org/10.1128/aac.46.1.1-11.2002

[81] R. A. Powers, Structural and functional aspects of extended-spectrum AmpC cephalosporinases, Curr. Drug. Targets. 17 (2016) 1051-1060.

[82] M. R. Meini, L. I. Llarrull, A. J. Vila, Overcoming differences: the catalytic mechanism of metallo- β-lactamases. FEBS lett. 589 (2015) 3419- 3432.

[83] B. A. Evans, S. G. Amyes, OXA β-lactamases, Clin. Microbiol. Rev. 27 (2014) 241-263

[84] C. Pulcini, K. Bush, W. A. Craig, N. Frimodt-Møller, M. L. Grayson, J. W. Mouton, Forgotten antibiotics: an inventory in Europe, the United States, Canada, and Australia, Clin. Infect. Dis. 54 (2012) 268–274. doi: 10.1093/cid/cir838.

[85] N. Cassir, J. M. Rolain, P. Brouqui, A new strategy to fight antimicrobial resistance: the revival of old antibiotics, Front. Microbiol. 5 (2014) 551.

[86] R. De Jongh, R. Hens, V. Basma, J. W. Mouton, P. M. Tulkens, S. Carryn, Continuous versus intermittent infusion of temocillin, a directed spectrum penicillin for intensive care patients with nosocomial pneumonia: stability, compatibility, population pharmacokinetic studies and breakpoint selection. J. Antimicrob. Chemother. 61 (2008) 382–388. doi: 10.1093/jac/dkm467

[87] E. M. Grimsey, L. J. Piddock, Do phenothiazines possess antimicrobial and efflux inhibitory properties?, FEMS. Microbiol. Rev. 43 (2019) 577-590.

[88] N. Srinivas, P. Jetter, B. J. Ueberbacher, M. Werneburg, K. Zerbe, J. Steinmann, B. Van der Meijden, F. Bernardini, A. Lederer, R. L. A. Dias, Peptidomimetic antibiotics target outer-membrane biogenesis in Pseudomonas aeruginosa, Science. 327 (2010) 1010-1013

[89] M. I. Hutchings, A. W. Truman, B. Wilkinson, Antibiotics: past, present and future, Current Opinion in Microbiology, 51 (2019) 72-80. ISSN 1369-5274, https://doi.org/10.1016/j.mib.2019.10.008.

[90] R. C. Jr. Moellering, Rationale for use of antimicrobial combinations, Am. J. Med. 75 (1983) 4–8.

[91] M. Tyers, G. D. Wright, Drug combinations: a strategy to extend the life of antibiotics in the 21st century, Nat. Rev. Microbiol. 17 (2019) 141-155.

[92] A. G. Brown, Naturally- occurring β- lactamase inhibitors with antibacterial activity, J. Antibiot. 29 (1976) 668–669.

[93] K. Bush, Game changers: new β- lactamase inhibitor combinations targeting antibiotic resistance in Gramnegative bacteria. ACS Infect. Dis. 4 (2018) 84–87.

[94] S. A. Amolegbe, C. A. Akinremi, S. Adewuyi, A. Lawal, M. O. Bamigboye, J. A. Obaleye, Some nontoxic metal-based drugs for selected prevalent tropical pathogenic diseases. J. Biol. Inorg Chem. 22 (2017) 1-18. doi: 10.1007/s00775-016-1421-4. Epub 2016 Nov 30. PMID: 27904956.

[95] M. B. Harbut, C. Vilchèze, X. Luo, M. E. Hensler, H. Guo, B. Yang, A. K. Chatterjee, V. Nizet, W. R. Jacobs, P. G. Schultz, Auranofin exerts broad-spectrum bactericidal activities by targeting thiol-redox homeostasis. Proc. Natl. Acad. Sci. USA. 112 (2015) 4453–4458. 10.1073/pnas.1504022112

[96] A. E Finkelstein, Auranofin: New oral gold compound for treatment of rheumatoid arthritis. Ann. Rheum. Dis. 35 (1976) 251–257.

[97] B. Wu, X. Yang, M. Yan, Synthesis and Structure–Activity Relationship Study of Antimicrobial Auranofin against ESKAPE Pathogens. J. Med. Chem. 62 (2019) 7751–7768.

[98] H. Sun, Biological Chemistry of Arsenic, Antimony and Bismuth, John Wiley & Sons, 2010.

[99] A. Hrioua, A. Loudiki, Farahi, F. Laghrib, M. Bakasse, S. Lahrich, S. Saqrane, M. A. El Mhammedi, Complexation of amoxicillin by transition metals: Physico-chemical and antibacterial activity evaluation, Bioelectrochemistry, 142 (2021) 107936. https://doi.org/10.1016/j.bioelechem.2021.107936.

[100] F. Li, J. G. Collins, F. R. Keene, Ruthenium complexes as antimicrobial agents. Chem. Soc. Rev. 44 (2015) 2529–2542.

[101] Y. Wang, B. Han, Y. Xie, H. Wang, R. Wang, W. Xia, H. Li, H. Sun, Combination of gallium(iii) with acetate for combating antibiotic resistant Pseudomonas aeruginosa. Chem. Sci. 10 (2019) 6099–6106.

[102] Q. L. Feng, J. Wu, G. Q. Chen, F. Z. Cui, T. N. Kim, J. O. Kim, A mechanistic study of the antibacterial effect of silver ions on Escherichia coli and Staphylococcus aureus, J. Biomed. Mater. Res. 52 (2000) 662–668.

[103] L. S. Wang, A. Gupta, V. M. Rotello, Nanomaterials for the treatment of bacterial biofilms. ACS Infect. Dis. 2 (2016) 3–4.

[104] A. Gupta, R. F. Landis, V. M. Rotello, Nanoparticlebased antimicrobials: surface functionality is critical, F1000Res. 5 (2016) 364.

[105] A. Gupta, S. Mumtaz, C. H. Li, I. Hussain, V. M. Rotello, Combatting antibiotic-resistant bacteria using nanomaterials, Chem. Soc. Rev. 48 (2019) 415-427.

[106] D. A. Edwards, Z. Adeel, R. G. Luthy, Distribution of nonionic surfactant an phenanthrene in a sediment/aqueous system. J. Environ. Sci. Technol. 28 (1994) 1550–1560.

[107] M. Aliyu, A. Y. Nor, H. Reza, A. Jaafar, Construction of an Electrochemical Sensor Based on Carbon Nanotubes/Gold Nanoparticles for Trace Determination of Amoxicillin in Bovine Milk, Sensors16 (2016) 56.

[108] M. H. Chiu, J. L. Chang, J. M. Zen, An Analyte Derivatization Approach for Improved Electrochemical Detection of Amoxicillin, Electroanalysis. 21 (2009) 1562-1567.

[109] R. Ojani, J. B. Raoof, S. Zamani, A novel voltammetric sensor for amoxicillin based on nickel–curcumin complex modified carbon paste electrode, Bioelectrochemistry. 85 (2012) 44–49.

[110] B. Rezaei, S. Damiri, Electrochemistry and Adsorptive Stripping Voltammetric Determination of Amoxicillin on a Multiwalled Carbon Nanotubes Modified Glassy Carbon Electrode, Electroanalysis. 21 (2009) 1577 – 1586

[111] M. Ferreira, I. K. Biernacka, A. M. Fonseca, I. C. Neves, O. S. G. P. Soares, M. F.R. Pereira, J. L. Figueiredo, P. Parpot, Study of the electroreactivity of amoxicillin on carbon nanotubes supported metal electrodes, Chem. Cat. Chem.10 (21) 4900-4909.

[112] F. Sopaj, M. A. Rodrigo, N. Oturan, F. I. Podvorica, J. Pinson, M. A. Oturan, Influence of the anode materials on the electrochemical oxidation efficiency. Application to oxidative degradation of the pharmaceutical amoxicillin, Chem. Eng. J. 262 (2015) 286–294

[113] A. A. Ensafi, A. R. Allafchian, B. Rezaei, Multiwall carbon nanotubes decorated with $FeCr_2O_4$, a new selective electrochemical sensor for amoxicillin determination, J. Nanopart. Res. 14 (2012)1244

[114] P. K. Brahman, R. A. Dar, K. S. Pitre, conducting polymer film based electrochemical sensor for the determination of amoxicillin in micellar media, Sensor. Actuat. B-chem. 176 (2013) 307– 314.

[115] M. Fouladgar, M. R. Hadjmohammadi, M. A.Khalilzadeh, P. Biparva, N. Teymoori, H. Beitollah, Voltammetric Determination of Amoxicillin at the Electrochemical Sensor Ferrocenedicarboxylic Acid Multi Wall Carbon Nanotubes Paste Electrode, Int. J. Electrochem. Sci. 6 (2011) 1355 – 1366.

[116] D. P. Santos, M. F. Bergamini, M. Valnice, B. Zanoni, Voltammetric sensor for amoxicillin determination in human urine using polyglutamic acid/glutaraldehyde film, Sensor. Actuat B-Chem. 133 (2008) 398–403.

[117] A. Hrioua, A. Farahi, S. Lahrich, M. Bakasse, S. Saqrane, M. A. El Mhammedi, Chronoamperometric Detection of Amoxicillin at Graphite Electrode using Chelate Effect of Copper(II) Ions:Application in Human Blood and Pharmaceutical Tablets, J. ChemistrySelect. 4 (2019) 8350 –8357.

[118] S. J. Lyle, S. S. Yassin, Polarographic studies of metal ion complexes of Ampicillin and Amoxycillin, Anal. Chim. Acta. 274 (1993) 225-230.

[119] J. Shan Ye, Chemically Modified Electrodes and Ultramicroelectrodes for the Detection of Redox-active Biomolecules, Thesis, The Hong Kong University of Science and Technology (1999).

[120] J. M. Zen, A. S. Kumar, D. M. Tsai, Recent updates of chemically modified electrodes in analytical chemistry, Electroanalysis. 15 (2003) 1073-1087.

[121] E. H. Falcao, F. Wudl, Carbon allotropes: beyond graphite and diamond, J. Chem. Technol. Biotechnol. 82 (2007) 524–531.
[122] B. T. Zhang, X. Zheng, H. F. Li, J. M. Lin, Application of carbon-based nanomaterials in sample preparation: a review. Anal. Chim. Acta. 784 (2013) 1–17.
[123] S. Lahrich, A. Hrioua, F. Laghrib, H. Hafdi, A. Bouzidi, M. Bakasse, M. A. El Mhammedi, Conversion of the Nitro Group to the Nitroso in Aromatic Compounds: Case of p-Nitrophenol Using the Catalytic Effect of Palladium. Chem. Slct. 4 (2019) 12320– 12327.
[124] I. Svancara, K. Vytras, K. Kalcher, A. Walcarius, J. Wang, Carbon paste electrodes in facts, numbers, and notes: a review on the occasion of the 50 years jubilee of carbon paste in electrochemistry and electroanalysis, Electroanal. 21 (2009) 7 – 28.
[125] Y. Zheng, L. Ye, L.Yan, Y. Gao, The electrochemical behavior and determination of quercetin in choline chloride/urea deep eutectic solvent electrolyte based on abrasively immobilized multi-wall carbon nanotubes modified electrode. Int. J. Electrochem. Sci. 9 (2014) 238-248.
[126] F. Laghrib, N. Ajermoun, A. Hrioua, S. Lahrich, A. Farahi, A. El Haimouti, M. Bakasse, M. A. El Mhammedi, Investigation of voltammetric behavior of 4-nitroaniline based on electrodeposition of silver particles onto graphite electrode, Ionics. 25 (2019) 2813-2821
[127] H. Hammani , A. Hrioua, S. Aghris , S. Lahrich, S. Saqrane, M. Bakasse, M. A. El Mhammedi, Activated charcoal as a capture material for dopamine, paracetamol and salicylic acid in human blood and pharmaceutical formulations, Mater. Chem. Phys. 240 (2020) 122111.
[128] S. Lahrich, B. Manoun, M. A. El Mhammedi, Catalytic effect of potassium in $Na_{1-x}KxCdPb_3(PO_4)_3$ to detect mercury (II) in fish and seawater using a carbon paste electrode, Talanta. 149 (2016) 158-167.
[129] M. A. El Mhammedi, M. Bakasse, R. Bachirat, A. Chtaini, Accumulation and trace measurement of paraquat at kaolin-modified carbon paste electrode, Mater. Sci. Eng. C 30 (2010) 833–838.
[130] M. Nosuhi , A. N. Ejhieh, Comprehensive study on the electrocatalytic effect of copper – doped nano-clinoptilolite towards amoxicillin at the modified carbon paste electrode – solution interface, J. Colloid. Interf. Sci. 497 (2017) 66–72.
[131] M. F. Bergamini, M. F. S. Teixeira, E. R. Dockal, N. Bocchi, É. T. G. Cavalheirob, Evaluation of Different Voltammetric Techniques in the Determination of Amoxicillin Using a Carbon Paste Electrode Modified with [N,N-ethylenebis(salicylideneaminato)] oxovanadium(IV), J. Electrochem. Soc. 153 (2006) E94-E98.

[132] G. Absalan, M. Akhond, H. Ershadifar, highly sensitive determination and selective immobilization of amoxicillin using carbon ionic liquid electrode, J. Solid. State. Electrochem. 19 (2015) 2491-2499.
[133] O.A. Shenderova, V.V. Zhirnov, D. W. Brenner, Carbon nanostructures, Crit. Rev. Solid. State. Mater. Sci. 27 (2002) 227-356.
[134] T. Madrakian, H. Ghasemi, A. Afkhami, E. Haghshenas, ZnO/rGO nanocomposite/ carbon paste electrode for determination of terazosin in human serum samples, RSC. Adv. 6 (2016) 2552–2558.
[135] C. Chen, X. Lv, W. Lei, Y. Wu, S. Feng, Y.Ding,J.Lv, Q. Hao, S. M. Chen, Amoxicillin on polyglutamic acid composite three-dimensional graphene modified electrode: Reaction mechanism of amoxicillin insights by computational simulations, Analytica. Chimica. Acta. 1073 (2019) 22-29.
[136] S. Iijima, Carbon nanotubes: past, present, and future. Physica. B 323 (2002) 1–5.
[137] F. Torrens, G. Castellano, Bundlet model for single-wall carbon nanotubes, nanocones and nanohorns, In Methodologies and Applications for Chemoinformatics and Chemical Engineering, (2013) 228-294. IGI Global.
[138] P. B. Deroco, R. C. R. Filho, O. F. Filho, A new and simple method for the simultaneous determination of amoxicillin and nimesulide using carbon black within a dihexadecylphosphate film as electrochemical senso, Talanta. 179 (2018) 115-123.
[139] F. Laghrib, S. Aghris, N. Ajermoun, A. Hrioua, M. Bakasse, S. Lahrich, M. A. El Mhammedi, Recent progress in controlling the synthesis and assembly of nanostructures: Application for electrochemical determination of p-nitroaniline in water. Talanta. (2020) 121234.
[140] F. Laghrib, N. Ajermoun, M. Bakasse, S. Lahrich, M. A. El Mhammedi. Synthesis of silver nanoparticles assisted by chitosan and its application to catalyze the reduction of 4-nitroaniline, Int. J. Biol. Macromol. 135 (2019) 752-759.
[141] W. Zhu, W. Liu, T. Li, X. Yue, T. Liu, W. Zhang, S. Yu, D. Zhang, J. Wang, Facile greensynthesis of graphene-Au nanorod nanoassembly for on-line extraction and sensitivestripping analysis of methyl parathion, Electrochim. Acta. 146 (2014) 419–428.
[142] A. Pollap, P. Knihnicki, P. Kus´trowski, J. Kozak, M. G. Ce¸pa, A. Kotarba, J. Kochana, Sensitive Voltammetric Amoxicillin Sensor Based on TiO_2 Sol Modified by CMK-3-type Mesoporous Carbon and Gold Ganoparticles, Electroanalysis. 30 (2018) 1– 12.

[143] T. M. Prado, F. H. Cincotto, F. C. Moraes, S. A. S. Machado, Electrochemical Sensor-Based Ruthenium Nanoparticles on Reduced Graphene Oxide for the Simultaneous Determination of Ethinylestradiol and Amoxicillin, Electroanalysis. 29 (2017) 1278 – 1285.
[144] N. Kumar, R. N. Goyal, Gold-palladium nanoparticles aided electrochemically reduced graphene oxide sensor for the simultaneous estimation of lomefloxacin and amoxicillin, Sensor. Actuat. B-Chem. 243 (2017) 658-668.
[145] A. Hatamiea, A. Echresha, B. Zargarb, O. Nura, M. Willandera, Fabrication and characterization of highly-ordered Zinc Oxide nanorods on gold/glass electrode, and its application as a voltammetric sensor, Electrochim. Acta. 174 (2015) 1261–1267.
[146] H. K. Maleh, F. T. Javazmi, V. K. Gupta, H. Ahmar, M. H. Asadi, A novel biosensor for liquid phase determination of glutathione and amoxicillin in biological and pharmaceutical samples using a ZnO/CNTs nanocomposite/catechol derivative modified electrode, J. Mol. Liq. 196 (2014) 258–263.
[147] M. M. Abdel-Galeil, H. S. El-Desoky, E. M. Ghoneim, A. Matsuda, Application of montmorillonite clay and mesoporous carbon as modifiers to carbon paste electrode for determination of amoxicillin drug, J. Electrochem. Soc. 164 (2017) 1003.
[148] A. Wonga, A. M. Santos, F. H. Cincottoc, F. C. Moraesb,O. F. Filhob, M. D.P.T. Sotomayora, A new electrochemical platform based on low cost nanomaterials for sensitive detection of the amoxicillin antibiotic in different matrices, Talanta. 206 (2020) 120252.
[149] A. J. Bard, L. R. Faulkner, Electroactive layers and modified electrodes, Electrochem. Methods. Fundamnetals. Appl. 2 (2001) 580–631.
[150] F.Ağın, Electrochemical Determination of Amoxicillin on a Poly(Acridine Orange) Modified Glassy Carbon Electrode, Anal. Lett. 49 (2016) 1366-1378.
[151] B. Norouziz, T. Mirkazemi, Electrochemical Sensor for Amoxicillin Using Cu/Poly (o-Toluidine) (Sodium Dodecyl Sulfate) Modified Carbon Paste Electrode, Russ. J. Electrochem. 52 (2016) 37–45.
[152] A. Farshadinia, M. Kolahdoozan, A new porous copolymer electrocatalyst: the optimal synthesis, characterization, and application for the measurement of amoxicillin, J. Appl. Electrochem. 49 (2019) 291-304.
[153] B. B. Prasad, B. Arora, Application of Polymer-Modified Hanging Mercury Drop Electrode in the Indirect Determination of Certain β-Lactam Antibiotics by Differential Pulse, Ion-Exchange Voltammetry, Electroanalysis. 15 (2003) 1212-1218.
[154] M. Ates, A review study of (bio)sensor systems based on conducting polymers, Mater. Sci. Eng. 33 (2013) 1853–1859.

[155] B. Uslu and I. Biryol,Voltammetric determination of amoxicillin using a poly N-vinyl imidazole, modified carbon paste electrode, J. Pharm. Biomed. Anal.20 (1999) 591.
[156] I. Biryol, B. Uslu, Z. Kucukyavuz, Voltammetric determination of amoxicillin using a carbon paste electrode modified with poly(4-vinyl pyridine), J. STP. Pharm. Sci. 8 (1998) 383–386.
[157] S. A. Piletsky, A. P. F. Turne, Electrochemical Sensors Based on Molecularly Imprinted Polymers, Electroanalysis. 14 (2002) 317-323.
[158] S. Zeinalia, H. Khoshsafarb, M. Rezaeib, H. Bagheric, Fabrication of a Selective and Sensitive Electrochemical Sensor Modified with Magnetic Molecularly Imprinted Polymer for Amoxicillin, Anal. Bioanal. Chem. Res. 5 (2018) 195-204.
[159] G. Yang, F. Zhao, molecularly imprinted polymer grown on multiwalled carbon nanotube surface for the sensitive electrochemical determination of amoxicillin, Electrochim. Acta. 174 (2015) 33-40.
[160] H. Essousi, H. Barhoumi, S. Karastogianni, S. T. Girousi, An Electrochemical Sensor Based on Reduced Graphene Oxide, Gold Nanoparticles and Molecular Imprinted Overoxidized Polypyrrole for Amoxicillin Determination, Electroanalysis. 32 (2020) 1– 14.
[161] D. Thevenot, K. Toth, R. A. Durst, G.S. Wilson, Electrochemical biosensors: recommended definitions and classification, Pure. Appl. Chem. 71 (1999) 635-659.
[162] S.Trashin, V. Rahemi, K. Ramji, L. Neven, S. M. Gorun, K. D. Wael, Singlet oxygen-based electrosensing by molecular photosensitizers, Nat. Commun, 8 (2017) 1-10.
[163] G. Merola, E. Martini, M. Tomassetti, L. Campanella, New immunosensor for β-lactam antibiotics determination in river waste waters, J. Sensor. Actuat. B-chem. 199 (2014) 301-313.
[164] A.Mehlhorn, P. Rahimi, Y. Joseph, Aptamer-based Biosensors for Antibiotic Detection: A Review, Biosensors. 8 (2018) 54.
[165] J. Songa, M. Huanga, N. Jianga, S. Zhenga, T. Mua, L. Menga,Y. Liua, J. Liua, G. Chena, Ultrasensitive detection of amoxicillin by TiO2-g-C3N4@AuNPs impedimetric aptasensor: Fabrication, optimization, and mechanism, J. Hazard. Mater. 391 (2020) 122024.
[166] T. R. Chowdhury, A. A. Shaikh, H. Akter, M. M. Neaz, P. K. Bakshi, A. S. Ahammad, Highly sensitive detection of amoxicillin based on gold nanoparticle-modified ITO electrode, J. ECS. Solid. State. Lett. 3 (2013) 14.
[167] I. S. Park, D. K. Kim, N. S. Kim, Characterization and food application of a potentiometric biosensor measuring beta-lactam antibiotics, J. microb. biote. 14 (2004) 698-706.

Chapter II

Experimental Techniques

I. Electrochemical techniques

Electroanalytical techniques are concerned with the interplay between electricity and chemistry, namely the measurement of electrical quantities such as current, potential or charge and their relationship to chemical parameters such as concentration, kinetics, reaction mechanisms, chemical status and other behavior of a species in solution. Similar information can be obtained concerning the electrode surface [1].

In most electrochemical techniques, there are three electrodes – the working electrode, the reference electrode and the counter (or auxiliary) electrode. The three electrodes are connected to a potentiostat, an instrument which controls the potential of the working electrode and measures the resulting current. In one typical electrochemical experiment, a potential is applied to the working electrode and the resulting current measured then plotted versus time. In another, the potential is varied, and the resulting current is plotted versus the applied potential. The different combinations of parameters and working electrode types make for a long list of techniques, including cyclic voltammetry, chronoamperometry, pulsed techniques, electrochemical impedance spectroscopy and others.

I.1. Cyclic Voltammetry

Cyclic Voltammetry **(**CV) is an electrochemical technique used to study the electrochemical properties related to electroactive surfaces. CV is a very versatile electrochemical method that enables understanding of the mechanisms of redox reactions, reversibility of a reaction, and electron transfer kinetics of an electroactive species in solution [2,3]. CV provides rapid information on thermodynamic redox processes, on the kinetics of heterogeneous electron-transfer reactions, and on coupled chemical reactions or adsorption processes. It is the foremost electrochemical experiment performed to characterize electrode material for every type of application [3].

The current is measured as a function of the linear potential applied. As species react at different potentials and with different intensity, the CV enables multiple detections in one measurement (qualitative), and estimation of their concentration in solution (quantitative). The current resulting from the potential application is due to the occurrence of redox reactions in the solution (Faradic current) and to the double layer charging (capacitive current) [4]. The current response is plotted as a function of voltage rather than time, unlike potential step measurements. In the case of a reversible reaction, the species is consecutively oxidised and reduced (or vice versa). The voltage is scanned using a triangular waveform shown in Fig. 1: In this case the

voltage is swept between two values (see above) at a fixed rate, starting from E_1; when the voltage reaches E_2 the scan is reversed and swept back to E_1. The time taken to sweep the potential range is the voltage scan rate (ν), calculated from the slope of V = f(t).

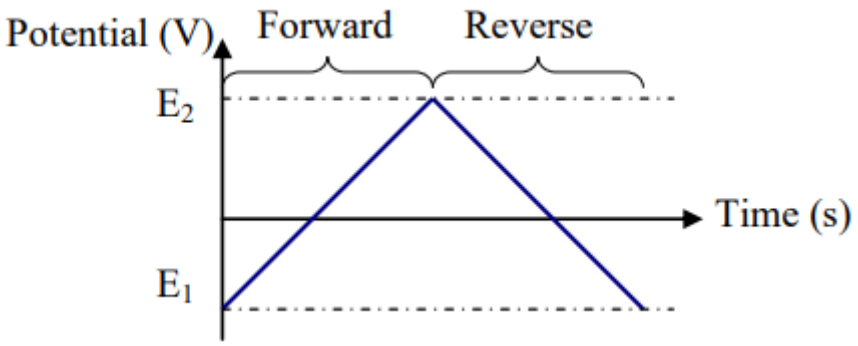

Figure 1*:* *Potential applied to the cell versus time.*

With the change of potential, the current passed through the electrode changes due to oxidation or reduction processes, therefore normally a cyclic voltammogram is a plot of current against potential [4]. An example of a cyclic voltammetry at macroelectrode is shown in Fig. 2.

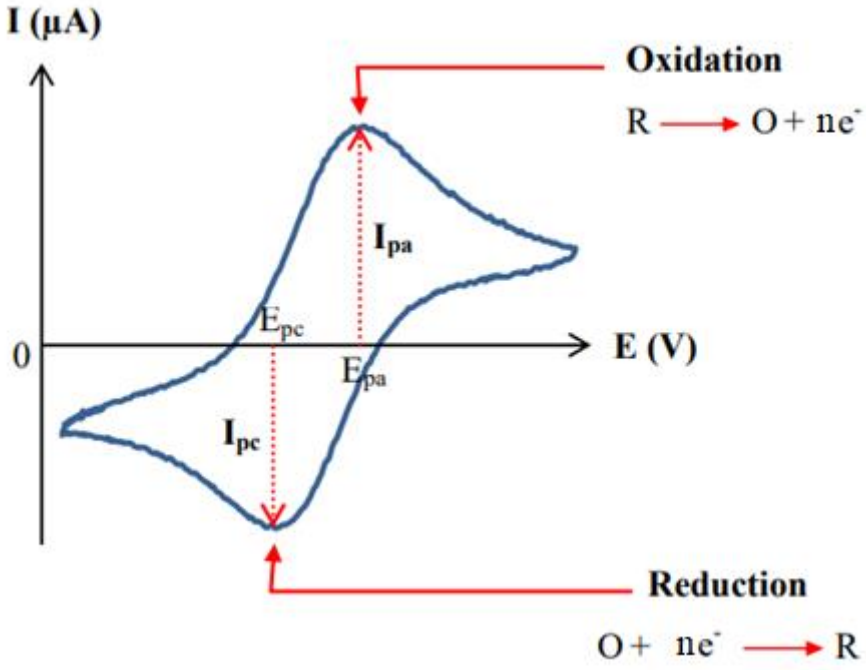

Figure 2: *Cyclic voltammogram of a reversible reaction using a macroelectrode.*

The measured parameters in cyclic voltammetry are anodic and cathodic peak potential (Epa and Epc), anodic and cathodic peak current (Ipa and Ipc) and the half peak potentials (Ep/2) at which the cathodic and anodic currents reach half of their peak value. According to International

Union of Pure and Applied Chemistry (IUPAC) convention, the anodic current is positive and the cathodic current is negative [5].

I.1.1. Reversibility

Based on the different electrode kinetics, the electrochemical reactions can be described as reversible, quasi-reversible and irreversible. An electrochemically reversible process occurs when the rate of electrode reaction is faster than that of the mass transport. Conversely, if the rate of electrochemical reaction is slower than the rate of mass transport, then the reactant is electrochemically irreversible. Normally with $D=10^{-5}$ cm^2 s^{-1} and at 298 K, the reversibility can be described by a heterogeneous rate constant, k^0. Matsuda and Ayabe [6] suggested that, for a reversible case, $k^0 > 0.3v^{1/2}$ *cm* s^{-1}, for a quasi-reversible case, k^0 in range of less than $0.3v^{1/2}$ cm s^{-1} and greater than $2\times10^{-5}v^{1/2}$ *cm* s^{-1}, and for a totally irreversible case, $k^0 < 2\times10^{-5}$ $v^{1/2}$ *cm* s^{-1}, where *v* is the scan rate, respectively.

If consider a simple one electron transfer process (with n = 1), the process can be described as Er, where the E stands for electron transfer and the subscript, r, stands for reversible process.

For a reversible limit case, the sweep peak current can be given by the Randles-Sevčik equation [7,8]:

$$i_p = 0.4463nFA\sqrt{\left[\frac{nF}{RT}\right]}c\sqrt{D}\sqrt{v} \qquad \text{Eq. 1}$$

For a reversible CV, the rate of electron transfer is controlled by diffusion. The separation of cathodic and anodic peak potentials is around 56/n mV. In real cases, the separation in range 60-70 mV can be considered as reversible. The peak potential in reversible process is independent of scan rate. The ratio of cathodic to anodic currents is unity at all different scan rates. As shown in Eq. 1, the peak current is proportional to the square root of the scan rate, therefore graph of log ip vs. log v is normally plotted to distinguish between a diffusion-controlled process and an adsorbed process. In practical cases, the slope equals to 0.5 indicates the process is under diffusion controlled; a slope of unity indicates the electroactive material is adsorbed on the electrode. For an irreversible case, Ei_{rr}, the Randles-Sevčik equation is modified to be:

$$i_p = 0.496nFA\sqrt{\left[\frac{\alpha nF}{RT}\right]}c\sqrt{D}\sqrt{v} \qquad \text{Eq. 2}$$

As it can be seen from Eq. 2, the peak current is still proportional to the square root of scan rate due to the diffusion-controlled process. An extra term, the symmetry coefficient of the electron

transfer process, is introduced in the Randles-Sevčik equation for irreversible case. For a single electron irreversible electrochemical process, the separation of peak potential varies with the change of scan rate at 298 K is given by:

$$\Delta E_p = \frac{59.4}{\alpha} + \text{constant} \qquad \text{Eq. 3}$$

where ΔEp is the potential difference between oxidative and reductive peaks. It is also known as approximately 30 mV shift per decade change in scan rate.

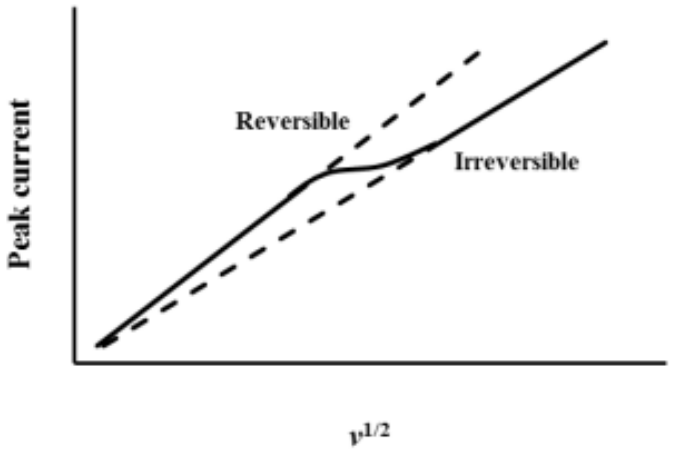

Figure 3: *Plot of peak current against square root of scan rates corresponding to reversibility.*

A quasi-reversible process sits in between reversible limit and irreversible limit. In practice, quasi-reversible processes appear reversible at slow scan rate and an irreversible behaviour at high scan rate as the limits which are described by Matsuda and Ayabe [6] . Normally a plot of peak potential versus $\log_{10}$ v is used to find the reversible limit. The peak potential initially independent on increasing scan rate and the peak potential starts to shift in high scan rates, therefore reversible limit equations can be applied in the reversible regime and irreversible limit equations can be applied in the irreversible regime. In addition, the transit between reversible to quasi-reversible and on to irreversible process can be described by plotting peak current against square root of scan rates (Fig. 3).

I.2. Square Wave Voltammetry

Square wave voltammetry (SWV), developed by Barker and Jenkins [9], is a powerful electrochemical technique that has been extensively used in electro-kinetic measurements, analytical application and mechanistic study of electrode processes [10]. It unifies the merits of several pulse voltammetric methods, including the background suppression and sensitivity of

differential pulse voltammetry (DPV), the diagnostic value of normal pulse voltammetry (NPV), and the direct interrogation of products of reverse pulse voltammetry (RPV). It also incorporates the advantages of cyclic voltammetry (insight into the electrode mechanism) and impedance techniques (kinetic information of fast electrode processes) [11]. The ability to achieve a wider time scale than other pulse voltammetric methods also adds its popularity. Currently SWV is regarded as one of the most advanced voltammetric techniques.

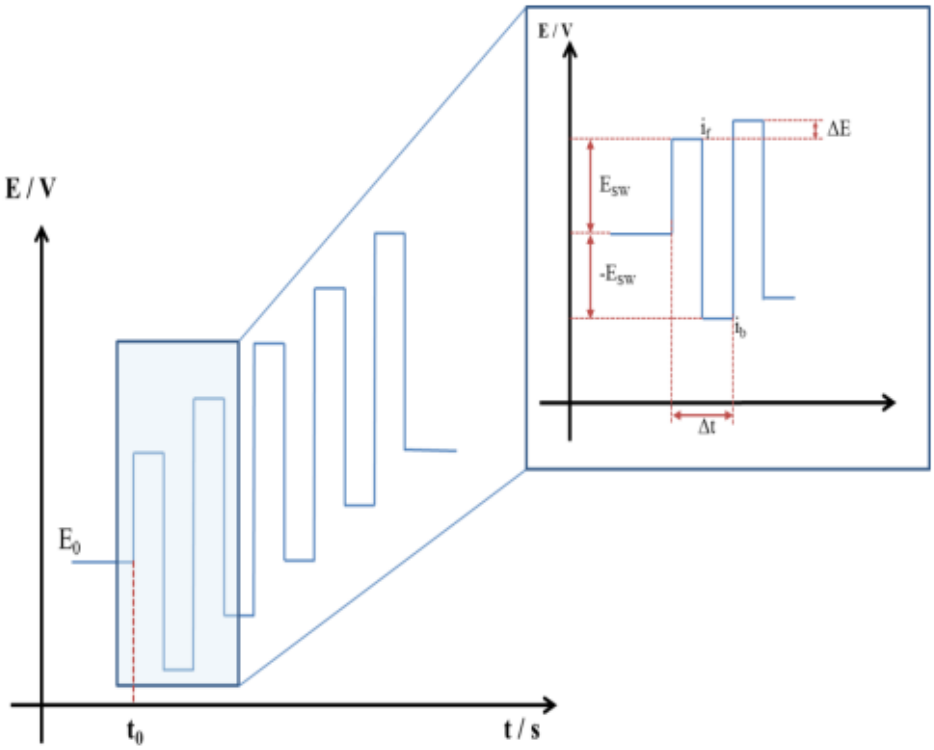

Figure 4: *A schematic diagram of the principle square wave voltammetry.*

A schematic diagram is shown in Fig. 4 for a potential-time change for a SWV. As shown in Fig. 4, the potential changes in a square wave form as increase experimental time. The initial potential starts at E_0, then the potential goes up to E_0+Esw, which Esw is amplitude, and it is held for $\Delta t/2$ (pulse duration) seconds and the potential then goes down to E_0+(-Esw). Δt is known as period, and the frequency can be illustrated to be $f = \Delta t^{-1}$. ΔE represents the potential increment of the staircase waveform. The currents are measured at the end of each pulse (both i_f and i_b). In practice, the net current, which subtracts i_b from i_f is normally shown in the software. the net current is usually shown as final view of a SW voltammogram. The charging current in this case can be negligible as the currents are measured after each pulse. Note that the backward current is positive and without a peak is due to small value of E_{SW}.

I.3. Chronoamperometry

Chronoamperometry belongs to the potential pulse techniques and can be employed to measure the current which arises after the capacitive current. Contrary to cyclic voltammetry where the potential is applied linearly, in chronoamperometry the potential is applied in steps (Fig. 5), from a value where the analyte is not oxidised or reduced, E_1, to a value where it is (E_2). In this step technique, the current is diffusion-controlled and plotted as a function of time (Fig. 5).

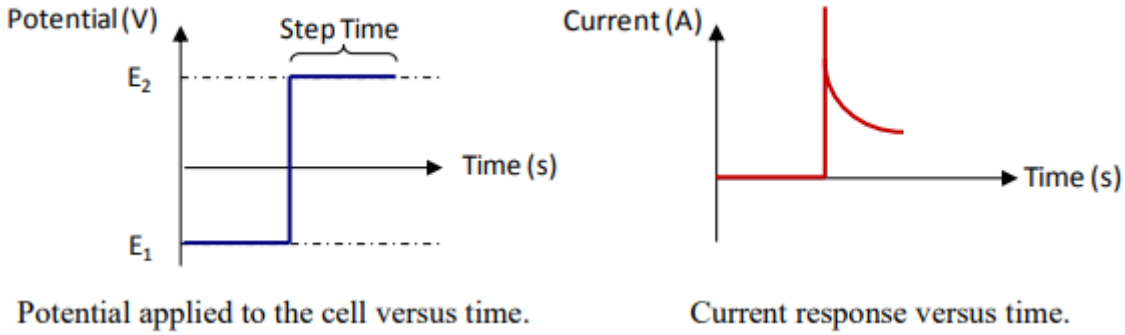

Figure 5: *Chronoamperometry voltammogram.*

The step time τ is the time for which the potential is maintained at the same value. It should be neither too short nor too long so that the current remains controlled by diffusion. If the step time is too short, the current measured includes the charging current. As the charging current decreases exponentially in time, it is negligible after a few milliseconds. At long times (of the order of 100 s), convection develops in the solution (from density gradients arising from the electrolysis products) causing positive deviations from the theoretical current [12]. When mass transport is only happening by diffusion, the current-time curve reflects the change in the concentration gradient at the electrode surface. This involves a gradual expansion of the diffusion layer associated with the diminution of the analyte, and hence decreased slope of the concentration profile as time progresses. The environment is maintained still to observe no effects other than diffusion [13]. The Cottrell equation (Eq. 4) describes the current decays with time, at a planar electrode. Typically, the current measured is then plotted versus $t^{-1/2}$ to get back to the concentration, the diffusion coefficient, the number of electrons transferred or the surface area [14].

$$i_p(t) = \frac{nFAC\sqrt{D}}{\sqrt{\pi t}} \qquad \text{Eq. 4}$$

Where n is the number of electrons involved in the reaction, F is the Faraday constant ($C.mol^{-1}$), A is the surface area (dm^2), C is the analyte concentration (mol/dm^3), D is the diffusion coefficient ($dm^2.s^{-1}$) and t is the time (s).

II. Spectroscopic techniques

II.1. UV-Visible spectroscopy

Ultraviolet (UV) absorption spectroscopy is perhaps the simplest and most employed instrumental technique for studying both the stability of ligand and their interactions with metal ions. The study of drug–metal interactions could be carried out by UV–Visible absorption spectroscopy by monitoring the changes in the absorption properties of the drug or the metal ions [15]. Usually, molecules used as ligands show an absorption band that can be clearly distinguished in the visible region.

II.1.1. Principle

A molecule or ion will exhibit absorption in the visible or ultraviolet region when radiation causes an electronic transition within its structure. Thus, the absorption of light by a sample in the ultraviolet or visible region is accompanied by a change in the electronic state of the molecules in the sample. The energy supplied by the light will promote electrons from their ground state orbital to higher energy, excited state orbital or anti-bonding orbital (Fig. 6).

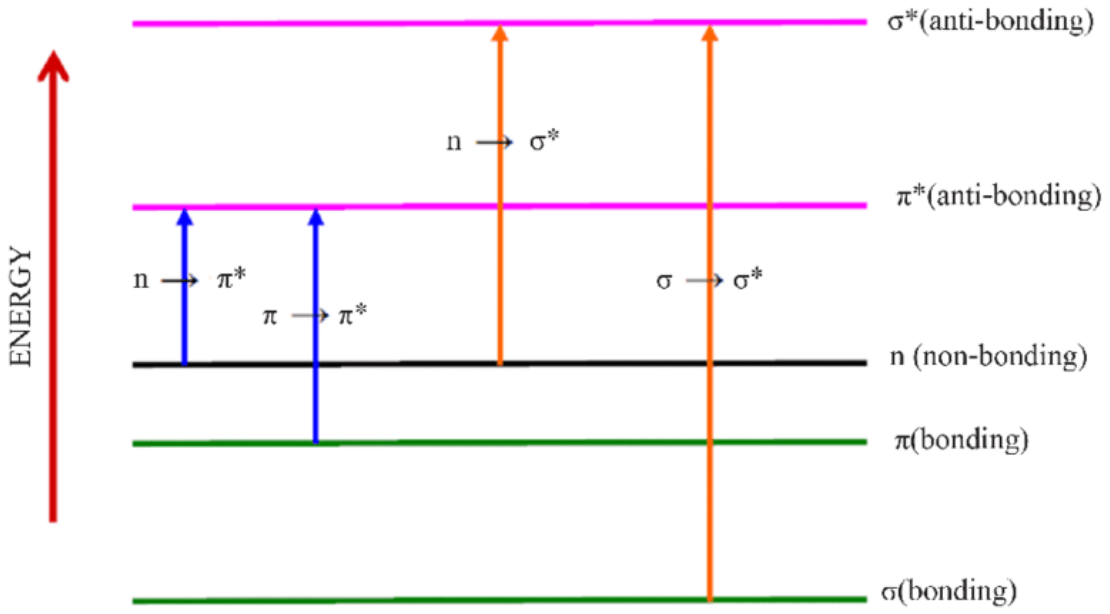

Figure 6: *Electron Transition graphically represented.*

Potentially, three types of ground state orbitals may be involved:

1. σ (Bonding) molecular
2. π (Bonding) molecular orbital
3. n (non-Bonding) atomic orbital.

In addition, two types of anti-bonding orbitals may be involved in the transition:

i) σ* (sigma star) orbital.

ii) π* (pi star) orbital.

There is no such thing as an n* anti-bonding orbital as the n electrons do not form bonds).

Thus, the following electronic transitions can occur by the absorption of ultraviolet and visible light:

- σ to σ*
- n to σ*
- n to π*
- π to π*

Both σ to σ* and n to σ* transitions require a great deal of energy and therefore occur in the far ultraviolet region or weakly in the region 180-240nm. Consequently, saturated groups do not exhibit strong absorption in the ordinary ultraviolet region. Transitions from then to π* and π to π* type occur in molecules with unsaturated centers, they require less energy and occur at longer wavelengths than transitions to σ* anti-bonding orbital. It will be seen presently that the wavelength of maximum absorption and the intensity of absorption are determined by molecular structure. Transitions to π* anti-bonding orbital which occurs in the ultraviolet region for a particular molecule may well take place in the visible region if the molecular structure is modified. Many inorganic compounds in solution also show absorption in the visible region. These include salts of elements with incomplete inner electron shells (mainly transition metals) whose ions are complexed by hydration. Such absorptions arise from a charge transfer process, where electrons are moved from one part of the system to another by the energy provided by the visible light [16]. The level of absorption intensity is identified by absorbance values at given energy and this value depends on the energy of excited light and concentration of chemical species in the solution for non-solid samples. The absorbance follows the Beer-Lambert's law [17]:

$$A=\varepsilon\, c\, l \qquad \text{Eq. 5}$$

Where: A is the measured absorbance, ε is the proportionality constant called absorptivity , l is the path length of the cell, c is the concentration of the analyte.

The optical absorption of chemicals species could be obtained experimentally by measuring the intensity of incident light and transmitted light. In this way it defined the transmittance (T) as:

$$T=\frac{It}{Ii} \qquad \text{Eq. 6}$$

Where: I_i is the intensity of incident light at a given wavelength (λ), I_t is the transmitted light intensity and T is the transmittance.

The logarithm of this "rate" corresponds to the energy absorbed at a particular wavelength and can be calculated by (Eq. 7) [17]:

$$A = log_{10}\left(\frac{It}{Ii}\right) = - log_{10}(T) \qquad \text{Eq. 7}$$

Where: A is the absorbance and T is the transmittance.

II.1.2. Instrumentation

The UV-Visible absorption spectrometer is an instrument used to perform measurements of absorbance, transmittance and reflectance. The operation is based on the extent of absorption of light when a beam of a light source is separated into individual wavelengths by a prism or diffraction grating. This monochromatic light is divided into two beams of equal intensity by a beam-splitter. On one side, the light is sent through a reference cuvette (white) and, on the other hand, through the sample under analysis. In this case, the UV-Visible spectrometer is called a double beam (Figure 7).

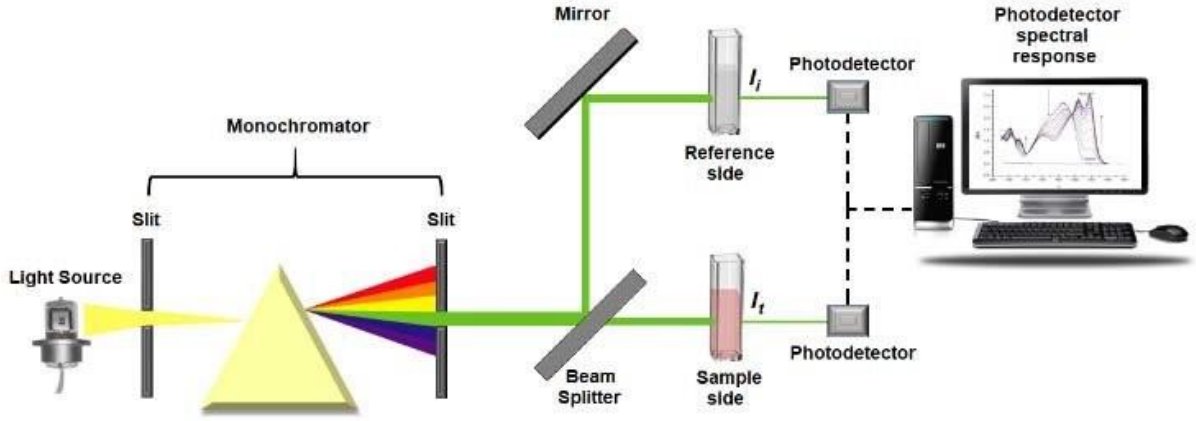

Figure 7: *Schematic representation of the dual-beam UV-VIS spectrometer.*

Both light rays are directed to detectors that compare their intensities as the ratio (rate) of light intensity through the sample and the reference medium. Over a short period of time, the UV-Visible absorption spectrometer automatically submits the sample to the incidence of light at wavelengths from the UV region (200 nm) to the visible region (800 nm) [18].

II.2. Fourier transform infrared spectroscopy—FTIR

Fourier spectroscopy" is a general term that describes the analysis of any varying signal into its constituent frequency components. The mathematical methods named after J.B.J. Fourier are

extremely powerful in spectroscopy [19]. Fourier transforms can be applied to a variety of spectroscopies including infrared spectroscopy known as Fourier transform infrared (FT-IR), nuclear magnetic resonance (NMR), and electron spin resonance (ESR) spectroscopy. FT-IR spectroscopy includes the absorption, reflection, emission, or photoacoustic spectrum obtained by Fourier transform of an optical interferogram. The power of the method derives from the simultaneous analysis of many frequency components in a single operation. A variety of spectroscopic techniques have been used to study various samples, but FT-IR spectrometers are growing in popularity since they offer speed, accuracy and sensitivity previously impossible to achieve with wavelength dispersive spectrometers [19].

In IR spectroscopy, IR radiation is passed through a sample. Some of the IR radiation is absorbed by the sample and some of it is passed through (transmitted). The resulting spectrum represents the molecular absorption and transmission, creating a molecular fingerprint of the sample. As two fingerprints never match, similarly no two unique molecular structures produce the same IR spectrum [20]. Therefore, IR spectroscopy can result in a positive identification (qualitative analysis) of every kind of material. In addition, the size of a peak in the spectrum is a direct indication of the amount of material present. With modern software algorithms, IR is an excellent tool for quantitative analysis and is among the top three analytical techniques in Web of Science (WoS) with 50 000 articles per year [20,21]. The peaks in the IR spectrum of a sample represent the excitation of vibrational modes of the molecules in the sample and thus are associated with the various chemical bonds and functional groups present in the molecules.

II.2.1. Principle

The IR region is commonly divided into three smaller areas: near-IR (400-10 cm^{-1}), mid-IR (4000)-400 cm^{-1}), and far-IR (14,000-4000 cm^{-1}) [22]. IR electromagnetic radiation is insufficient to excite electrons, unlike UV-vis excitation or x-rays [23], but intensifies the molecular and rotational vibrations. The far IR region of the spectrum (lower energy toward 400 000 nm) quantifies changes induced by rotational vibrations, while the near IR region includes both vibrational-rotational vibrations (toward 700 nm). The absorption frequency varies with vibrational modes, while the intensity depends on how effectively molecules absorb energy, which depends in turn on the change in the dipole moment. Compounds with a dipole moment selectively absorb infrared (IR) radiation according to their characteristic functional groups—hydroxyl, nitirle, amide, for example (Fig. 8). As the compounds absorb energy the molecule vibrates more–stretching and bending–depending on its geometry. The vibrational modes correspond to distinct energies, and molecules absorb IR radiation only at certain

wavelengths and frequencies. Chemical bonds vibrate at characteristic frequencies, and when exposed to IR radiation, they absorb the radiation at frequencies that match their vibration modes. Measuring the radiation absorption frequency produces a spectrum that can be used to identify functional groups and compounds. An IR spectrogram plots the absorbance vs the wavelengths varying from (700 to 400 000 nm and wave numbers from 14 000 to 25 cm^{-1}). Symmetrical molecules like diatomic gases—N_2, H_2, and O_2—have no dipole moment and consequently have no characteristic IR spectrum fingerprint [24].

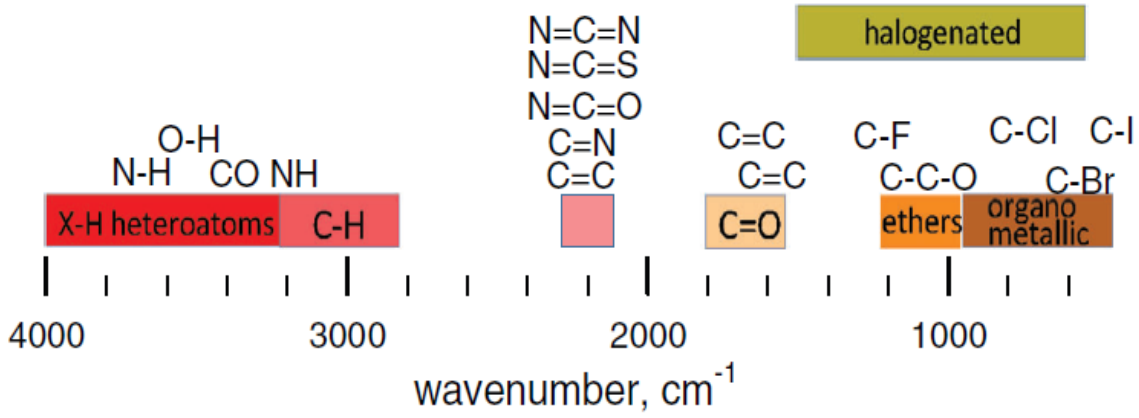

Figure 8: *Range of IR spectroscopic stretching bands.*

IR photons have enough energy to cause groups of atoms to vibrate with respect to the bonds that connect them. Like electronic transitions, the vibrational transitions correspond to distinct energies, and molecules absorb IR radiation only at certain wavelengths and frequencies. Chemical bonds vibrate at characteristic frequencies, and when exposed to IR radiation, they absorb the radiation at frequencies that match their vibration modes. Measuring the radiation absorption frequency produces a spectrum that can be used to identify functional groups and compounds [22].

II.2.2. Instrumentation

There are three basic spectrometer components in an FT: a radiation source, an interferometer, and a detector. The interferometer divides radiant beams, generates an optical path difference between the beams, and generates interference signals measured as a function of the optical path difference by the detector. As its name implies, the interferometer produces interference signals, which contain IR spectral information generated after passing through the sample. The most preferred interferometer is a Michelson interferometer, consisting of three active components: a moving mirror, a fixed mirror, and a beam splitter. The two mirrors are

perpendicular to each other. The beam splitter is a semi reflecting device and is often made by depositing a thin film of germanium onto a flat potassium bromide (KBr) substrate. Radiation from the broadband IR source is collimated and directed into the interferometer and impinges on the beam splitter producing two beams of roughly the same intensity. One beam strikes the fixed mirror and returns to the beam splitter. The other beam goes to the moving mirror. The motion of the moving mirror makes the total pathlength variable versus that taken by the fixed mirror beam. When these two beams meet up again at the beams splitter, they recombine, and the difference in their path lengths create constructive and destructive interference, an interferogram. The recombined beam passes through the sample. The sample absorbs all the wavelengths characteristic of its spectrum and then subtracts specific wavelengths from the interferogram. The detector now reports variation in energy-versus-time for all wavelengths simultaneously. A laser beam is superimposed to provide a reference for the operation of the instrument. Fourier transform function convert the intensity-versus-time spectrum into an intensity-versus-frequency spectrum [25] (Fig. 9).

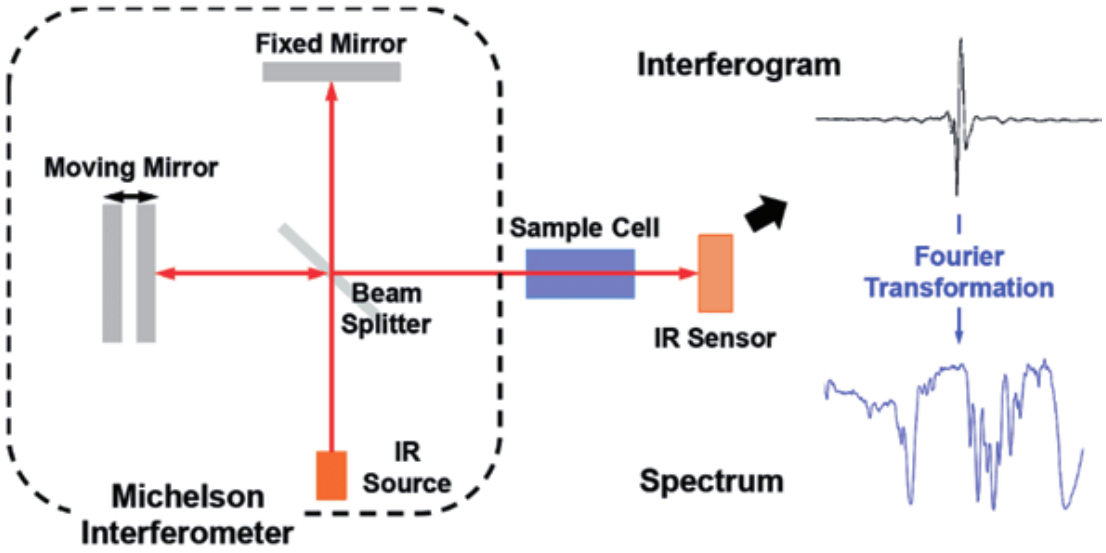

Figure 9: *Schematic diagram of a Fourier transform infrared instrument.*

References

[1] P.T. Kissinger, W. R. Heineman, Cyclic voltammetry. J. Chem. Educ. 60 (1983) 702.

[2] M. Aliofkhazraei, Modern electrochemical methods in nano, surface and corrosion science, BoD–Books on Demand. ed., 2014.

[3] D. K. Gosser, Cyclic voltammetry: simulation and analysis of reaction mechanisms, New York: VCH. 43 (1993).

[4] R. G. Compton, C. E. Banks, Understanding voltammetry, World Scientific. (2018).

[5] A. S. Hameed, Phosphate based cathodes and reduced graphene oxide composite anodes for energy storage applications, Springer. (2016).

[6] H. Matsuda, Y. Ayabe, Zur Theorie der Randles-Sevčikschen Kathodenstrahl-Polarographie. Zeitschrift für Elektrochemie, Berichte der Bunsengesellschaft für physikalische Chemie. 59 (1995) 494-503.

[7] J. E. B. Randles, A cathode ray polarograph. Part II.—The current-voltage curves , Trans. Faraday Soc. 44 (1948) 327-338. doi: 10.1039/TF9484400327.

[8] J. E. B. Randles, A cathode ray polarograph, Trans. Faraday Soc. 44 (1948) 322-327. doi: 10.1039/TF9484400322.

[9] Š. Komorsky-Lovrić, Measurement of the kinetics of adsorbed cinnoline by square-wave voltammetry », Anal. Bioanal. Chem. 373 (2002) 777-780. doi: 10.1007/s00216-002-1364-1.

[10] V. Mirceski, S. Komorsky-Lovric, M. Lovric, Square-wave voltammetry: theory and application. Springer Science & Business Media (2007).

[11] V. Mirceski, R. Gulaboski, M. Lovric, I. Bogeski, R. Kappl, M. Hoth, Square-wave voltammetry: a review on the recent progress. Electroanalysis. 25 (2013) 2411-2422.

[12] A. Kamat, A. Huth, O. Klein, S. Scholl, Chronoamperometric Investigations of the Electrode–Electrolyte Interface of a Commercial High Temperature PEM Fuel Cell , Fuel Cells. 10 (2010) 983-992. doi: 10.1002/fuce.201000014.

[13] D. H. Evans, M. J. Kelly, Theory for double potential step chronoamperometry, chronocoulometry, and chronoabsorptometry with a quasi-reversible electrode reaction , Anal. Chem. 54 (1982) 1727-1729. doi: 10.1021/ac00248a016.

[14] K. C. Honeychurch, Printed thick-film biosensors. Printed films. (2012) 366-409.

[15] H. Sun, A stabilizing and denaturing dual-effect for natural polyamines interacting with G-quadruplexes depending on concentration, *Biochimie*. 93 (2011) 1351-1356. doi: 10.1016/j.biochi.2011.06.007.

[16] Y. R. Sharma, *Elementary Organic Spectroscopy*. S. Chand Publishing. (2007).

[17] K. Fuwa, B. L. Valle, The Physical Basis of Analytical Atomic Absorption Spectrometry. The Pertinence of the Beer-Lambert Law, ACS Publications. 35 (2002) 942-946. https://pubs.acs.org/doi/pdf/10.1021/ac60201a006.

[18] M. S. Braga, O. F. Gomes, R. F. V. V. Jaimes, E. R. Braga, W. Borysow, et W. J. Salcedo, Multispectral colorimetric portable system for detecting metal ions in liquid media », in 2019 4th International Symposium on Instrumentation Systems, Circuits and Transducers (INSCIT). IEEE. (2019) 1-6. doi: 10.1109/INSCIT.2019.8868861.

[19] D. R. Vij, Handbook of applied solid state spectroscopy. Springer Science & Business Media. ed. (2007).

[20] R. J. Markovich, C. Pidgeon, Introduction to Fourier transform infrared spectroscopy and applications in the pharmaceutical sciences. Pharmaceutical research. 8 (1991) 663-675.

[21] G. S. Patience, C. A. Patience, et F. Bertrand, Chemical engineering research synergies across scientific categories, Can. J. Chem. Eng. 96 (2018) 1684-1690. doi: 10.1002/cjce.23165.

[22] A. Dutta, Chapter 4 - Fourier Transform Infrared Spectroscopy, Editor(s): Sabu Thomas, Raju Thomas, Ajesh K. Zachariah, Raghvendra Kumar Mishra, In Micro and Nano Technologies, Spectroscopic Methods for Nanomaterials Characterization, Elsevier, (2017) Pages 73-93, SBN 9780323461405, https://doi.org/10.1016/B978-0-323-46140-5.00004-2.

[23] F. S. Rocha, A. J. Gomes, C. N. Lunardi, S. Kaliaguine, et G. S. Patience, Experimental methods in chemical engineering: Ultraviolet visible spectroscopy—UV-Vis, Can. J. Chem. Eng. 96 (2018) 2512-2517 doi: 10.1002/cjce.23344.

[24] M. O. Guerrero-Pérez, G. S. Patience, Experimental methods in chemical engineering: Fourier transform infrared spectroscopy—FTIR. Can. J. Chem. Eng. 98 (2020) 25-33.

[25] J. R. Ferraro, L. J. Basile, Fourier transform infrared spectra: applications to chemical systems. Academic press. eds. (2012).

Chapter III

Chronoamperometric Detection of Amoxicillin

I. Introduction

Amoxicillin (AMX) is a semi-synthetic β-lactam antimicrobial agent used in the treatment and prevention of bacterial infections in animals and humans [1]. It not only possesses antimicrobial activity against most gram-positive and gram-negative bacteria, but it also presents higher absorption rate, following oral administration, than other β-lactam antibiotics. The World Health Organization (WHO) has categorized it as a critically important antimicrobial agent in human medicine [2]. However, AMX can cause harmful effects to humans, like central nervous system (CNS) disorders, spermatogenesis and many more [3]. Thus, it is necessary to develop a sensitive method for the determination of AMX.

Many analytical techniques have been reported for the determination of AMX such as spectrometry [4-7], chromatography [8-9] and chemiluminescence [10]. Furthermore, most of the mentioned methods are expensive, needing complex pretreatments, consuming large samples volumes and time. Therefore, electrochemical methods with their high sensitivity, fast response, easy operation and cost-effective, have been widely used for the determination of AMX, such as cyclic voltammetry [11], square wave voltammetry [12], differential pulse anodic stripping voltammetry [13] and linear sweep voltammetry [12].

Some of the previous studies reported that the detection of AMX has been based on metal ion-catalyzed hydrolysis of the antibiotic [5,7], where the antibiotic–metal complex is considered as intermediate in the hydrolytic reaction [12]. Among the metal ions, copper (II) is an essential transition metal ion for the human diet and biochemical processes, participating in various physiological reactions of living organisms [14-15]. In the human body amoxicillin can interact with copper (II) ions which are present as free ions or coordinatively bounded to bioligands, these reactions can influence processes of the biosynthesis of antibiotics, so the knowledge of this interaction is of great importance [16-18].

The copper (II) ion catalyzed hydrolysis of AMX has been widely investigated [5-6]. This metal-catalyzed hydrolysis seems to have a complex chemistry, involving the catalyzed effect of the metal ion as well as complex formation. So far, various analytical methods including spectrophotometry [5,19], fluorimetric [20], pH-potentiometry [21] and electrospray ionization mass spectrometry (ESI-MS) [22], have been used for studied the interaction of AMX with copper (II) ions, only in one study this interaction was studied by electrochemical method [4]. To our best knowledge, this study is among the first to investigate copper-amoxicillin complex ions by square wave voltammetry (SWV) and chronoamperometry. Moreover, there were no reports on the detection of amoxicillin by chronoamperometry. Therefore, we have undertaken

chronoamperometric measurements for the determination of (AMX) in the presence of copper (II) ions at carbon paste electrode. The complexation reaction of the Cu(II) by AMX was characterized by UV-visible spectroscopy, Infrared spectroscopy (IR) and square wave voltammetry (SWV). The influence of different organic compounds on the AMX determination and the effect of coexisting of other metal ions in electrolytic solution were studied. The method is successfully applied for the determination of AMX in blood samples and pharmaceutical tablets.

II. Experimental

II.1. Reagent

Amoxicillin (98% purity) was obtained from Sigma–Aldrich Laboratories. Copper (II) sulfate, nitrate of iron (II), nickel (II), cobalt (II), zinc (II), aluminum (III) and lead (II) were obtained from Scharlau, Janssen Chimica, Merck and Sigma-Aldrich and were used as received. Phosphate buffer solution (pH =7) used as supporting electrolyte was prepared by mixing appropriate amounts of potassium hydrogen phosphate and potassium dihydrogen phosphate (Sigma–Aldrich). Tablets containing amoxicillin labeled 1g was obtained from a commercial source. Blood samples were obtained from healthy volunteers.

II.2. Apparatus

All electrochemical experiments were investigated using a VOLTALAB PGZ 100 potentiostat controlled by voltamaster 4 data acquisition software. An electrochemical cell involving three electrode using a carbon paste electrode (CPE) as working electrode, platinum wire as counter electrode and Ag/AgCl in saturated KCl as the reference electrode. Spectrophotometric measurements were made on a UV/Vis spectrophotometer (Shimadzu spectrophotometer, model biochrom). Infrared (IR) spectra were taken in a PerkinElmer Fourier transform FT-IR spectrometer (FTIR-2000). The values of pH were adjusted using the pH-meter (Radiometer, SENSION^{TM}, PH31, Spain).

II.3. Procedure

II.3.1. Electrochemical Studies

Chronoamperometric analysis of AMX was performed using CPE. The working electrode was placed in an electrochemical cell containing 30 mL of 0.1 M phosphate buffer solution (pH 7) and 0.1 mM copper (II). The working electrode operated at -150 mV vs Ag/AgCl under a slow constant stirring of 100 rpm. When a stable baseline current was acquired, a volume of 0.5 mL

of different known concentrations of AMX was added and the response was recorded. Square-wave voltammograms were recorded between 0.0 and +1.0 V vs. Ag/AgCl. All measurements were obtained at room temperature.

II.3.2. Spectrophotometric measurements

The reaction of the Cu(II) ions with AMX was studied spectrophotometrically under various experimental conditions. The effect of different Cu(II) concentrations on the absorption spectra of AMX was studied after a reaction time of 5 min (randomly selected) at room temperature. Thereafter, the reaction time was investigated, within the range from 2 min to 90 min. The absorbance measurement was carried out at a wave number (λ) ranging between 400 and 900 nm.

II.3.3. Preparation of solid complex

The solid AMX–Cu complex was prepared by adding 25 mL of a 0.01 M metal solution to 25 mL of a 0.01 M AMX dissolved in a phosphate buffer solution (pH=7) with continuous stirring at room temperature for 48h. The product was filtered through a filter paper, and it was dried by keeping it at room temperature. An aliquot of the solid complex (1%) was thoroughly mixed with KBr (99%) and pressed to prepare the pellet for IR measurement.

II.3.4. Sample preparation

Amoxicillin medicaments were purchased from local pharmacy. Each tablet contains 1g of AMX. They were powdered in a mortar and a portion of the powder equivalent to the average weight of one tablet was dissolved in PBS (pH 7). Then, the prepared samples of amoxicillin were analyzed using the developed electrochemical method. The human blood obtained from healthy volunteers was centrifuged at 4000 rpm for 30 min to separate serum and plasma. The amperometric measurement is implemented in 30 mL of serum containing 0.1 M PBS and 0.1 mM Cu(II) with the injection of serum spiked with 1.0×10^{-4} M, 5.0×10^{-5} M and 1.0×10^{-5} M of AMX.

III. Results and discussions

III.1. Electrochemical behavior of AMX/Cu

The electrochemical behavior of AMX/Cu at carbon paste electrode (CPE) was investigated using cyclic voltammetry (CV) and square-wave voltammetry (SWV). Cyclic voltammograms for the electro-oxidation of 1 mM AMX in PBS at pH 7.0, as shown in Fig.1 A, present an

oxidation wave at 0.85 V. which is attributed to the oxidation of OH group of the phenolic sites of the AMX (ϕ–OH) [23]. The mechanism proposed for the electrochemical oxidation of AMX is (Scheme 1):

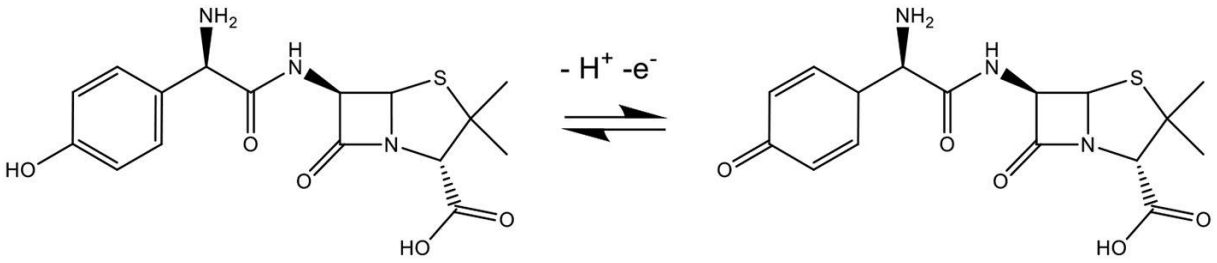

Scheme 1: *Proposed mechanism for the electrochemical oxidation of AMX.*

The presence of 0.1mM Cu(II) reveals a considerable influence on the electrode response. It observed that the anode current of AMX in the presence of Cu(II) is significantly lower than that where copper does not exist in the solution, which could be due to the formation of an electro-inactive compound as result of the reaction between AMX and Cu(II).

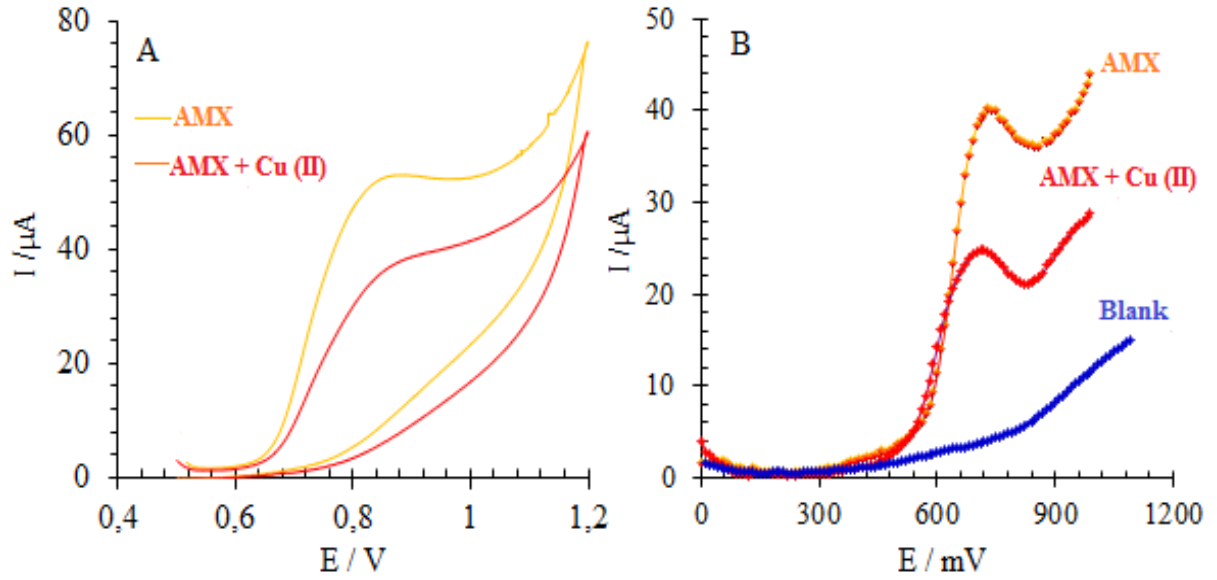

Figure 1: *(A) Cyclic voltammograms of 1.0×10^{-3} M AMX, 1.0×10^{-3} M AMX + Cu(II) in PBS pH=7 at CPE and (B) Square-wave voltammograms of 1.0×10^{-4} M AMX, 1.0×10^{-4} M AMX + Cu(II), and PBS pH=7 (blank) at CPE.*

The electro-oxidation square-wave voltammograms of 0.1 mM AMX in both absence and presence of 0.1 mM of Cu(II) in PBS (pH=7) are compared in the fig. 1B, as can be seen, the anodic peak potential of amoxicillin oxidation on carbon paste electrode is about 0.7 V. The presence of Cu(II) had a tremendous influence on the electrode response, it is apparent that the

anodic current of AMX in the presence of Cu(II) is significantly less than that of a solution without it. This decrease is directly related to both to the decrease in the concentration of AMX and the formation of new formed product, which cannot be oxidized at the working electrode.

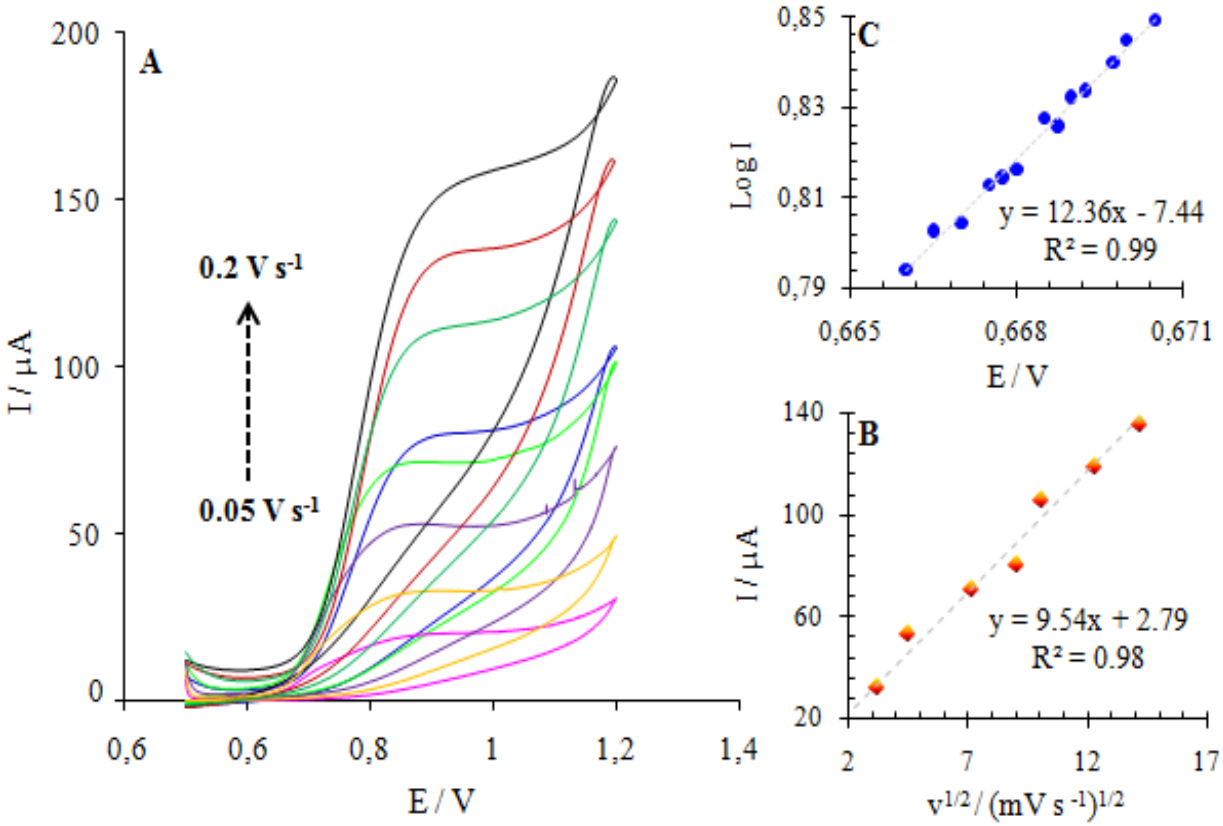

Figure 2: *(A) Cyclic voltammogramms of 1.0×10^{-3} M AMX in PBS (pH=7) for various scan rates (0.05 – 0.2 Vs^{-1}); (B) Variation in peak current of AMX with root of scan rate; (C) Tafel plot for 1.0×10^{-3} M AMX in PBS (pH=7) at scan rate 20 mV s^{-1}.*

Fig. 2A shows the cyclic voltamograms of AMX recorded at different scan rates in the range from 0.05 V to 0.2 V. The effect of peak current of 1.0×10^{-3} M AMX vs. square root of scan rate was recorded (Fig. 2B). A good linear relationship was obtained, showing that the oxidation reaction of AMX is controlled by diffusion process, which confirms the Randles–Sevcik law. Furthermore, to calculate the electronic transfer coefficient and number of electrons transferred in the rate determining step, a plot between peak potential and log I of AMX oxidation was registered (Fig. 2C). From the slope of this plot, a value of 0.44 for αnα was obtained according to the following equation (Eq. 1):

$$b = 2.303RT/\alpha n_{\alpha}F \qquad \text{Eq. 1}$$

With b: the slope of Tafel plot (V); α the transfer coefficient and n_α the number of electrons transferred in the rate determining step [24].

Indeed, the electron transfer coefficient was found to be α= 0.4 by assuming n = 1.

III.2. Spectroscopic characterization of AMX/ Cu(II) complex

The reaction of Cu(II) ions with AMX was studied spectrophotometrically with UV-Visible. The UV-visible spectra of 1.0×10^{-4} M AMX in phosphate buffer solution (pH=7) shows a strong absorption band at 229 nm corresponding to the β-lactam bond [25] and a second band of low intensity at 272 nm relating to aromatic rings as it is illustrated in Fig. 3A. However, in presence of Cu^{2+} ions, a new absorption band appeared clearly at 324 nm when the mole ratio amoxicillin: Cu(II) ion was equal to 1:1 or 1:2 and the band at 229 nm which originated from the β-lactam bond was significantly deformed due to the complex formed with Cu(II) demonstrating the involvement of the C=O of the lactam ring in the chelation process. The effect of the reaction time was investigated in the range from 2 min to 120 min. As can be seen in Fig. 3B, the band centered at 324 nm appears at the beginning of reaction, but no other changes have been recorded after longer duration.

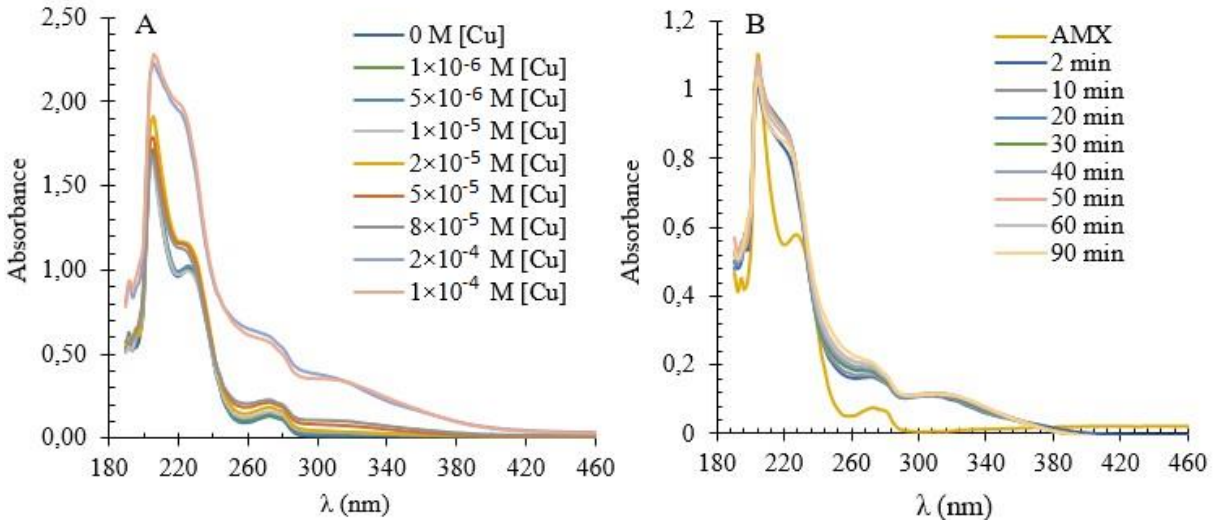

Figure 3: *(A) Effect of concentration of Cu (II) on the UV-visible spectra of 1.0×10^{-4} M AMX in phosphate buffer solution (pH=7) at contact time of 5 min. (B) Absorption spectra of 1.0×10^{-4} M AMX with 1.0×10^{-4} M Cu (II) in phosphate buffer as a function of react.*

IR spectra of AMX and Cu(II)-AMX were recorded in a spectral domain between 4000 and 400 cm^{-1} (Fig. 4). Tablets for IR were prepared by mixing 1 % of the solid complex and 99 % of KBr.

For the free AMX ligand, the band at 3157 cm^{-1}, is due to ν(NH) vibration of the amino group, the other band at 3057 cm^{-1} may be due to the vibration of the imino group. Ligand band at 3485 cm^{-1} was assigned to ν(OH) [26].

The next diagnostic band in the free ligand is this of stretching of phenolic OH, which appears at 3381 cm^{-1}. The band at 1778 cm^{-1} attributed to ν(C=O) of the β-lactam group for AMX, the strong band at 1687 cm^{-1} is characteristic of the C=O group of the amide ν (–CO–NH–). The carboxylic group band of the AMX appears at 1255 cm-1, sharp bands at (1590, 1485 cm-1) are assigned to asymmetric νas(COO-) and symmetric νs(COO-) stretching of carboxylate respectively.

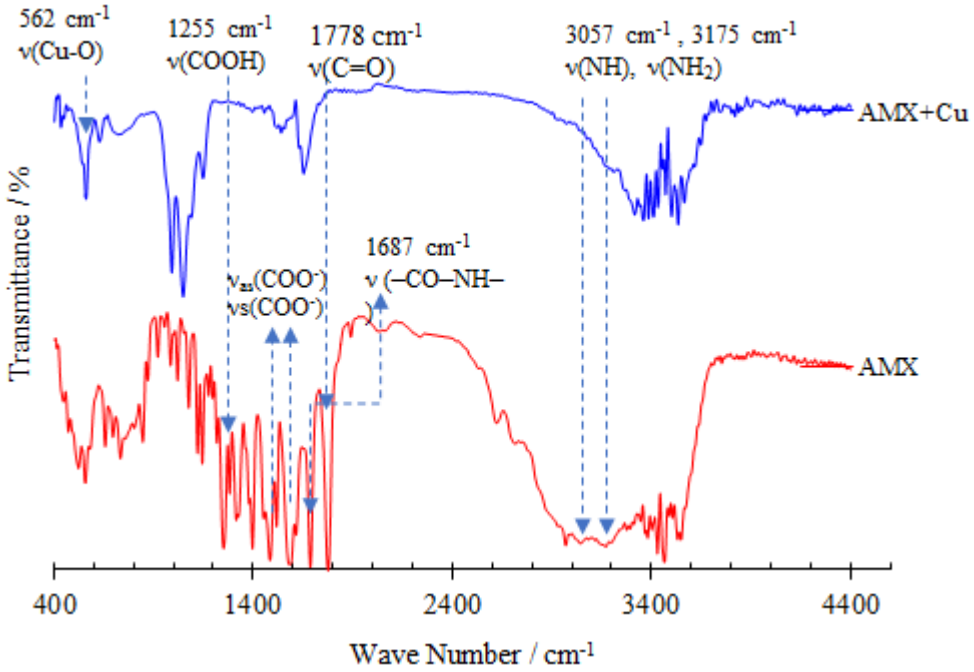

Figure 4: *IR spectra of Amoxicillin and Amoxicillin complex: AMX-Cu.*

IR spectra of the complex AMX-Cu confirmed the absence of the β-lactam ring, indicating the involvement of the C=O of the lactam ring in the chelation process. The carboxylic group band of the AMX disappears also in the spectra of the AMX-Cu complex and this indicates the participation of the carboxylate in the complex formation. The shift of ν(NH) of the amide group (–CO–NH–) toward lower wave numbers, from 1687 cm^{-1} to 1654 cm^{-1} on complexation suggests coordination via the NH of the amide group. The two bands of NH_2 and NH groups are shifted on complexation indicating the involvement of both in complex formation. New band at 562 cm^{-1} can be attributed to ν(Cu–O) of carbonyl [27].

The coordination model for Cu-AMX complex proposed thereby includes two nitrogen donors provided by the primary amine and the amid group and two oxygen donors from the carbonyl group C=O group and the carboxylic group, according to the following reaction mechanism (Scheme 2):

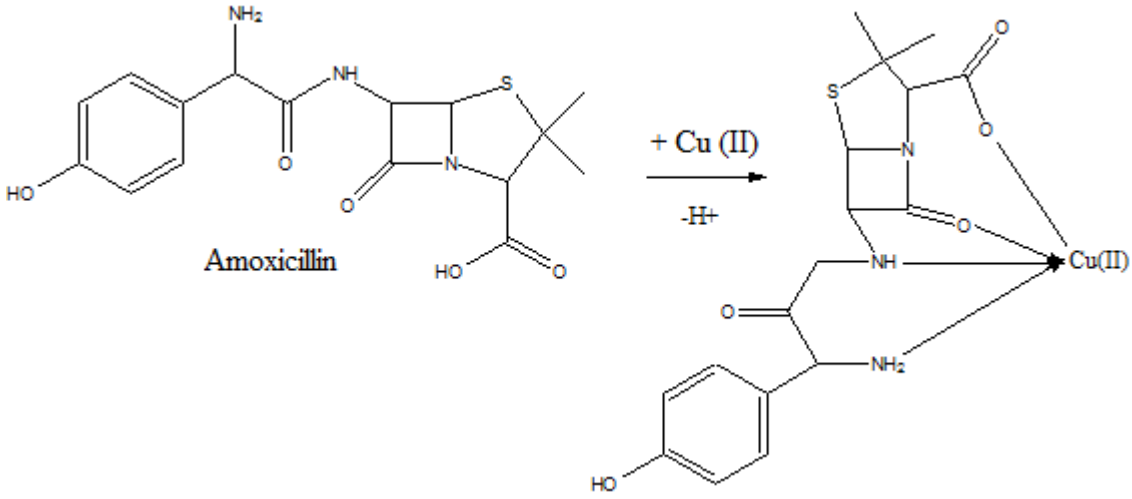

Scheme 2: *The proposed structure of the Cu(II)-amoxicillin complex [28].*

The shift of ν(NH) of the amide group (–CO–NH–) toward lower wave numbers, from 1687 cm^{-1} to 1654 cm^{-1} on complexation suggests coordination via the NH of the amide group. The two bands of NH_2 and NH groups are shifted on complexation indicating the involvement of both in complex formation. New band at 562 cm^{-1} can be attributed to ν(Cu–O) of carbonyl [27]. The coordination model for Cu-AMX complex proposed thereby includes two nitrogen donors provided by the primary amine and the amid group and two oxygen donors from the carbonyl group C=O group and the carboxylic group, according to the following reaction mechanism (Scheme 2).

III.3. Complexation study of Cu(II)/AMX by chronoamperometry

Chronoamperometry, as well as other electrochemical techniques, was employed for the study of electrode processes at the working. The protocol for AMX determination was based on the reaction between AMX and copper (II) ions electrode by setting the working electrode at optimum applied potential. To select an optimal detection potential for amoxicillin, the effect of applied potential on the current response was tested in the range of 200mV to −300mV (Fig. 5). The maximum current response corresponding to the injection of $1x10^{-4}$ M AMX was observed for an applied potential of -150mV. Thus -150 mV was chosen as the applied potential for AMX detection in successive experiments.

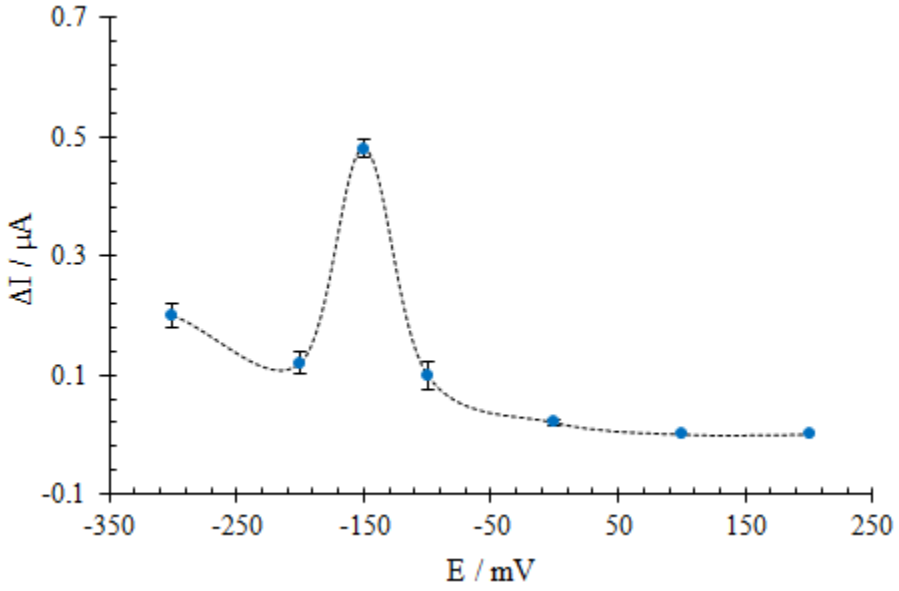

Figure 5: *Influence of the applied potential on the response of 1.0×10^{-3} M AMX obtained in PBS using chronoamperometry measurements.*

The optimization of the reaction time between AMX and copper (II) was afterward studied. Fig. 6A shows that when adding 0.5 mL of 1.0×10^{-4} M AMX to 1.0×10^{-4} M copper (II) ions, a significant increase in signal current was recorded, and the response current reached maximum steady state current within 2 min of AMX injection and remained almost constant throughout the experiment. Thus, 2 min was chosen as the optimum reaction time for AMX detection for subsequent experiments.

To further investigate the behavior of copper (II) in the presence of AMX at CPE, successive additions of 0.5 mL 1.0×10^{-4} M AMX in PBS (pH 7) were established using chronoamperometry (Fig.6 B). For each injection, a sharp increase in the amperometric current is observed, which was related to the decrease in copper (II) ions concentration in the electrochemical cell after their chemical reaction with AMX. In addition, the variation of current intensity (ΔI) is directly related to the concentration of the AMX added. As displayed in the chronoamperogram, a significant increase in signal intensity (ΔI) was reported after each injection of 0.5 mL of 1.0×10^{-4} M AMX.

Chronoamperometry has been employed for the estimation of the diffusion coefficient of AMX in the solution. For an electroactive material with diffusion coefficient D, the corresponding current to the electrochemical reaction (under diffusion control) is described by Cottrell equation (Eq. 2) [28].

$$I = nFAD^{0.5}C_0(\pi t)^{-0.5} \qquad \text{Eq. 2}$$

where I is the measured current, A is the electrochemically active area, D is the diffusion coefficient ($cm^2\ s^{-1}$) and C_0 bulk concentration of AMX (mol cm^{-3}).

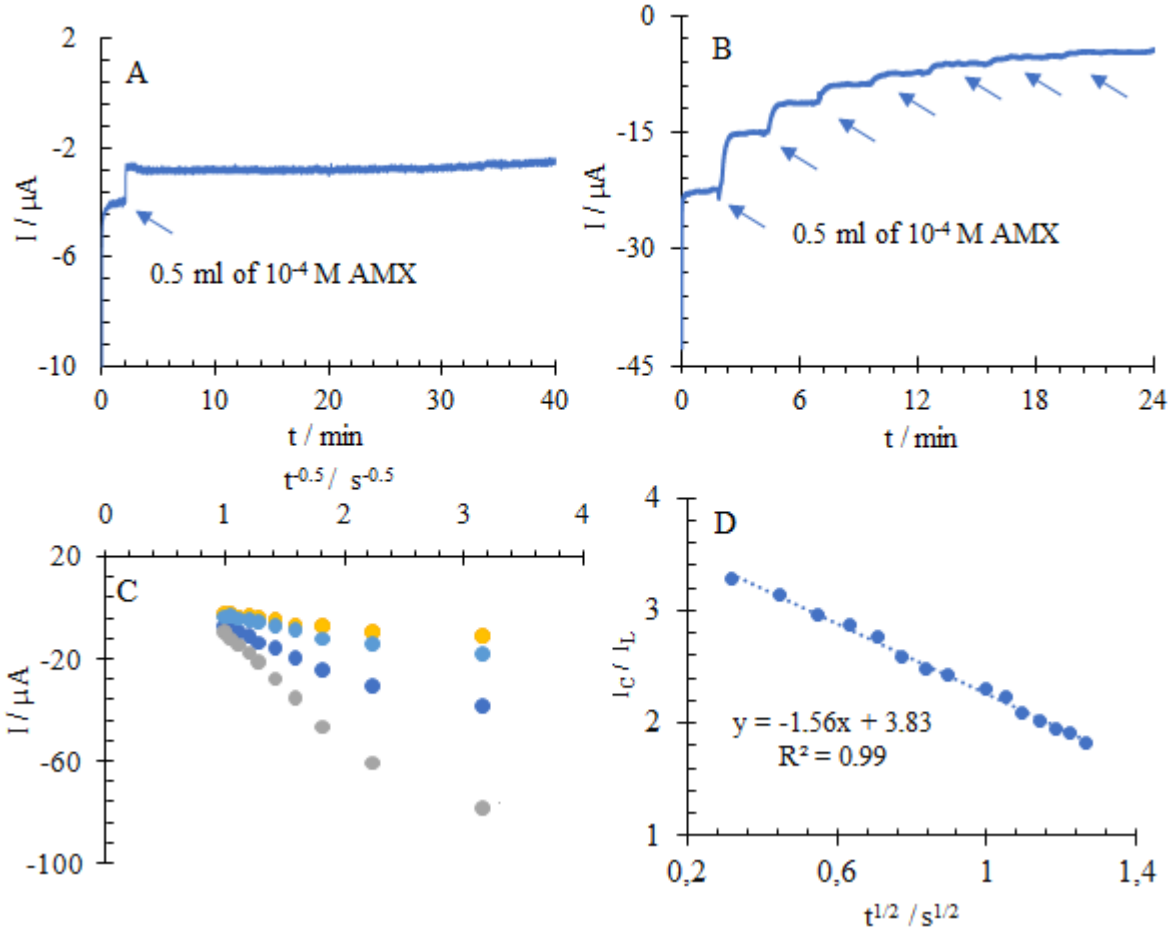

Figure 6: *(A) Chronoamperogram obtained by addition of 0.5 mL of 1.0×10^{-4} M AMX in an electrochemical cell containing 1.0×10^{-4} M Cu(II) for a reaction time of 40 min, (B) chronoamperogram obtained by successive addition of 0.5 mL of 1.0×10^{-4} M AMX in solution containing 1.0×10^{-4} M Cu(II). (C) Variation of current intensity as a function of the inverse of root of reaction time for various concentration of AMX, and ((D) dependence of IC/IL on $t_{1/2}$ derived from chronoamperograms.*

Fig.6C shows the experimenal plots of I vs. $t^{-0.5}$ with the best fits for different concentrations of AMX. From the slopes of the resulting straight lines and using the Cottrell equation (Eq. 2), the mean value of the D was found to be $4.82 \times 10^{-5}\ cm^2\ s^{-1}$.

The reaction constant (k) of Cu-AMX, for the reaction between AMX and Cu(II) was further predicted according to the Galus method (Eq. 3) [29].

$$I_C / I_L = \pi^{1/2} (kC_b t)^{1/2} \qquad \text{Eq. 3}$$

where I_C is the electrical signal of AMX in the presence of copper (II), I_L is the limiting current in the absence of copper (II), C_b is the bulk concentration of AMX, and t is the contact time (s). The reaction constant k was calculated using the above equation. Based on the slope of the I_C/I_L versus $t^{1/2}$ plot (Fig.6D), k can be obtained for a given AMX concentration. The average value of k was found to be 188.9 mol^{-1} cm^2.

III.4. Amperometric detection of Amoxicillin

III.4.1. Calibration curve

Chronoamperometric response of AMX was recorded for various concentrations of copper (II) by adding a series of AMX concentrations under magnetic stirring on the CPE at a constant potential of -150 mV. As summarized in Table 1, a low detection limit (DL) has been obtained for a copper (II) concentration of 1.0×10^{-4} M.

Table 1: *Results obtained from linear regression curves for the determination of AMX for different concentration of Cu (II).*

[Cu (II)] / M	DL(µM)	QL(µM)	R^2	Slope
5.0×10^{-4}	0.153	0. 51	0.985	0.0216
1.0×10^{-4}	0.088	0.29	0.987	0.0328
5.0×10^{-5}	0.12	0.40	0.987	0.0274

A linear correlation between the current response and the AMX concentration was found in the range from 1.46×10^{-5} M to 1.95×10^{-7} M (Fig.7), which can be represented by a regression equation as I(µA) = 0.328 [AMX] (µM) + 0.013 (R^2=0.987). The limit of detection (DL) was calculated through the ensuing formulas $3S_b/m$ [30], where S_b is the standard deviation of the blank signal (obtained based on 8 measurements on the blank solution) and m is the slope of the calibration curve. Therefore, the DL was found to be 8.84×10^{-8} M.

The detection limit was calculated to be 8.84×10^{-8} M. To show advantages of the proposed method on the determination of amoxicillin, these values are comparable with values reported by some previously reported works [12,23,31-35]. The corresponding results are summarized in Table 2. Analytical performance of the proposed method is competitive to the previously reported AMX detection.

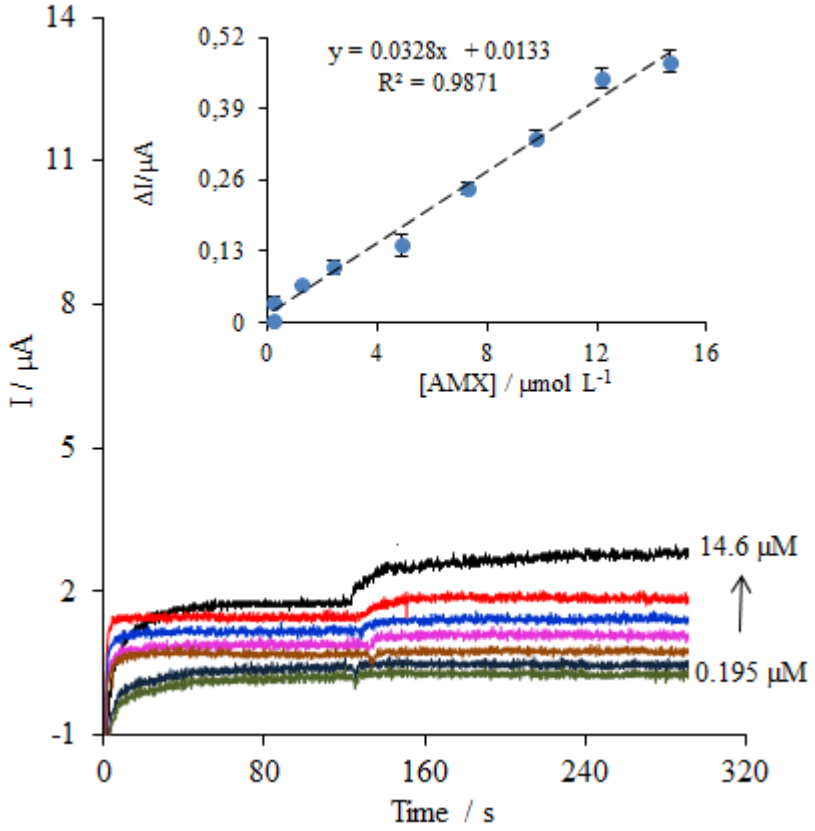

Figure 7: *Chronoamperograms of AMX for different concentrations within the range 1.95 × 10^{-7} M to 1.46 × 10^{-5} M at carbon paste electrode and calibration curve as figured in insert.*

Table 2: *Comparison of the characteristics of the developed method with previously reported works on the determination of amoxicillin.*

Method	Electrode	DL (µM)	LDR (µM)	Ref
Chromatography	_	0.041	0.041-1.36	[31]
LC-MS/MS	_	0.0136	0.0136-54.7	[32]
Spectrophotometry	_		13.6-82	[33]
SWV	Glutaraldehyde/GA/GCE	0.92	2-25	[12]
SWV	Cu(II)-NCL-CPE	0.02	0.04-100	[23]
DPV	B-Diamond	0.25	0.5- 40	[34]
CV	MWCNTs modified GCE	0.2	0.6-8.0 and 10.0-80.0	[35]
Chronoamperometry	CPE	0.088	0.195-14.6	This work

III.4.2. Interference studies

The interference of different metal ions such as Fe(II), Cd(II), Ni(II), Al(III), Co(II), Zn(II) and Pb(II) on the AMX determination was investigated (Fig.8). Under the optimal operational conditions two of the following metallic ions analyzed –Fe(II), Zn(II)– produced an interfering electrochemical signal, and no interference was observed for other metals. The interference observed from Fe(II) ions, may be due to their interaction with the β-lactam ring of the AMX. However, free Fe(II) ions have low stability in aqueous solutions due to their spontaneous oxidation to Fe(III), and Cu(II) reduction occurred simultaneously. The lowest recovery is obtained for the Zn(II) ions taking into account that in the literature, Zn (II) ions are often used to catalyze the amoxicillin degradation reaction [36]. The interferences of the Zn(II) and Fe(II) can be removed by selective precipitation using the azelaic acid [37].

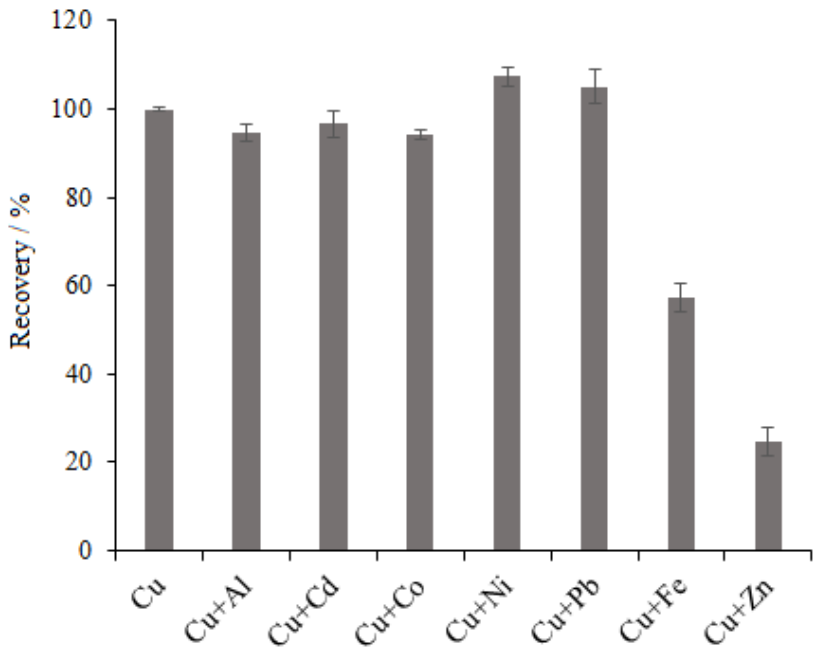

Figure 8: *Influence of coexisting substances on the determination of 1.0×10^{-4} M AMX.*

The influence of various organic compounds on the determination of AMX was also studied. Table 3 shows the effect of paracetamol, salicylic acid, 4-nitrophenol, ascorbic acid and dopamine on the recovery of AMX and Cu(II) reaction. The results showed that all the organic compounds mentioned above dont interfere in the reaction of AMX with copper in all portions.

Table 3: *Interferences effect of organic compounds on the determination of 1.0×10-4 M AMX at carbon paste electrode.*

Interfering	Concentration (1×10^{-5} M)	Recovery (%)	RSD
Paracetamol	5.0	91.64	3.43
	10.0	92.55	4.64
	50.0	94.13	3.85
Salicylic acid	5.0	93.65	4.03
	10.0	96.14	3.38
	50.0	98.86	0.85
4-nitrophenol	5.0	92.51	1.58
	10.0	94.10	2.07
	50.0	97.27	1.14
Ascorbic acid	5.0	92.10	3.75
	10.0	94.78	1.47
	50.0	96.14	2.40
Dopamine	5.0	94.35	2.21
	10.0	95.71	4.05
	50.0	98.19	3.51

III.4.3. Analytical application in real samples

Analytical application in real sample was explored by determining AMX in pharmaceutical samples and blood. The AMX content in the pharmaceutical tablets was measured using the standard addition method. For this purpose, the required amount of powdered formulations was taken and the test solutions were prepared as described in the experimental section.

The chronoamperograms were then recorded with optimized parameters, and the AMX content was determined using a calibration graph. The reported and calculated values of the AMX content in the respective pharmaceutical tablets are compared in Table 4. The results obtained show that the amount calculated is in perfect agreement with the amount claimed.

Table 4: *Recovery results obtained for the determination of AMX in pharmaceutical tablets.*

Name of drugs	AMX found (mg/tablet)	RSD (%)	Recovery (%)
Augmentin	1033.31	2.68	103.3
Aximycine	1061.39	2.59	106.10
Novoclin	1019.32	6.06	101.93
Pneumocid	1006.12	4.25	100.63

For analytical determination of AMX in blood, a spike recovery test was carried out by the addition of different amounts of AMX to blood. The results are summarized in Table 5. All the measurements were repeated for three times under the same conditions. The recovery of the spiked samples varied from 91.83% to 97.16%. These results showed that proposed method was satisfactory applied for analytical determination of amoxicillin in real samples.

Table 5: *Recovery results obtained for the determination of AMX in human blood.*

AMX Added (1×10^{-4} M)	AMX Found (1×10^{-4} M)	Recovery (%)
0	<DL	-
0.1	0.092	91.83±0.63
0.5	0.480	96.13±1.41
1	0.970	97.16±1.98

IV. Conclusion

As a conclusion, a new electrochemical method with very high sensitivity has been developed for the detection of AMX after complexation with copper (II) at carbon paste electrode. The kinetic parameters such as electron transfer coefficient and reaction constant were also determined using various electrochemical approaches. A mechanism for the oxidation of AMX at the electrode has been proposed. Chronoamperometric detection of AMX was obtained in the concentration range from 1.46×10^{-5} M to 1.95×10^{-7} M. The detection limit was found to be 8.84×10^{-8} M. The proposed method was employed for the amperometric determination of AMX in real samples such as drugs and human blood.

References

[1] V. Pandit, S. Suresh, H. Joshi, Gastro retentive drug delivery system of amoxicillin: formulation and in vitro evaluation, Int. J. Pharma.Chem. 1 (2010) 1-10.

[2] World Health Organization, Toxicological evaluation of certain veterinary drug residues in food. Vol. 66. Geneva (2012).

[3] R. Sharma, R. N. Goyal, Estimation of amoxicillin in presence of high concentration of uric acid and other urinary metabolites using an unmodified pyrolytic graphite sensor, J. Electrochem. Soc. 162 (2015) 8-13.

[4] A. Sher, M. Veber, M. Marolt-Gomiscek, Spectroscopic and polarographic investigations: copper(II)-penicillin derivatives, Int. J. Pharm. 148 (1997) 191-199.

[5] A. Garcia-Reiriz, P. C. Damiani, A. C. Olivieri, Different strategies for the direct determination of amoxicillin in human urine by second-order multivariate analysis of kinetic spectrophotometric data, Talanta 71 (2007) 806-815.

[6] A. Ferna´ndez-Gonza´lez, R. Badı´a, M.E. Dı´az-Garcı´a, Comparative study of the micellar enhanced spectrophotometric determination of b-lactamic antibiotics by batch and flow injection analysis using a multisimplex design, J. Pharm. Biomed. Anal. 29 (2002) 669-679.

[7] P. B. Issopoulos, Analytical investigations of β-lactam antibiotics in pharmaceutical preparations—II. Spectrophotometric determination of cephalexin, cephradine, ampicillin and amoxycillin using copper (II) acetate as a completing agent, J. Pharm. Biomed. Anal.6 (1988) 321-327.

[8] Z. F. Zhang, Y. Lu, G. J. Liang, Y. D. Wang, W. Liu, Study on the determination and stability of amoxicillin sodium and clavulanate potassium for injection by HPLC, Chinese J. Pharma. Anal. 16 (1996) 366-369.

[9] L. Sun, L. Jia, X. Xie, K. Xie, J. Wang, J. Liu, L. Cui, G. Zhang, G. Dai, J. Wang, Quantitative analysis of amoxicillin, its major metabolites and ampicillin in eggs by liquid chromatography combined with electrospray ionization tandem mass spectrometry, J. Food. Chem. 192 (2016) 313-318.

[10] F. A. Aly, N. A. Alarfaj, A. A. Alwarthan, Sensitive assay for clavulanic acid and sulbactam in pharmaceuticals and blood serum using a how-injection chemiluminometric method, Anal. Chim. Acta 414 (2000) 15-23.

[11] M. F. Bergamini, M. F. S. Teixeira, E.R. Dockal, N. Bocchi, E.T.G. Cavalheiro, Evaluation of different voltammetric techniques in the determination of amoxicillin using a carbon paste

electrode modified with [N,N-ethylenebis(salicylideneaminato)]oxovanadium(IV), J. Electrochem. Soc. 153 (2006) 94-98.

[12] D. P. Santos, M. F. Bergamini, M. V. B. Zanoni, Approach on the electrochemical reactivity of poly-L-Glutamic acid against doxorubicin and its application in the development of a voltammetric Sensor, Int. J. Electrochem. Sci. 5 (2010) 1399-1410.

[13] N. Kumar, R. Rajendra, N. Goya, Gold-palladium nanoparticles aided electrochemically reduced graphene oxide sensor for the simultaneous estimation of lomefloxacin and amoxicillin, Sens. Actu. B http://dx.doi.org/doi:10.1016/j.snb.2016.12.025.

[14] Yuan, Xiu, A. Ninh Pham, Christopher J. Miller, and T. David Waite. Copper-catalyzed hydroquinone oxidation and associated redox cycling of copper under conditions typical of natural saline waters. J. Environ. Sci. Technol. 47 (2013) 8355-8364.

[15] A. N. Pham, A. L. Rose, T. D. Waite. Kinetics of Cu (II) reduction by natural organic matter. J. Phys.Chem. 116 (2012) 6590-6599.

[16] Davies, B.Richard, E. P. Abraham.Metal cofactor requirement of β-lactamase II. J. Biochem. 143 (1974) 129-135.

[17] A. Kucers, N.McBennett , The Use of Antibiotics, Medical Books, London, 1988.

[18] M. I. Page, The mechanisms of reactions of. beta.-lactam antibiotics. J.Aec. Chem. Res. 17 (1984) 144-150.

[19] P. G. Navarro, P. J. Martínez De Las Parras, A. M.Garcia, Reaction of Sodium Amoxicillin with Cu(ll) Ion in a Methanolic Medium, J. Pharm.Sci. 80 (1991) 904-907.

[20] A. Fernández-González, R. Badía, M. E. Díaz-García, Insights into the reaction of β-lactam antibiotics with copper(II) ions in aqueous and micellar media: Kinetic and spectrometric studies, J. Anal.Biochem. 341 (2005) 113–121.

[21] S. V. Lapshin, V. G. Alekseev, Copper (II) complexation with ampicillin, amoxicillin, and cephalexin. Russ. J. Inorg. Chem 54 (2009) 1066-1069.

[22] R. Sekar, S. K. Kailasa, Y. C. Chen, H. F. Wu, Electrospray ionization tandem mass spectrometric studies to probe the interaction of Cu(II) with amoxicillin, J. Chin. Chem. Lett. 25 (2014) 39–45.

[23] M. Nosuhi, A. Nezamzadeh-Ejhieh, Comprehensive study on the electrocatalytic effect of copper - doped nano-clinoptilolite towards amoxicillin at the modified carbon paste electrode - solution interface. J. Colloid. Interface Sci. 497 (2017) 66-72.

[24] J. A. Harrison, Z. A. Khan, The oxidation of hydrazine on platinum in acid solution, J. Electroanal. Chem. Interfacial. Electrochem. 28 (1970) 131-138.

[25] X. Weng, W. Cai, S. Lin, Z. Chen, Degradation mechanism of amoxicillin using clay supported nanoscale zero-valent iron, J. Appl. Clay Sci. 147 (2017) 137-142.

[26] S. M. Refat, M. A. Hussein Al-Maydama, M. Fathi Al-Azab , R. Ragab Amin , M.S. Yasmin Jamil, Synthesis, thermal and spectroscopic behaviors of metal–drugcomplexes: La(III), Ce(III), Sm(III) and Y(III) amoxicillin trihydrate antibiotic drug complexes, J. Spectrochim. Acta A. Mol. Biomol. Spectrosc. 128 (2014) 427-446.

[27] M. A. Zayed, S. M. Abdallah, Synthesis and structure investigation of the antibiotic amoxicillin complexes of d-block elements, Spectrochim. Acta A 61 (2005) 2231-2238.

[28] E. A. Nadia El-Gamel, Metal chelates of ampicillin versus amoxicillin: synthesis, structural investigation, and biological studies, J. coord. chem. 63 (2010) 534-543.

[29] Z. Galus, Fundumentals of electrochemical analysis, Ellis Horwood, New York, (1976).

[30] J. Uhrovcˇ ı´k, Strategy for determination of LOD and LOQ values – some basic aspects. Talanta 119 (2014) 178–180.

[31] A. Aghazadeh, G. Kazemifard, Simultaneous determination of amoxycillin and clavulanic acid in pharmaceutical dosage forms by LC with amperometric detection, J. Pharm. Biomed. Anal. 25 (2001) 325-329.

[32] S. G. Pingale, M. A. Badgujar, K. V. Mangaonkar, N. E. Mastorakis, Determination of amoxicillin in human plasma by LC-MS/MS and its application to a bioequivalence study, WSEAS Transact. Biol. Biomed. 9 (2012) 1-13.

[33] H. Salem, G. A. Saleh, Selective spectrophotometric determination of phenolic β-lactam antibiotics, J. Pharm. Biomed. Anal. 28 (2002) 1205-1213.

[34] L. Švorc, J. Sochr, M. Rievaj, P. Tomcík, D. Bustin,Voltammetric determination of penicillin V in pharmaceutical formulations and human urine using a boron-doped diamond electrode, Bioelectrochemistry 88 (2012) 36-41.

[35] B. Rezaei, S. Damiri, electrochemistry and adsorptive stripping voltammetric determination of amoxicillin on a multiwalled carbon nanotubes modified glassy carbon electrode, elecrtoanalysis 21 (2009) 1577-1586.

[36] P. Gutiérrez Navarro , I. Hernández Blázquez, B. Quintero Osso, J. Mart´ınez de las Parras, M I. Mart´ınez Puentedura, A. Márquez Garc´ıa, Penicillin degradation catalysed by Zn(II) ions in methanol, Int. J. Biol. Macromol. 33 (2003) 159-166.

[37] F. Zimmermann, E. Meux, N. Oget, J. M. Lecuire, J. L. Mieloszynski, Précipitation sélective de cations métalliquesau moyen d'acide azélaïque issu de l'oxydationde l'acide oléique, J. Phys. IV France 122 (2004) 223-228.

Chapter IV

Electrochemical Investigation of Amoxicillin Interaction With Some Metal Ions Related To Complexation Process

I. Introduction

β-lactam antibiotics are among the most successful drugs used for individual therapy, and they represent around 50-70% of total antibiotic consumption [1]. Among β-lactam antibiotics, amoxicillin has a particular importance, due to its effectiveness against a broad spectrum of bacterial infections and its pharmacological and pharmacokinetic properties, it is also used for the prevention and treatment of respiratory, urinary, gastrointestinal, and bacterial skin infections [2-4].

The interactions between amoxicillin and metal ions have acquired a growing interest due to their potential applications [5-7]. It has been demonstrated that amoxicillin interacts effectively with several metal ions due to the presence of donor sites like the O- and N- containing functional groups in its chemical structure [8-9].

On the other hand, because of their biological importance, several studies have demonstrated metal-antibiotic complex formation in different conditions using thermal and spectroscopic methods. They showed that metals can react with AMX by different binding modes [10-14]. In their work, El-Gamel reported that the majority of solid chelates derived from various metal complexes with ampicillin and amoxicillin have octahedral geometry, while the Cu (II) and UO_2(VI) complexes have a four- and seven-coordination.The synthesis and characterization of all chelates was performed using different analytical methods [11]. Interaction of amoxicillin, ampicillin, and cephalexin with Al(III) in aqueous solution and amoxicillin interaction (AMX–) with divalent metals like Zn(II), Mn(II), Ni(II), Co(II) and Cd(II) in aqueous solution at 20°C of an ionic strength of 0.1 (KNO_3) by pH-metric titration were reported [12,13]. Orabi investigated the acid-base equilibria of amoxicillin in different solvents and water mixtures and pure water with the determination of the formation constant of the complexes formed by reaction of the ligands with Mg(II), Ca(II), Cu(II), Zn(II), Ni(II), Ce(III), Co(II), Pr(III), Eu(III), Gd(III), Ho(III), Er(III), and Yb(III) [14].

The complexation reaction of amoxicillin and metal ions were obtained with the molar ratio of 1:1, 1:2, and 2:1 (AMX:M). Almost all reaction of the amoxicillin complexation with metal ions were studied by spectroscopic methods, while all the electrochemical papers reported in the literature have been focused on the determination of AMX [15-23]; however, they did not investigate the interference of metal ions [15-21]. In the previous chapter, we reported that the electrochemical behavior of AMX is influenced by the presence of certain metal ions. The present chapter was undertaken in order to conduct an in-depth study to elucidate the effect of metal ions such as Cu(II), Zn(II), Fe(III) on the electrochemical behavior of AMX.

On the other hand, the chelation of transition metal ions modifies their redox potential and can inhibit the oxidation of some transition metals such as Cu(I) and Fe (II) [24-27] by the formation of Ligand-Metal complex. The complexation effect on redox potentials [28,29] has incited us for further study of amoxicillin stability concerning its oxidation by metal ions as complexing agents. In this chapter, the electrochemical mechanism of AMX oxidation was investigated using square wave voltammetry. The oxidation protection of OH groups of amoxicillin by metal ions such as Cu(II), Zn(II), Fe(III) was studied by different electrochemical methods.

II. Experimental

II.1. Reagents

All chemicals used in this study were of analytical grade. Amoxicillin trihydrate $C_{16}H_{19}N_3O_5S.3H_2O$ (95%) was purchased from Aldrich, while the metal salts $Fe(Cl)_3$, $CuSO_4$ and $ZnSO_4 \cdot 7H_2O$ were obtained from fluka. The phosphate buffer solution was prepared from dipotassium hydrogen phosphate (K_2HPO_4) and potassium dihydrogen phosphate (KH_2PO_4) (Sigma–Adrich). Distilled water was used in all experiments.

II.2. Apparatus

The electrochemical experiments were carried out using a potentiostat (Voltalab PGZ 100) controlled by Voltamaster 4 data acquisition software with a three-electrode electrochemical cell: a Pt wire was used as a counter electrode, Ag/AgCl electrode as a reference, and the carbon paste electrode (CPE) as the working electrode. The UV-Visible spectra of the ligand and complexes solutions were measured by a recording Shimadzu spectrophotometer, model biochrom, at room temperature. Infrared (IR) spectra were taken in a PerkinElmer Fourier transform (FT)–IR spectrometer (FTIR-2000). All pH measurements were performed using a pH-meter (Radiometer, SensION^{TM}, pH^{31}, and Spain).

II.3. Procedure

II.3.1. Operational conditions of electrochemical measurements

Curves of cyclic voltammetry (CV) and square-wave voltammetry (SWV)were recorded at carbon paste electrode (CPE) in phosphate buffer solution (pH=7) containing 1.0×10^{-4} M amoxicillin in the absence and presence of different concentrations of metal ions (Cu (II), Zn(II), Fe(III)).

II.3.2. UV-Visible spectroscopy analysis

The UV-visible spectral studies of the interaction between metal ions and AMX were carried out at room temperature by ranging wavelengths between 190 and 900 nm. The AMX concentration in all the experiments was kept at 1.0×10^{-4} M. The effect of metal ions concentration on the absorption spectra of AMX was studied in the range from 1.0×10^{-6} to 2.0×10^{-4} M after a reaction time of 5 min. The effect of reaction time was also investigated.

II.3.3. Synthesis of the metal complexes

The solid M–AMX complexes were prepared by adding 10 mL of a 0.01 M metal salt solution to 10 mL of a 0.01 M AMX solution dissolved in a phosphate buffer solution (pH=7). The solution was stirred continuously at room temperature for 2h. The resulted precipitate was filtered through a filter paper, and then it was dried by keeping it at room temperature.

III. Results and discussion

III.1. Electrochemical behavior of Amoxicillin

The AMX is electro-oxidizable by CPE at positive potentials. Several buffer solutions were used for AMX oxidation on unmodified electrode, but no voltammetric signal was observed. The condition under which a good signal can be observed is using phosphate buffer solution (pH=7.0). Cyclic voltammogram obtained for the electrochemical oxidation of amoxicillin (5.0×10^{-4} M) in phosphate buffer solution at pH 7.0, was shown in Fig. 1.

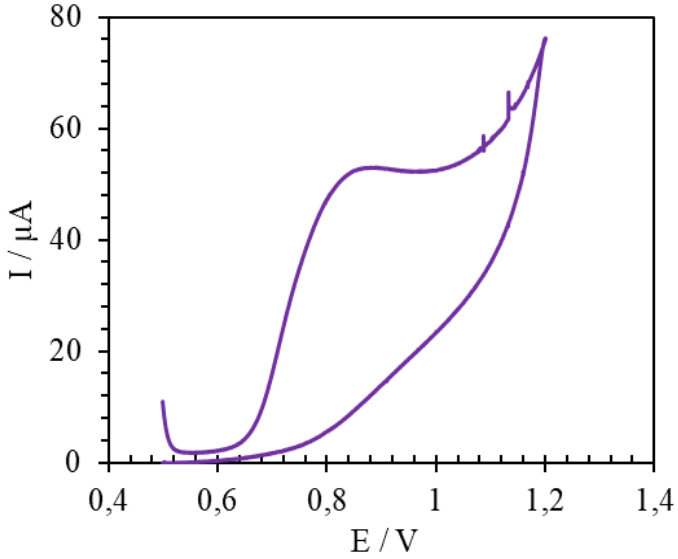

Figure 1: *Cyclic voltammograms of 1.0×10^{-3} M AMX in PBS (pH=7) at CPE.*

Square-wave voltammograms in the presence of selected metal ions were recorded at the CPE in phosphate buffer solution (pH =7) within the potential range from 0.2V to 1.2V (Fig. 2). It

reveals that in the presence of Cu(II) ions, the current intensity of the anodic peak of AMX at 0.7 V decreases, while at the same time, a new peak appears at 0.98V, that can be ascribed to the oxidation of amoxicillin bonded with Cu(II) ions in the coordinative compound (AMX-Cu). In the presence of Zn(II), the SWV shows a significant decrease in the current intensity of the anodic peak of AMX, which could be due to the formation of an electro-inactive compound as a result of the complexation reaction between AMX and Zn(II).

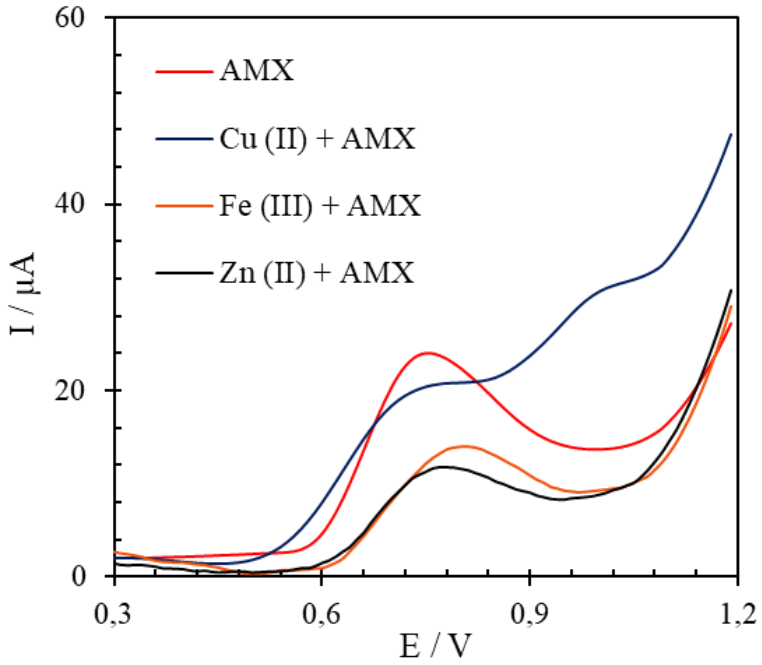

Figure 2: *Square-wave voltammograms of 1.0×10^{-4} M AMX; 1.0×10^{-4} M AMX + 1.0×10^{-4} M Cu(II); 1.0×10^{-4} M AMX +1.0×10-^{4} M Zn(II); 1.0×10^{-4} M AMX + 1.0×10^{-4} M Fe(III).*

Table 1: *Effect of metal ions on the oxidation peak current and potential of AMX in PBS (pH=7).*

Metal ions	Anodic peak potential (V)	Anodic peak current (µA)
—	0.75	24.06
Cu(II)	0.76	20.56
	0.98	30.60
Fe(III)	0.81	14.4
Zn(II)	0.77	11.84

Fig. 2. shows the electrochemical behavior of amoxicillin in the presence of Fe(III). After the addition of Fe(III), the positive shift of the oxidation peak potential was observed, although the current intensity decreased. These changes in oxidation peak for AMX in the presence of Fe(III) suggests an interaction between these two species.

The positive shift in the oxidation potential is due to the complexation reaction between the AMX ligand and the metal ions. The interaction of AMX with all these metal ions leads to a decrease in AMX anodic peak intensity in all cases. The strongest interaction was observed between AMX and Cu(II), which is due to the appearance of a new peak (AMX-Cu) at Ep +0.2 V. The effect of metal ions on the oxidation peak current and potential of AMX are summarized in table 1.

III.2. Amoxicillin binding studies

III.2.1. Electrochemical studies of the interaction of metal chelates with amoxicillin

In order to study the interaction between AMX and the selected metal ions (Cu(II), Zn(II), Fe(III)), change of the electrochemical behavior of AMX were observed upon the addition of metal ions. SWV voltammograms were performed at different concentrations of metal ions. All experimental conditions were kept constant except for the addition of different metal ions concentrations.

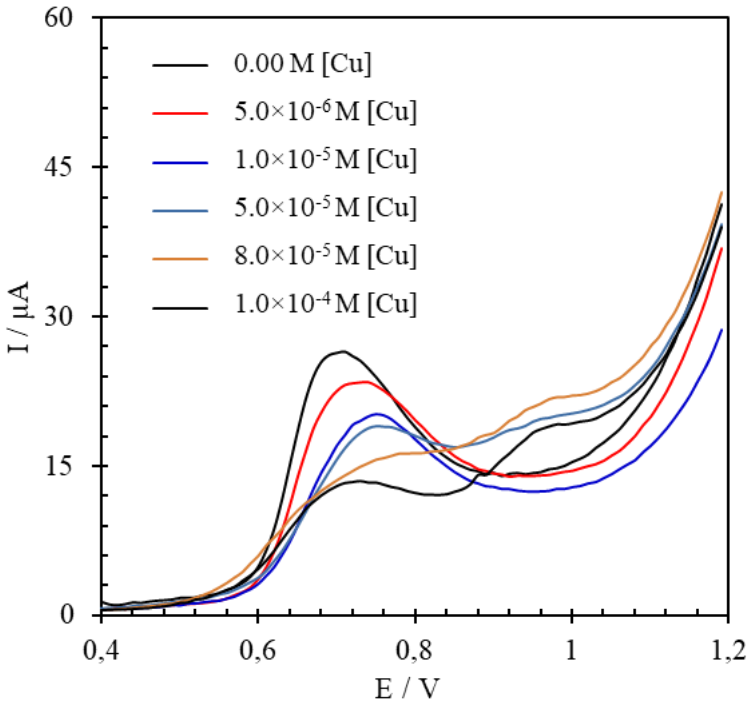

Figure 3: *Effect of concentration of Cu (II) on square-wave voltammograms of 1.0×10-4 M AMX in PBS (pH=7) at contact time of 5 min.*

Fig. 3 shows a series of voltammograms in the absence and presence of varying concentrations of Cu(II) ranging between 5.0×10^{-4} M and 5.0×10^{-6} M, after a reaction time of 5 min. The result revealed that the intensity of the anodic peak of amoxicillin decreased when the concentration of Cu(II) ions increased from 5.0×10^{-6} M to 1.0×10^{-6} M, a second anodic peak was detected at 0.96 V for the Cu (II) concentration between 5.0×10^{-5} M and 1.0×10^{-4} M. These results demonstrated that at higher ligand concentrations the peak at 0.7 V begins to decrease, while a new peak at 0.96 V arises, which is related to the formation of the complex compound with higher ligand content.

The influence of reaction time was also examined in the range 5–90 min, the obtained results did not show any significant changes in the SW voltammogram of 1.0×10^{-4} M AMX in the presence of 1.0×10^{-4} M Cu(II) with time. When Cu(II) was added to the solution containing AMX, the anodic peak at 0.96 V was immediately recorded, which proves that AMX interacts very rapidly with Cu(II). These results will be further verified in UV-visible spectroscopy section.

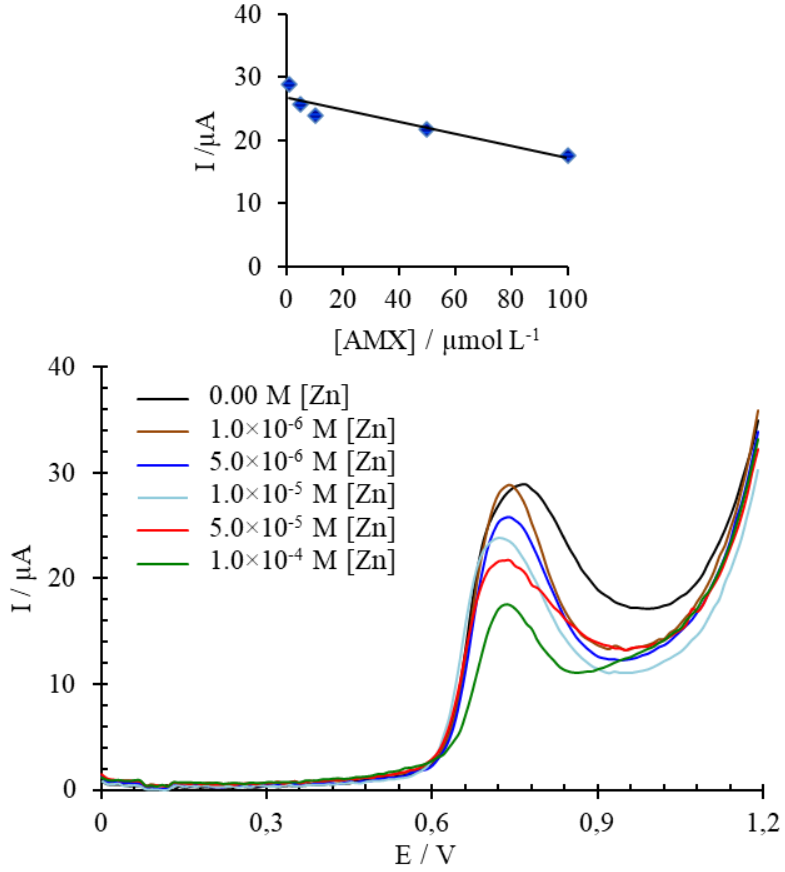

Figure 4: *Effect of concentration of Zn (II) on square-wave voltammograms of 1.0×10^{-4} M AMX in PBS (pH=7) at contact time of 5 min and variation of current intensity as a function of Zn(II) concentration as figured in insert.*

The interaction of amoxicillin with Zn(II) ions was also investigated using square-wave voltammetry. Fig. 4 shows a series of SW voltammograms in the absence and presence of varying concentrations of Zn(II) ions, ranging between 1.0×10^{-6} M and 1.0×10^{-4} M. The obtained voltammograms showed a decrease in the intensity of the oxidation peakof AMX at 0.7 V by increasing Zn(II) concentration. The oxidation peak of AMX is proportional to the added concentration of Zn(II) (Fig. 4 insert), confirming that Zn(II) interacted with AMX quantitatively. This result encourages the possibility of developing a method based on the detection of AMX consumed by Zn(II), in the absence of other interfering metals. The decrease in the intensity with the addition of Zn(II) reflects the binding progress of amoxicillin to Zn(II) ions.

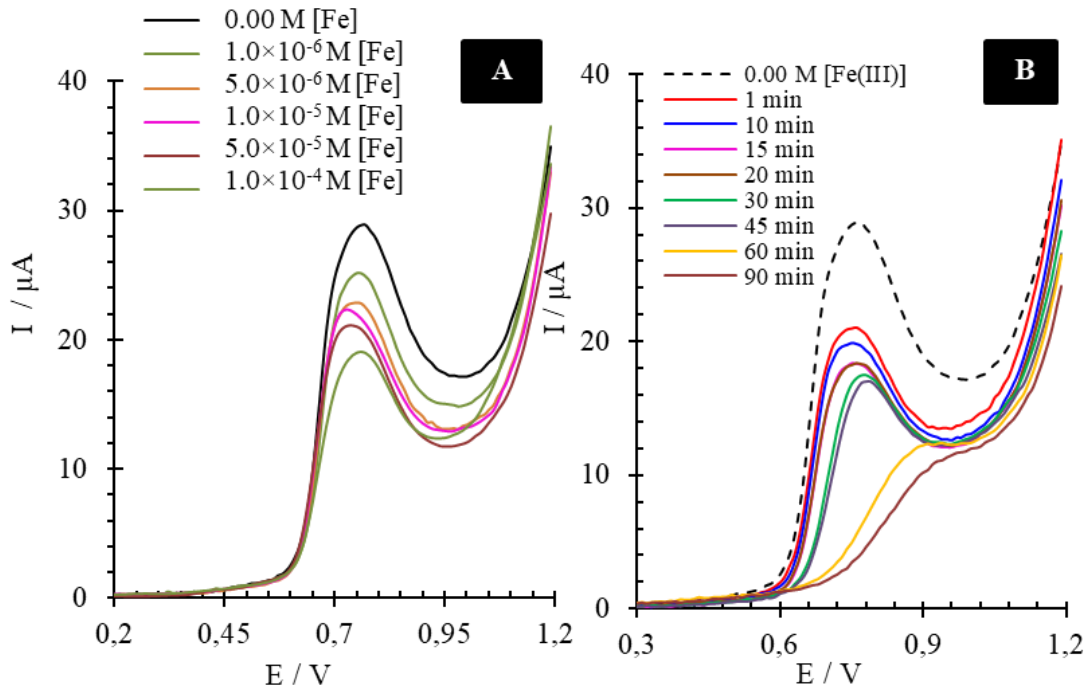

Figure 5: *(A) Effect of concentration of Fe (III) on square-wave voltammograms of 1.0×10^{-4} M AMX in PBS (pH=7) at contact time of 5 min. (B) Square-wave voltammograms of 1.0×10^{-4} M AMX with 1.0×10^{-4} M Fe(III) in PBS as a function of reaction time.*

The influence of reaction time was also studied; the obtained results show that the intensity of the anodic peak of AMX increased insignificantly with time. We suppose that this behavior is caused by an unknown electrochemical process of amoxicillin in the presence of zinc ions.

The square-wave voltammetric behavior of amoxicillin in the presence of varying concentrations of Fe(III) ions is shown in Fig. 5A. The oxidation peak current of amoxicillin at 0.7 V decreased with increasing Fe(III) ions concentration from 1.0×10^{-6} M to 1.0×10^{-4} M. This

observation indicates that some of the amoxicillin molecules interacted with Fe (III) ions, so their concentration in the aqueous solution decreased; as a result, a decrease in the intensity of the anodic peak of amoxicillin has been noticed. This result suggests that a binding event between amoxicillin and Fe(III) ions has occurred.

The influence of reaction time was also investigated in the range [5–90 min]. The results (Fig. 5B) show that the peak current decreased with an increase of the reaction time from 5 to 90 min, which can be attributed to the interaction of amoxicillin with Fe(III). The presence of Fe(III) decreases clearly the anodic current of AMX in the first 5 min of the reaction, then after 20 min of reaction time, a less significant decrease in AMX peak height was observed. The potential of the anodic peak of AMX shifts to more positive values as the time increases from 30 min to 90 min, the most significant shift was observed for 60 and 90 min of reaction time. This displacement in the oxidation potential indicates that AMX oxidation becomes less favorable with increasing reaction time.

The reduction of amoxicillin concentration and the positive shifts in the oxidation potentials are both consistent with the complexation of AMX to the metal ion [32]. In some cases, metal ions have a catalytic effect onto hydrolysis and the degradation of amoxicillin [33-35]. The metal ion−catalyzed degradation likely occurred via complexation of β-lactam antibiotic with carboxyl group and tertiary nitrogen, followed by hydrolytic opening of the β-lactam ring [36].

III.2.2. UV–visible absorption spectra of amoxicillin in the presence of metal ions

UV-Visible absorption spectroscopy is considered the simplest and most commonly used instrumental technique for studying drug interactions with metals. This technique was applied to confirm the electrochemical results. Amoxicillin have an absorption band that can be clearly distinguished in the visible region. An easy way to determine if there is an interaction between the drug and metals. This interaction express by the appearance of new bands or the displacement of the maximum band position to another wavelength between the time the ligand is free in solution and when bonded to metals.

The UV spectrum of AMX shows two major absorption bands in which, one around 230 nm corresponding to the β-lactam band [37] and a relatively low one at 272 nm of aromatic rings, as shown in Fig. 6A. However, in the presence of Cu(II) ions, the obtained spectra indicated a new absorption band near 325 nm, which appears clearly when the molar ratio amoxicillin: Cu(II) was equal to 1:1 or 1:2. This absorption is attributed to the formation of the coordinative compound (AMX-Cu) [38], with a significant increase in the band intensity at 230 nm, strongly

suggesting the formation of a complex. The band around 325 nm was also observed in the complexation of AMX with Fe(III) (Fig. 6B).

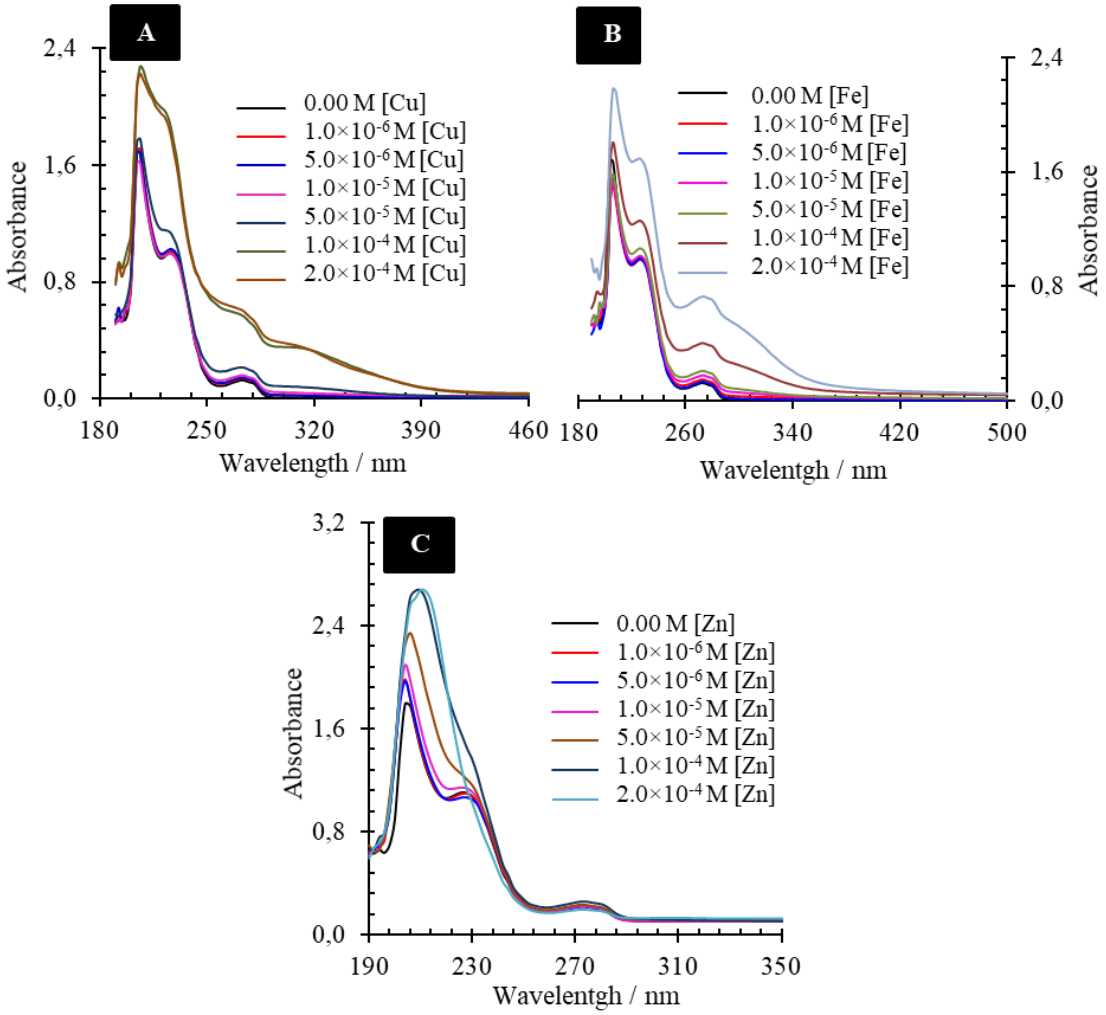

Figure 6: *(A) Effect of concentration of Cu(II), (B) Fe (III), (C) Zn(II) on UV-visible spectra of 1.0×10^{-4} M AMX in PBS (pH=7) at contact time of 5 min.*

These results suggest that the observed UV-visible absorption bond at 325 nm is not from the hydrolysis process but is attributed to the formation of the metal-AMX complex. In contrast, when Zn(II) was allowed to complex with AMX, the new absorbance band at 325 nm was not observed. However, the band intensity at 230 nm increased with the increase in Zn(II) ions concentration as shown in Fig. 6C, which indicates that the coordination of AMX complex engaging the carbonyl oxygen atom at the β-lactam ring of amoxicillin [11,39], confirming the possibility of complex formation between AMX and Zn(II) ions.

Fig. 7 exhibits the time-dependent UV-Visible absorption spectra of 1.0×10^{-4} M AMX in the presence of 1.0×10^{-4} M of metal ions (Cu(II), Zn(II)). As can be seen in Fig. 7A, once Zn(II)

was added to the solution, the absorption band at 230 nm was immediately reshaped, and no major change was observed with the increasing time of the reaction. These results clearly suggest that the AMX can interact very rapidly with Zn(II) species in solution. The new band with the maximum absorbance around 325 nm associated to the complexation of AMX with Cu(II) appears at the beginning of the reaction, but no other changes have been recorded after a longer duration (Fig. 7B). Therefore, it can be concluded that the interaction of amoxicillin with Cu(II) is rapid.

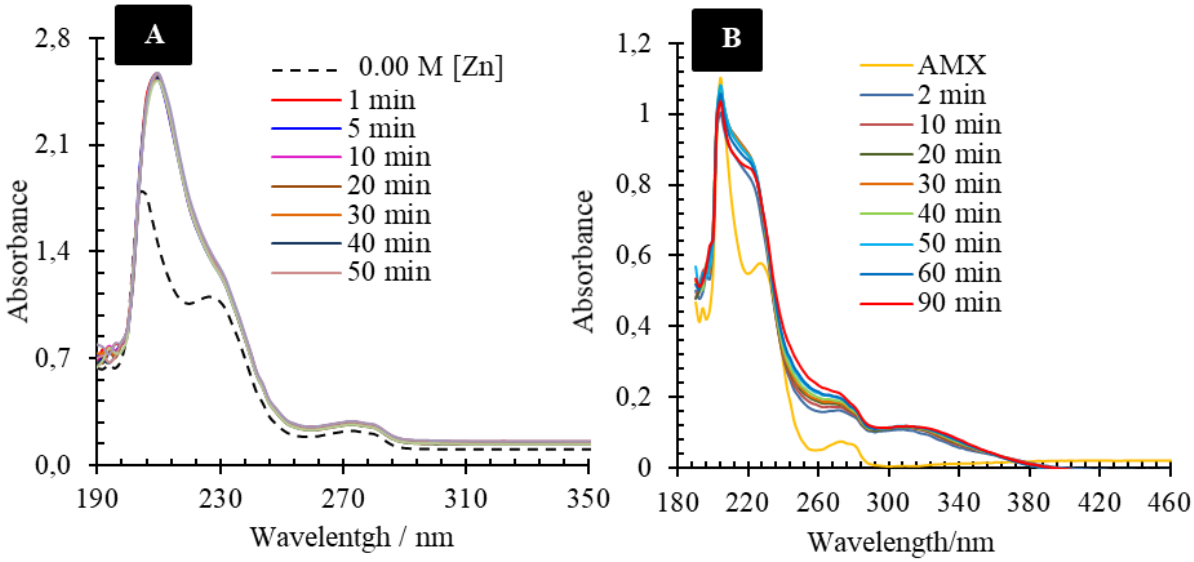

Figure 7: *UV-visible spectra of: (A) 1.0×10^{-4} M AMX+ 1.0×10^{-4} M Cu(II), (B) 1.0×10^{-4} M AMX+ 1.0×10-4 M Zn (II) in phosphate buffer as a function of reaction time.*

III.3. Characterization of AMX/ Metal complex

The electrochemical behavior of the complex between amoxicillin and metal ions was studied. As can be seen from the SW voltammograms of AMX-Cu complex (Fig. 8A), the oxidation potential of amoxicillin (0.7 V) was shifted, becoming more positive (0.9 V), this means that it is much easier to oxidize the ligand (AMX) than the complex (AMX-Cu), so coordination can be a new method of preventing amoxicillin oxidation. The new approach is based on the use of Cu(II) as chelates that stabilize AMX by increasing its oxidation potential, then inhibit its oxidation at 0.7 V.

Several electrochemical studies, designed to probe the ability of various ligands to bind free metals in solution [40-44]. The most of these studies suggested that the shifts in redox peak values in the presence of ligands or chelators in solution confirm the complex formation, which is qualitatively similar to the result observed in the present work [40-42]. The SW

voltammograms of AMX-Zn and AMX-Fe(III) complex were also carried out compared to that of free AMX (Fig. 8A). The results indicated that the anodic peak of metal-bound AMX is less intense than that of the unbound AMX; this confirms the strong interaction of AMX with Zn(II) and Fe (III) ions. The SWV of AMX-Fe(III) shows also a new peak at 0.5 V, which can be attributed to the reduction of Fe(III) to Fe(II), so the chelating effect of Fe(III) against AMX was confirmed.

It has been reported in the literature that amoxicillin submits a hydrolysis procedure involving oxidation in an alkaline medium to obtain an intense yellow product at 395 nm [45]. To exclude the possibility that the electrochemical behavior of amoxicillin is associated to hydrolysis products, the UV-Visible spectra of AMX-Metal complex were collected in Fig. 8B, as reported earlier in UV-visible spectra of free AMX, that showed two absorption bands at 229 nm and 272 nm. In the case of AMX-Metal complex, the new absorption band appears at 347 nm, which is attributed to the formation of the coordinative compound (AMX-Metal) [38,46]. Nonetheless, it is concluded that the observed electrochemical behavior is attributed to the formation of AMX-Metal complex.

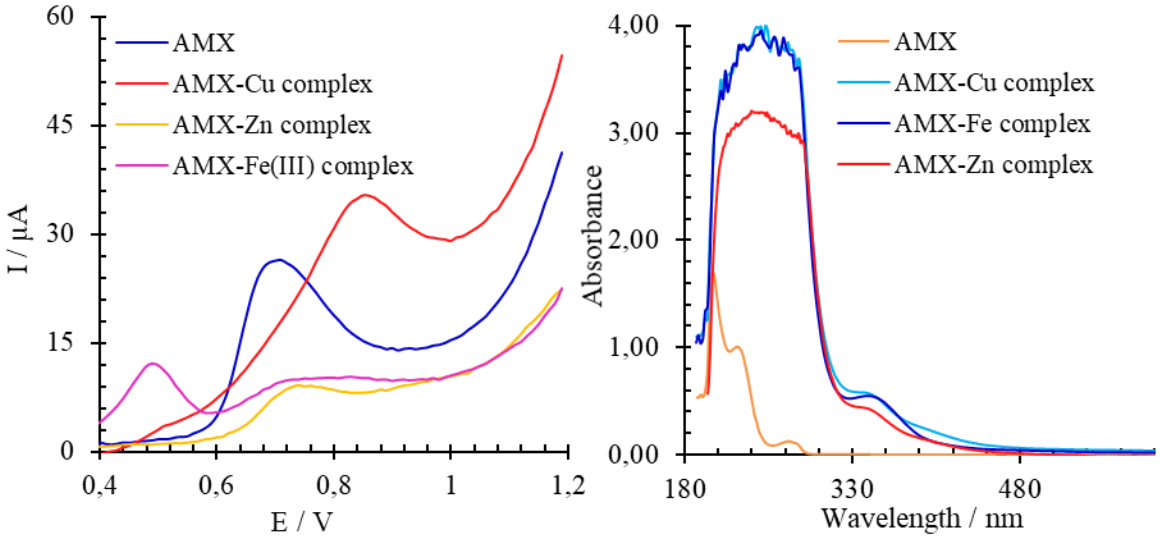

Figure 8: *(A) Square-wave voltammograms of AMX, AMX-Cu complex, AMX-Fe(III) complex, AMX-Zn complex, (B) UV-visible spectra of AMX-Cu complex, AMX-Fe(III) complex, AMX-Zn complex.*

The infrared spectra of AMX ligand and its metal complexes were recorded in the range 400–4000 cm^{-1} (Fig. 9). The band at 3000–3400 cm^{-1}, in the free ligand is due to the presence of the water. Ligand bands at 3157 and 3057 cm^{-1} were assigned to $\nu(NH_2)$ and $\nu(NH)$ respectively. These bands were absent in all complexes, suggesting the involvement of these sites in the

chelation process. The bands at 3485 in the free ligand attributed ν(OH), appears in all complexes almost at the same wavenumber as the ligand [47-49]. The carbonyl group of the β-lactam ring appears as strong band at 1778 cm^{-1}. This band ν(C=O) disappears upon the complexation, indicating the involvement of the C=O of the β-lactam ring in the chelation process [50-51]. The strong band at 1687 cm^{-1} is assigned to the C=O group of the amide. This band ν (–CO–NH–) is negatively shifted (Δν=33-40 cm^{-1}) with some variation in the strength of the intensity (changed from strong band to shoulder one) in all complexes [52].

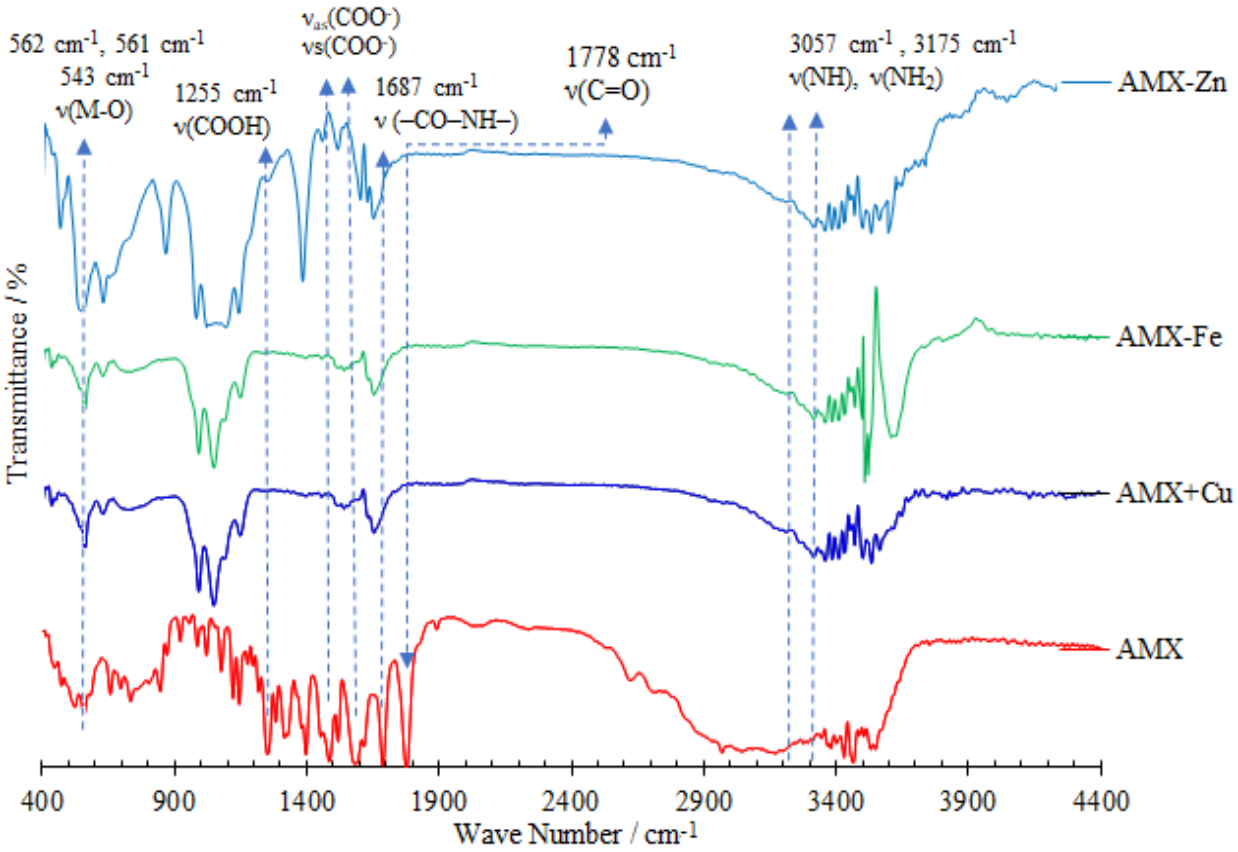

Figure 9: *IR spectra of Amoxicillin and Amoxicillin complexes.*

The carboxylic group band of the Amoxicillin appears at 1255 cm^{-1} but disappears in the spectra of the AMX-metal complexes, which indicates the involvement of carboxylic group in the complexes formation [39]. Sharp bands at 1590 cm^{-1} and 1485 cm^{-1} are assigned to the asymmetric and symmetric stretching of the AMX carboxylate, respectively. The ν_s (COO^-) shifted toward lower wavenumbers, while the ν_{as} (COO^-) shifted towards higher wavenumber indicating the participation of the carboxylate in the coordination [53]. The appearance of new bands at 562 cm^{-1}, 561 cm^{-1} and 543 cm^{-1} can be attributed to ν(M-O) of the carbonyl [10]. As

a result, the coordination of the AMX to the metal ions is proved to be through the amino, imino, carboxylate, and β-lactamic carbonyl groups.

IV. Conclusion

As a conclusion, this study reports on Metal–AMX interactions and their study by square wave voltammetry, IR and UV–Visible. These techniques are used to confirm the complex formation between AMX and transition metals such as Cu(II), Zn(II) and Fe(III). The oxidation potential of AMX was shifted, generally becoming more positive in the presence of Cu(II) and Fe(III), while the current intensity decreased for all metals. Square wave voltammetry experiments revealed the capability of metals to change the electrochemical behavior of AMX. This electrochemical approach confirms the oxidation protection of OH groups of amoxicillin by complexation process. The UV-visible results are in agreement with the electrochemical studies. The acquired findings demonstrated that AMX can form complexes with Cu(II), Zn(II) and Fe(III) ions.

References

[1] K. Kümmerer, Antibiotics in the aquatic environment–a review–part I, Chemosphere. 75 (2009) 417-434.

[2] R. Rao, P.S. Kaur, S. Nanda, Amoxicillin: a broad-spectrum antibiotic. Int. J. Pharm. Pharm. Sci. 3 (2011) 30–37.

[3] J. C. Soussa, Manual de antibióticos antibacterianos. Fernando Pessoa University, Oporto, Portugal. See, (2005) 219–221.

[4] K. Bush, in Antibiotic and Chemotherapy: Anti-Infective Agents and Their Use in Therapy. R.G. Finch, D. Greenwood, S.R. Norrby, R.J. Whitley, Editors, p. 224–278, Churchill Livingstone (2003).

[5] J. Delgado, W.A. Remers, Textbook of Organic Medicinal and Pharmaceutical Chemistry, J. Med. Chem., 42, 2491 (1991).

[6] H. Bello, M. Dominguez, G. Gonzalez, R. Zemelman, S. Mella, H. Young, S.G.B. Amyes. In vitro activities of ampicillin, sulbactam and a combination of ampicillin and sulbactam against isolates of Acinetobacter calcoaceticus–Acinetobacter baumannii complex isolated in Chile between 1990 and 1998. J. Antimicrob. Chemother. 45 (2000) 712-713.

[7] R. S. Satoskazr, S. D. Bhandarkar, S. S. Ainapure, Pharmacology and Pharmacother Apeutics, Indian J. Pharmacol. 29 (1997) 330.

[8] M. Castanheira, H. Sader, S. Desphande, M. Lalitagauri, R. Thomas, R.N. Jones, Antimicrobial activities of tigecycline and other broad-spectrum antimicrobials tested against serine carbapenemase-and metallo-β-lactamase-producing Enterobacteriaceae: report from the SENTRY Antimicrobial Surveillance Program. Antimicrob. Agents Chemother. 52 (2008) 570-573.

[9] S. Subramanian, C.L. Roberts, C. H. Anthony, M. H. Martin, W. S. Edwards, M. J. Rhodes, B. J. Campbell, Replication of colonic Crohn's disease mucosal Escherichia coli isolates within macrophages and their susceptibility to antibiotics. J. Antimicrob. Agents. Chemother. 52 (2008) 427-434.

[10] M. A. Zayed, S. M. Abdallah, Synthesis and structure investigation of the antibiotic amoxicillin complexes of d-block elements, Spectrochim. Acta A. 61 (2005) 2231-2238.

[11] E. A. Nadia El-Gamel, Metal chelates of ampicillin versus amoxicillin: synthesis, structural investigation, and biological studies, J. coord. chem. 63 (2010) 534-543.

[12] V. G. Alekseev, V. G. Zamyslov. Al (III) complexes with the ampicillin, amoxicillin, and cephalexin anions. Russ. J. Coord. Chem .33 (2007) 254-257.

[13] V. G. Alekseev, O. I. Lyamtseva, I. S. Samuilova, Complexation of Manganese(II), Cobalt(II), Nickel(II), Zink(II), and Cadmium(II) Cations with Amoxicillin, Russ. J. Inorg. Chem. 52 (2007) 433-435.

[14] A. S. Orabi, Physicochemical Properties of Ampicillin and Amoxicillin as Biologically Active Ligands with Some Alkali Earth, Transition Metal, and Lanthanide Ions in Aqueous and Mixed Solvents at 20, 30, and 40 ◦C, J. Solution. Chem. 34 (2005) 95-111.

[15] R. Sharma, R. N. Goyal, Estimation of amoxicillin in presence of high concentration of uric acid and other urinary metabolites using an unmodified pyrolytic graphite sensor, J. Electrochem. Soc. 162 (2015) 8-13.

[16] A. S. Kumar, S. Sornambikai, L. Deepik, J. Zen, Highly selective immobilization of amoxicillin antibiotic on carbon nanotube modified electrodes and its antibacterial activity, J. Mater. Chem. 20 (2010) 10152–10158.

[17] M. Nosuhi, A. Nezamzadeh-Ejhieh, Comprehensive study on the electrocatalytic effect of copper-doped nano-clinoptilolite towards amoxicillin at the modified carbon paste electrode - solution interface. J. Colloid. Interface Sci. 497 (2017) 66-72.

[18] D. P. Santos, M. F. Bergamini, M. V. B. Zanoni, Approach on the electrochemical reactivity of poly-L-Glutamic acid against doxorubicin and its application in the development of a voltammetric Sensor, Int. J. Electrochem. Sci. 5 (2010) 1399-1410.

[19] K. Chullasat, P. Nurerk, P. Kanatharana, F. Davis, O. Bunkoed, A facile optosensing protocol based on molecularly imprinted polymer coated on CdTe quantum dots for highly sensitive and selective amoxicillin detection, J. Sensor. Actuat. B-Chem, 254 (2018) 255-263.

[20] N. Kumar, R. Rajendra, N. Goya, Gold-palladium nanoparticles aided electrochemically reduced graphene oxide sensor for the simultaneous estimation of lomefloxacin and amoxicillin, J. Sensor. Actuat. B-Chem, http://dx.doi.org/doi:10.1016/j.snb.2016.12.025.

[21] Z. Frontistis , M. Antonopoulou , D. Venieri , I. Konstantinou , D. Mantzavinos, Boron-doped diamond oxidation of amoxicillin pharmaceutical formulation: Statistical evaluation of operating parameters, reaction pathways and antibacterial activity, J. Environ. Manage. 195 (2017) 100-109

[22] P. K. Brahman, R. A. Dar, K. S. Pitre, Conducting polymer film based electrochemical sensor for the determination of amoxicillin in micellar media, J. Sensor. Actuat. B-Chem. 176 (2013) 307– 314

[23] A. Hrioua, A. Farahi, S. Lahrich, M. Bakasse, S. Saqrane, M. A. El Mhammedi, Chronoamperometric Detection of Amoxicillin at Graphite Electrode using Chelate Effect of

Copper(II) Ions : Application in Human Blood and Pharmaceutical Tablets, J. Chem. Select. 4 (2019) 8350 –8357

[24] R. J. Mailloux, X. Jin, W. G. Willmore, Redox regulation of mitochondrial function with emphasis on cysteine oxidation reactions. J. Redox biology. 2 (2014) 123-139.

[25] Zhu, Ben-Zhan, W. E. Antholine, B. Frei, Thiourea protects against copper-induced oxidative damage by formation of a redox-inactive thiourea-copper complex. J. Free Radical Biology and Medicine. 32 (2002) 1333-1338.

[26] R. L. Levine, L. Rodney, J. A. Williams, E. P. Stadtman, E. Shacter, Carbonyl assays for determination of oxidatively modified proteins, J. In Methods in enzymology. 233 (1994) 346-357.

[27] K. A. Mies, J. I. Wirgau, A. L. Crumbliss, Ternary complex formation facilitates a redox mechanism for iron release from a siderophore, J. Biometals. 19 (2006) 115-126.

[28] N. M. Marshall, D. K. Garner, T. D. Wilson, Y. G. Gao, H. Robinson, M. J. Nilges, Y. Lu, rationally tuning the reduction potential of a single cupredoxin beyond the natural range. J. Nature. 462 (2009) 113.

[29] J. A. Zuris, D. A. Halim, A. R. Conlan, E. C. Abresch, R. Nechushtai, M. L. Paddock, P. A. Jennings, Engineering the redox potential over a wide range within a new class of FeS proteins. J. Am Chem Soc. 132 (2010) 13120-13122.

[30] C. Brett, A. M. O. Brett, Electroanalysis, Oxford Chemistry Primers, 1998.

[31] C. Brett, A. M. O. Brett, Electrochemistry: Principles, Methods and Applications, Oxford Science Publications, 544 (1993).

[32] M. A. Rizvi, Complexation Modulated Redox Behavior of Transition Metal Systems (Review), Russ. J. Gen. Chem. 85 (2015) 959–973.

[33] J. Chen, P. Sun, X. Zhou, Y. Zhang, C. Huang, Cu(II)-catalyzed transformation of benzylpenicillin revisited: The overlooked oxidation. Environ. Sci. Technol. 49 (2015) 4218−4225.

[34] P. G. Navarro, I. H. Blázquez, B. Q. Osso, P. J. M. de las Parras, M. I. M. Puentedura, A. A. M. García, Penicillin degradation catalysed by Zn(II) ions in methanol. Int. J. Biol. Macromol. 33 (2003) 159−166.

[35] J. Chen, Y. Wang, Y. Qian, T. Huang, Fe(III)-promoted transformation of β-lactam antibiotics: Hydrolysis vs oxidation, J. Hazard. Mater. 335 (2017) 117−124.

[36] W. A. Cressman, E. T. Sugita, J. T. Doluisio, P. J. Niebergall, Cupric ion-catalyzed hydrolysis of penicillins: Mechanism and site of complexation. J. Pharm. Sci. 58 (1969) 1471−1476.

[37] X. Weng, W. Cai, S. Lin, Z. Chen, Degradation mechanism of amoxicillin using clay supported nanoscale zero-valent iron, J. Appl. Clay Sci. 147 (2017) 137-142.
[38] A. Ferna´ndez-Gonza´lez, R. Badı´a, M. E. Dı´az-Garcı´a, Insights into the reaction of b-lactam antibiotics with copper(II) ions in aqueous and micellar media: Kinetic and spectrometric studies, J. Anal. Biochem. 341 (2005) 113–121.
[39] M. Imran, J. Iqbal, T. Mehmood, S. Latif, Synthesis, characterization and in vitro screening of amoxicillin and its complexes with Ag (I), Cu (II), Co (II), Zn (II) and Ni (II), J. Biol. Sci. 6 (2006) 946 -949.
[40] A. El-Jammal, D.M. Templeton, Electrochemical Oxidation of some Therapeutic 3-hydroxypyridin-4-one Iron Chelators, J. Electrochim. Acta. 38 (1993) 2223–2230.
[41] A. El-Jammal, D.M. Templeton, Iron-hydroxypyridone redox chemistry: kinetic and thermodynamic limitations to Fenton activity, J. Inorg. Chim. Acta. 245 (1996) 199– 207.
[42] N. Raman, K. Pothiraj, T.Baskaran, DNA interaction, antimicrobial, electrochemical and spectroscopic studies of metal (II) complexes with tridentate heterocyclic Schiff base derived from 2′-methylacetoacetanilide. J. Mol. Struct. 1000 (2011), 135-144.
[43] M. Zatloukalová, V. Křen, R. Gažák, M. Kubala, P. Trouillas, J. Ulrichová, J. Vacek, Electrochemical investigation of flavonolignans and study of their interactions with DNA in the presence of Cu (II). J. Bioelectrochemistry, 82 (2011) 117-124.
[44] S. Mahadevan, M. Palaniandavar, Chiral discrimination in the binding of tris (phenanthroline) ruthenium (II) to calf thymus DNA: an electrochemical study. J. Bioconjugate. Chem. 7 (1996) 138-143.
[45] G. A. Saleh, Two selective spectrophotometric methods for the determination of amoxicillin and cefadroxil, Analyst. 121 (1996) 641.
[46] T. H. O. Norte1, R. B. P. Marcelino, R. P. L. Moreira, I. Binatti, M. C. V. M. Starling, C. C. Amorim, E. S. Pereira, W. R. Rocha, and R. M. Lago, ESI-MS, UV-Vis, and Theoretical Investigation of Fe3-Amoxicillin Complexation during Coagulation, J. Environ. Eng. 3 (2018) 04018001.
[47] G. G. Mohamed, N. E. A. El-Gamel, F. A. Nour El-Dien, Preparation, chemical characterization, and electronic spectra of 6-(2-pyridylazo)-3-acetamidophenol and its metal complexes, Synth. React. Inorg. Met. Org. Chem. 31 (2001) 347-358.
[48] S. M. Refat, M. A. Hussein Al-Maydama, M. Fathi Al-Azab, R. Ragab Amin, M. S. Yasmin Jamil, Synthesis, thermal and spectroscopic behaviors of metal–drug complexes: La (III), Ce (III), Sm (III) and Y (III) amoxicillin trihydrate antibiotic drug complexes, J. Spectrochim. Acta A. Mol. Biomol. Spectrosc. 128 (2014) 427-446.

[49] A. S. Orabi, Monatsh. Physical properties of some new uranyl complexes with ligands derived from acetone, Chem. 129 (1998) 1139-1149.
[50] N. Kanooco, R.V. Singh, J.P. Tandon, Synthesis and Structural Studies of Cxovanadium (V) Complexes of Semicarbazones, Syn. React. Inorg. Met. Org. Chem. 17 (1987) 837-847.
[51] A. L. Ram, M.N. Singh, S. Das, Complexes of Uranyl Nitrate, Uranyl Acetate, Uranyl Thiocyanate and Uranyl Chloride with Benzoyl, Salicyloyl and Isonicotinoyl Hydrazines, Synth. React. Inorg. Met.-Org.Chem. 16 (1986) 513-325.
[52] A. Bravo, J. R. Anacona. Synthesis and characterization of metal complexes with ampicillin, J. Coord. Chem. 44 (1998) 173-182.
[53] R. D. Stefano, M. Scopelliti, C. Pellerito, T. Fiore, R. Vitturi, M. S. Colomba, P. Gianguzza, G.C. Stocco, M. Consiglio, L. Pellerito, Organometallic complexes with biological molecules: XVII. Triorganotin (IV) complexes with amoxicillin and ampicillin, J. Inorg. Biochem., 89 (2002) 279-292.

Chapter V

Complexation of Amoxicillin by Transition Metals: Physico-Chemical And Antibacterial Activity Evaluation

I. Introduction

Antibiotic-resistant (AR) bacteria and the deadly infections they can cause, are a subject of public health threat [1-2]. Indeed, a 2020 report from the World Health Organization (WHO) global antimicrobial surveillance system highlighted antibiotic resistance as "a major public health problem" [3]. Therefore, there is an urgent need for the advancement of novel strategies to improve the antibacterial therapy. Among them, one strategy aims at the development of novel drugs by chelating existing drugs to enhance their antibacterial activity [4-6]. In addition, the most advanced avenue today is to inhibit the action of beta-lactamases, produced by certain bacteria. These enzymes make them resistant to antibiotics which belong to the beta-lactam family.

Metallic particles have attracted much attention because of their effectiveness in biological applications due to their high surface-area-to-volume ratio [7-8], possessing multiple mechanisms for bactericidal effect, such as binding with bacteria DNA, blocking energy recycling, and releasing Ag^{+} ion [9-11]. In addition, transition metals in traces such as copper, iron and zinc possess a wide variety of coordination properties and reactivity, which can be used to form complex with organic drugs as ligands [12-13]. The ability to form different complex compounds which may be redox active or not, is the reason for the important role of the transition metal cations in sophisticated cellular biochemistry [14-15]. The coordination of these metals with antibiotics prevents the microbe's proliferation, enabling novel mechanisms of action by enhancing the antimicrobial property of the antibiotic [16-17]. Therefore, some metal−antibiotic complexes are more potent as compared to free antibiotic [18-19]. Comparative studies show that they have better antibacterial activity against *E. Coli*, *E. Aureus*, *E. Feacalis* than the parent antibiotics. Metallo-antibiotics can also interact with various types of biomolecules, such as proteins, receptors, lipids, DNA and RNA, and this makes them very bioactive [20-21].

Amoxicillin (AMX) is a bacteriolytic β-lactam antibiotic drug, and, like other penicillins, its bio-functional activity is related to β-lactam ring that inhibits the carboxypeptidase and transpeptidase enzymes that are required for peptidoglycan biosynthesis [22]. It is complexing agents for several metal ions due to the presence of range electron donor atoms in its chemical structure [23-24]. Reports indicate that the coordination of AMX to metal ions appears to be important for enhancing antibacterial activity of this drug [25-27]. AMX−metal complexes can also release valuable trace elements needed to maintain life when administered in the form of drugs [28]. The present chapter was undertaken in order to study in detail the antibacterial

activity of new families of complexes AMX−M (M= Cu, Fe and Zn) against *Escherichia. coli*, by using agar disc diffusion method as well as the synthesis and characterization methods we used.

II. Experimental

II.1. Chemicals, materials, and apparatus

All chemicals used in this study were of analytical grade. Amoxicillin trihydrate $C_{16}H_{19}N_3O_5S.3H_2O$ (95%) was purchased from Aldrich, while the metal salts $Fe(Cl)_3$, $CuSO_4$ and $ZnSO_4 \cdot 7H_2O$ used for the complexation were obtained from fluka. The phosphate buffer solution (0.1 mol L^{-1}, pH=7) was prepared from dipotassium hydrogen phosphate (K_2HPO_4) and potassium dihydrogen phosphate (KH_2PO_4) (Sigma–Adrich). The graphite powder was purchased from Carbone Lorraine (Lorraine, France; ref 9900). Distilled water was used in all experiments.

The electrochemical measurements (square wave voltammetry) were carried out using a Voltalab PGZ 100 potentiostat controlled by Voltamaster 4 data acquisition software with a standard cell consisting of a Pt wire as a counter electrode, an Ag/AgCl electrode as a reference and carbon paste electrode (CPE) as working electrode. The UV-Visible spectra of AMX and AMX-M complexes solutions were taken with a Shimadzu spectrophotometer, model biochrom. Infrared (IR) spectra were recorded on a PerkinElmer Fourier transform (FT)–IR spectrometer (FTIR-2000). The pH-meter (Radiometer, SensION^{TM}, pH^{31}, and Spain) was used for all pH measurements.

II.2. Analytical procedure

II.2.1. Synthesis of the metal complexes

Metal complexes were from 1:1 stoichiometric ratios of the ligand (0.01 mol L^{-1}) to metal ions (0.01 mol L^{-1}). The drug was dissolved in phosphate buffer solution (0.1 mol L^{-1}, pH=7) while the metal salts were dissolved in minimum distilled water. The resulting mixture was stirred for 2 h and left to cool for precipitation. The solid complexes were filtered, washed with deionized water, and dried in a vacuum desiccator over anhydrous calcium chloride.

II.2.2. Voltammetric measurement

Square-wave voltammetry (SWV) was recorded at carbon paste electrode (CPE) in phosphate buffer solution (pH=7.0) containing the ligand (AMX) and its metal complexes.

II.2.3. Antibacterial activity evaluation

The antibacterial activity of the three-synthesized AMX−M complexes was evaluated on the bacterial strain of *E. coli* which was isolated from two Moroccan patients that were found to be resistant to AMX. The bacterial strain was isolated and purified, following several subcultures, then cultured in petri dishes containing agar at 37 ° C for 24 hours. One or more colonies of the pure culture were picked and transferred to physiological water. A sample from the inoculum is used to inoculate new petri dishes containing Mueller Hinton medium. Using the swab technique, we spread 100 µL fractions of an *E. coli* suspension (approximately 10^8 bacteria / ml) on the surface of the nutrient agar. Sterile Wittman paper discs, 6 mm in diameter, were loaded with 25 µg mL^{-1} of the AMX−Zn, AMX-Fe and AMX−Cu complexes. The discs are then placed on the surface of the agar. A control disc with AMX alone of the same concentration was also put in the box. Petri dishes are incubated at 37 ° C for 24 hours. The results are expressed as diameters of the zone of inhibition produced around the discs. Three replicates were made for each biological testing and the results are expressed as the mean ± SD (standard deviation).

For time-kill assays, a 0.5 McFarland culture was prepared in the Mueller Hinton broth (MHB). The bacteria were diluted to a final concentration of 10^7 CFU/mL. Then AMX and their metal complexes were added at concentrations of 75 µg mL^{-1} for both isolates. The tubes were then incubated at 35 °C and 100 µl samples were taken at 0, 2, 4, 6, 8 and 24 h. The aliquots were then plated onto agar plates to assess viable bacteria by CFU (Colony-forming unit) counting. After 24 h of incubation at 35 °C, plates were examined for growth [29]. tubes containing only the MHB culture and the MHB culture with AMX were inoculated and served as controls.

For biofilm formation assay and estimation of bacterial cell density cultures were incubated overnight at 37 °C without shaking. The amount of biofilm was measured by crystal violet staining. The viability of the biofilm-associated bacteria was assessed on microscope cover glasses immersed in medium and cultured as described above [30]. Microcolonies formed on the glass surface were imaged on a microscope.

The microbiological part of this work was carried out at the CHERFAOUI Medical Analysis Laboratory, Khouribga, Morocco

III. Results and Discussions

III.1. Synthesis and characterization of the metal complexes

The UV-visible spectra of 1.0×10^{-4} mol L^{-1} of AMX in phosphate buffer solution (pH=7) shows an electronic absorption band in the UV region with a maximum absorption at 229 and

272 nm (Fig. 1). This maximum was observed due to presence of the chromophoric groups: sulfide, carboxyl, and β-lactam amide. The λ_{max} at 229 nm and 272 nm are related to the amide n-π* transition in the β-lactam chromophore and π-π* aromatic ring excitation, respectively [31-32]. For AMX complexations with Cu(II) and Fe(III) ions metal ions**,** the UV–Visible spectra showed the appearance of a new absorption band at 325 nm (Fig. 1A,B) when the molar ratio of AMX:M was 1:1 or 1:2, indicating the formation of the coordination compound (AMX-M). In contrast, in the presence of Zn(II) ions, the UV–Visible spectra (Fig. 1C) did not exhibit such an absorption band, while the band characteristic of β-lactam group of AMX reshaped with a very slight red shift and disappears when the molar ratio of AMX:Zn was 1:2. The energy levelsn, π, π* are disturbed upon complexation and thus the absorption maxima have been red shifted. [33-35], while the disappearance of the absorption band at the molar ratio 1:2 can be explained by the hydrolytic cleavage of the β-lactam ring after the complexation process with Zn(II) [31,36].

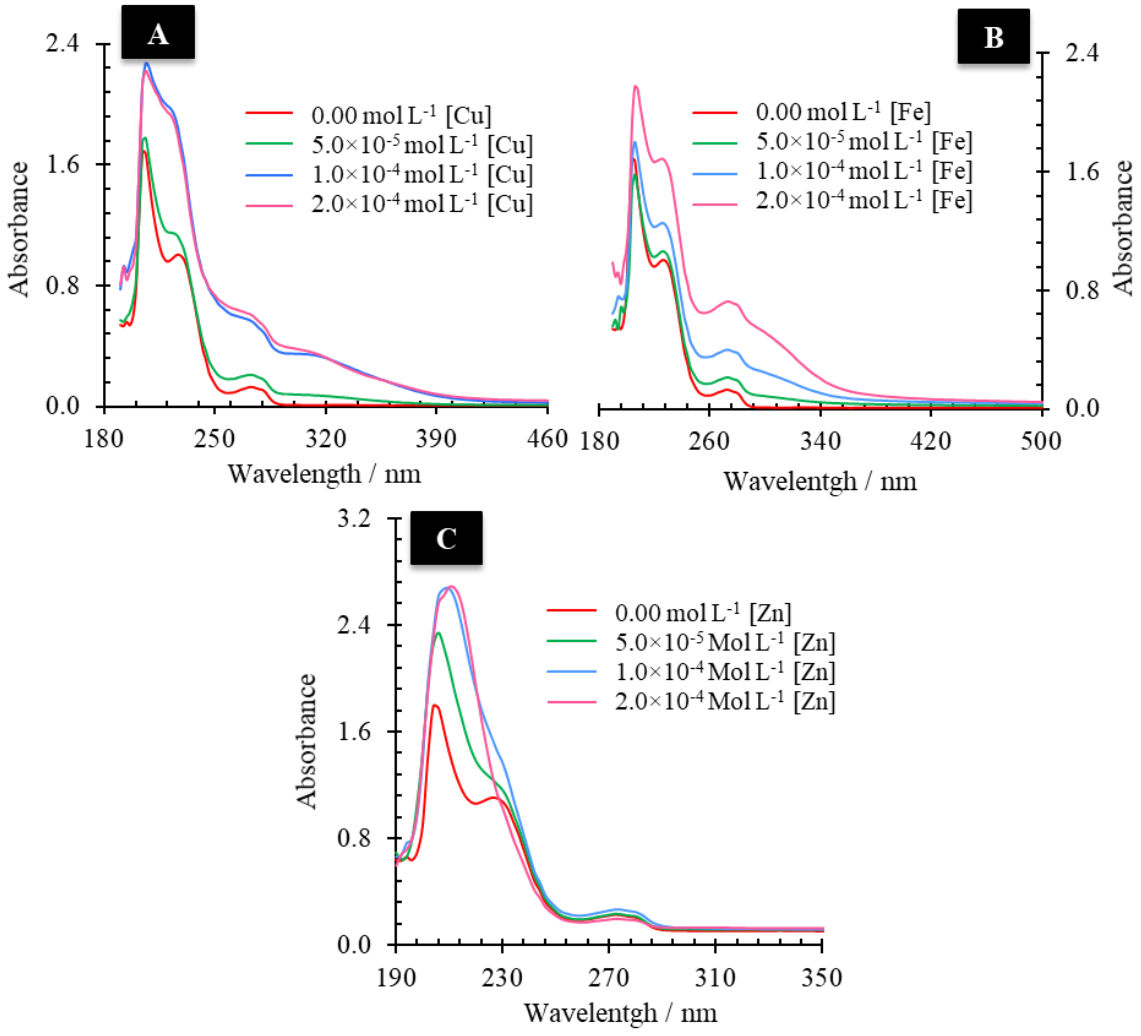

Figure 1: *(A) Effect of concentration of Cu(II), (B) Fe (III), (C) Zn(II) on UV-visible spectra of 1.0×10-4 M AMX in PBS (pH=7) at contact time of 5 min.*

The metal complex stoichiometry can be calculated using the continuous variation method [37-38]. Job plots show an intersection point corresponding to a 1:1 metal: AMX molar ratio (Fig. 2A.B.C).

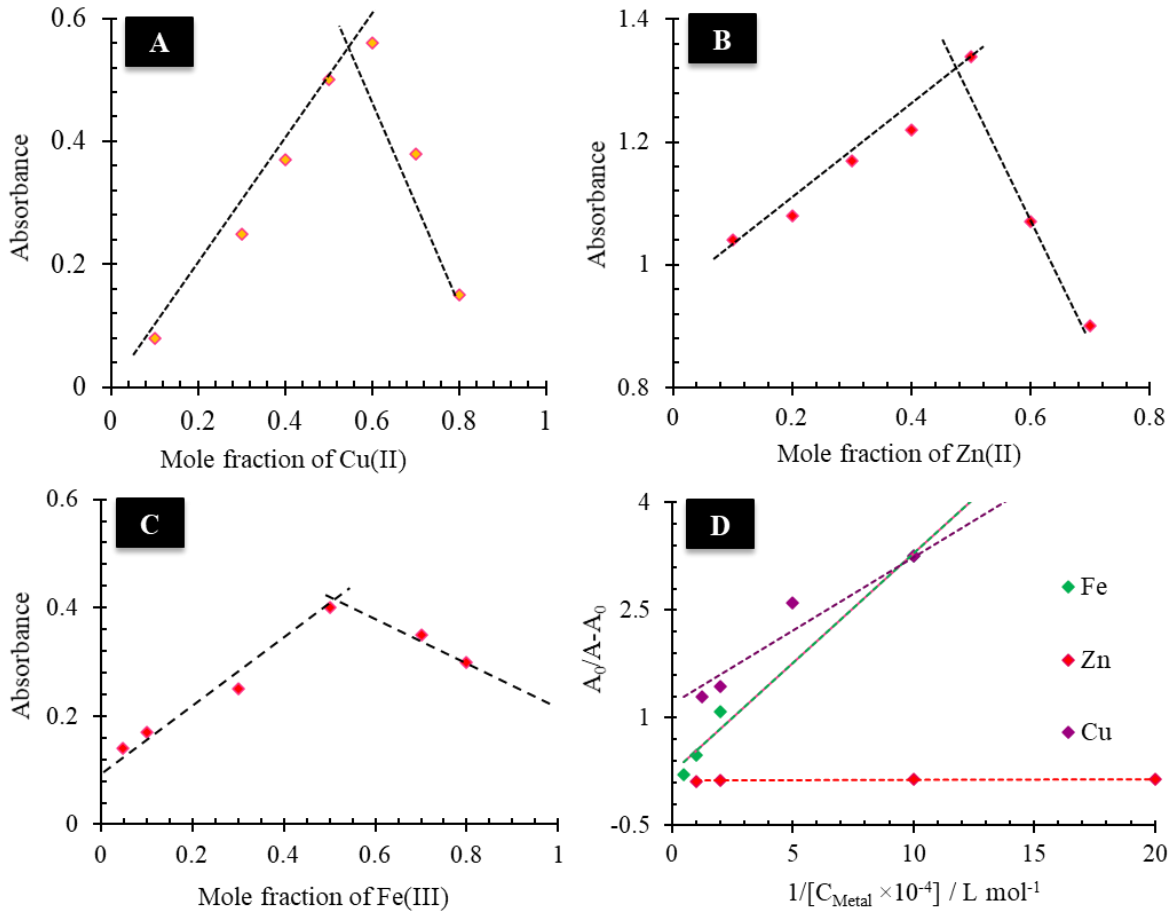

Figure 2: *Job's plot for amoxicillin complex: (A) Cu(II), (B) Fe (III), (C) Zn(II). (D). Plots of $A_0/(A - A_0)$ vs. 1/[Metal] for the determination of binding constants of Complex-AMX adducts. The linear regression equations for Fe, Zn and Cu were respectively: y = 0,3062x + 0,2245 (R^2 = 0,98), y = 0,0015x + 0,1219 (R^2 = 0,92), y = 0,2039x + 1,1984 (R^2 = 0,98).*

The binding constant/association constant (K) of the AMX with Cu(II), Fe(III) and Zn(II) can be determined according to Benesi–Hildebrand equation [39]:

$$\frac{A_0}{A - A_0} = \frac{\varepsilon_G}{\varepsilon_{H-G} - \varepsilon_G} + \frac{\varepsilon_G}{\varepsilon_{H-G} - \varepsilon_G} \times \frac{1}{K[Metal]}$$

Where A_0 and A are the absorbance's of the drug and its complex, respectively, and ε_G and ε_{H-G} are the absorption coefficients of the drug and the drug–metal complex, respectively. The association constant (K) can be obtained from the intercept-to-slope ratios of $A_0/(A - A_0)$ vs.

1/[Metal] plots (Fig. 2D). The binding constant/association constant (K) of the AMX with Cu(II), Fe(III) and Zn(II) were found to be 7.17×10^2, 7.65×10^2 and 4.46×10^4 M , respectively. The infrared spectroscopy (IR) is one of the important analytical techniques used employed for describing the process of complex formation. Comparing with the IR spectra of free AMX, the assignments of bonding sites of the ligand with metal ions are discussed (Fig. 3).

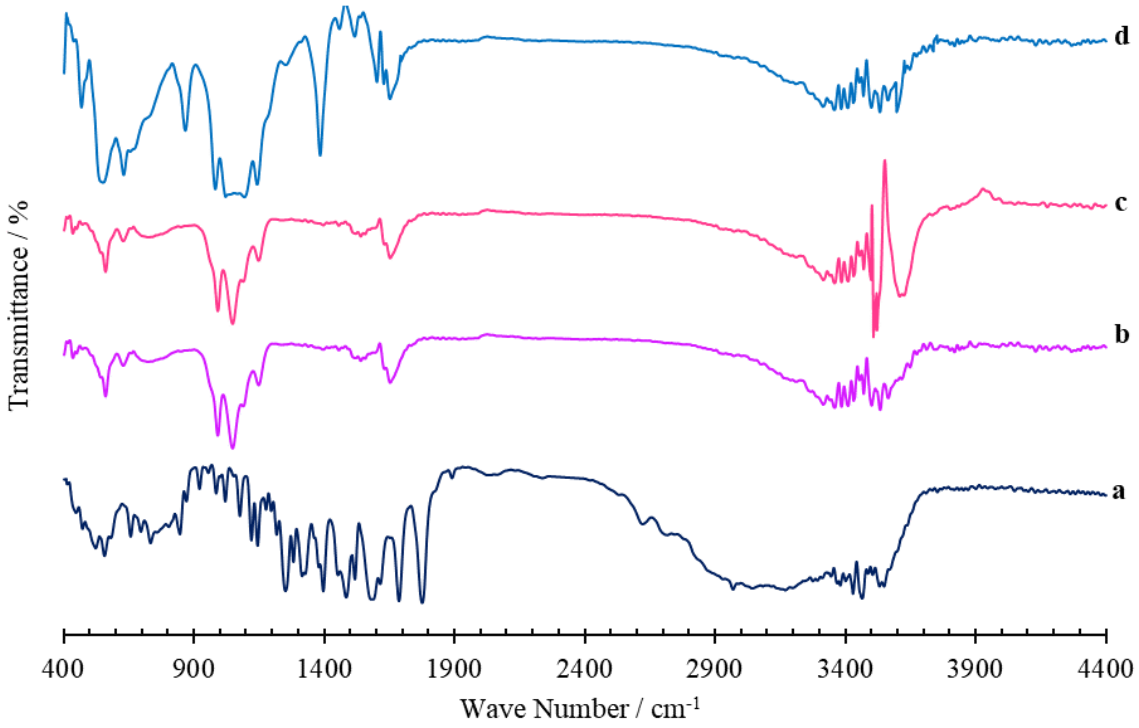

Figure 3: *IR spectra of (a) Amoxicillin and (b) AMX-Cu, (c) AMX-Fe and (d) AMX-Zn complexes.*

The band observed at 3000–3710 cm^{-1} in the free AMX is a broad one due to the presence of H_2O. The ligand bands at 3057 and 3157 cm^{-1} were assigned to ν(NH_2) and ν(NH) respectively. These bands disappeared in the spectra of all complexes, indicating a coordination of AMX with the metallic ions through its amino and imino. The band observed at 3485 cm^{-1} of the free ligand is attributed to ν(OH), also appears in all complexes almost at the same wavenumber as the ligand [40-41]. The C=O group of the β-lactam ring in the free ligand was noted at 1778 cm^{-1} [42-43] but disappears in the spectra of the AMX-metal complexes, which indicates that this carbonyl group is taking part in the complex formation. The carbonyl group of the amide appears as strong band at 1687 cm^{-1} [44], this band ν (–CO–NH–) has the same appearance in the complexes but with a negative shift (Δν = 33–40 cm^{-1}) with some variation in the strength of the intensity (changed from strong band to shoulder one) in all complexes. The carboxylic group band of free ligand appears at 1255 cm^{-1}, but this band was not observed in the IR spectra

of the AMX-metal complexes. Sharp bands at (1590, 1485 cm^{-1}) are assigned to asymmetric and symmetric stretching of carboxylate group of AMX respectively. The νs (COO-) shifted toward over wave numbers, while the νas (COO-) shifted towards higher wave number which indicates the coordination of carboxylate group with the metal atoms [45-46]. These overall data suggested that the amino, imino, carboxylate, β-lactamic and carbonyl groups are involved in coordination of the AMX to the metal ions.

The application of electrochemical methods to study the coordination of metal ions to drugs provides a useful complement to the previously used methods such as UV–Visible spectroscopy.

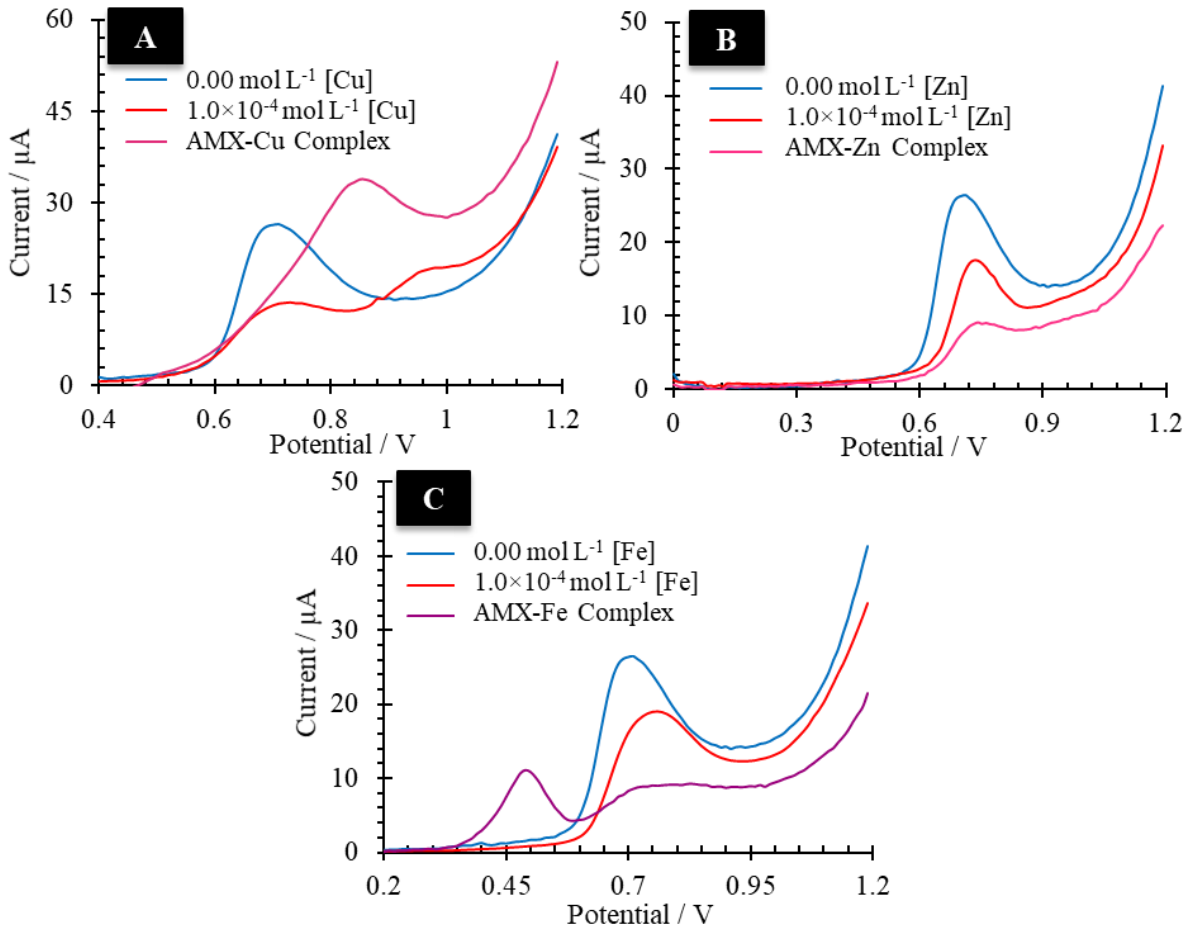

Figure 4: *Square-wave voltammograms of (A) 1.0×10^{-4} M AMX; 1.0×10^{-4} M AMX +1.0×10^{-4} M Cu(II); AMX-Cu complex, (B) 1.0×10^{-4} M AMX; 1.0×10^{-4} M AMX + 1.0×10^{-4} M Zn(II); AMX-Zn complex, (C) 1.0×10^{-4} M AMX; 1.0×10^{-4} M AMX + 1.0×10^{-4} M Fe(III); AMX-Fe complex.*

The electrochemical behavior of AMX in the absence and presence of metal ions was investigated on carbon paste electrode (CPE) using square-wave voltammetry (SWV). As shown in Fig. 4, in the absence of metal ions, the SW voltammogram for the electro-oxidation

of 1.0×10^{-4} M AMX in PBS (pH 7.0), exhibits an oxidation peak at 0.7 V (Epa) which is attributed to the oxidation of the OH group of the phenolic sites of the AMX (φ-OH) [24].

Upon addition of Cu(II) (1.0×10^{-4} M), the anodic peak currents (Ipa) decreased and a second anodic peak appeared at 0.96 V (Fig. 4A). These results suggesting that there exists an interaction between AMX and Cu(II) ions. The important positive shift of the anodic peak potential was observed in the SW voltammogram of the complex (AMX−Cu). The decrease in Ipa values and the positive shift of the oxidation potential are due to the complexation phenomena. Fig. 4B shows the effect of the addition of 1.0×10^{-4} M Fe(III) to a solution of 1.0×10^{-4} M AMX in PBS (pH 7.0), on the square wave voltammetry of AMX. The current decrease and a slight shift of anodic peak potential to a more positive value is due to the binding of AMX. The cause for the decrease in the peak current was that the concentration of electroactive species decreased which indicates the formation of slowly diffusing product (AMX−Fe). Similarly, the SWV of AMX−Fe(III) complex indicated a sequential drop in anodic peak current and exhibits a new peak at 0.5 V attributed to the reduction of Fe(III) to Fe(II).

Fig. 4C describes the square wave voltammetric behavior of AMX on CPE in the absence and presence of one equivalent of Zn (II) in 0.1 M PBS, by adding Zn(II). The decrease in the peak current value and the slightly positive shift of the oxidation potential are due to the reduction in diffusion coefficient as the AMX is bound to the Zn(II) ion.

The electrochemical studies of AMX−metal complex show that the binding of the metal ions to AMX leads to a decrease in AMX anodic peak intensity with the shift in oxidation potential. These results confirm the stability of AMX against oxidation by metal ions as complexing agents. This complex formed is likely to have a role in the antimicrobial activity.

III.2. Antimicrobial activity of the metal complexes

The antibacterial efficacy of the ligand (AMX) and its metal complexes (AMX−M) have been studied for their antibacterial activities against *E. coli* (patient 1) by disk diffusion method (Fig. 5) [47]. The parameters characterizing the bactericidal properties of compounds are the inhibition zone diameter (IZD) [mm] defined as the area around the disk with antibiotic in which bacteria are unable to grow. The inhibition zone diameters of the ligand and metal complexes AMX−Cu, AMX−Zn and AMX−Fe are 0, 18, 13 and 25 mm, respectively. The antibacterial activity was absent for the ligand (AMX), while the synthesized metal complexes exhibited promising antibacterial activity against E. coli bacteria. In addition, the complexes (AMX-Fe) and (AMX-Cu) possesses pronounced antibacterial activity in comparison with (AMX-Zn). The inhibition zones around the disks are also categorized according to the critical

values for these metal complexes, in order to determine the clinical category of susceptibility (resistant if (IZD) <14 mm), intermediate (moderately sensitive) (if (IZD) between 14-20 mm) and susceptible (if (IZD) ≥21mm)) [48].

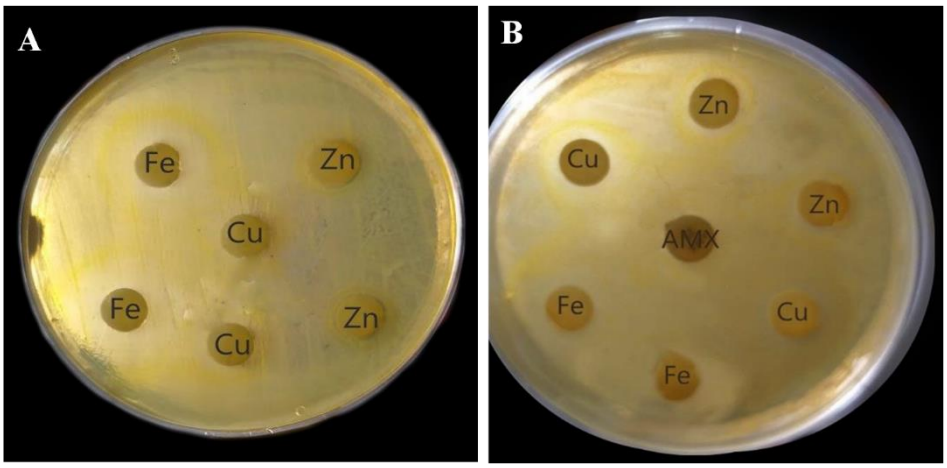

Figure 5: *Antibacterial activity of (A) Amoxicillin complexes, (B) Amoxicillin complexes and control drug (25 µg/mL Amoxicillin disk).*

E. coli has sensitive and an intermediate sensitivity to the AMX-Fe complex and AMX-Cu, respectively. While being resistant to AMX and AMX-Zn complex. The antibacterial activity of AMX complexes is probably due to the nature of the metal ion and the chelate stability. Metal-complexed antibiotics are highly effective against resistant strains. Some metal ions, such as iron, copper and zinc, continue to be of interest in the field of bioinorganic research because they may also influence a drug-induced metalloenzyme inhibition mechanism in some pathogens that are responsible for infections, influenza, tumors, inflammation, etc.

III.3. Determination of the minimum inhibitory concentrations (MICs)

The minimum inhibitory concentration (MIC) [µg/mL] which is the lowest concentration of the bactericide inhibiting bacteria growth [49]. The minimum inhibitory concentrations (MICs) against *E. coli* (patient 2) of synthesized metal complexes were determined by agar plate disc diffusion method (Fig. 6). The various concentrations (10, 25, 50, 75 and 100 µg/mL) of these complexes were used.

The MIC values of AMX and their metal complexes were exploited by the plot of arithmetic square of the inhibitory zone diameter (IZD^2) values against the logarithmic concentrations of the metal complexes (Fig. 7). The intercept on the concentration axis represents the MIC.

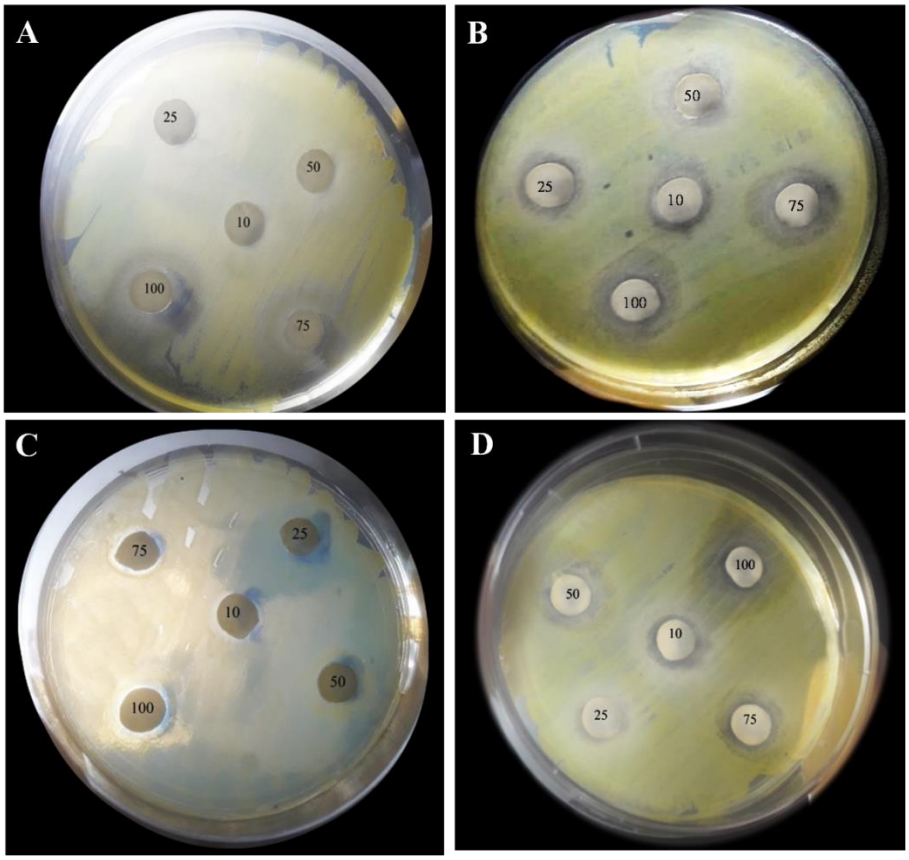

Figure 6: *Antibacterial activity of (A) Amoxicillin, (B) AMX-Cu complex, (C) AMX-Zn complex and (D) AMX-Fe complex at different concentration (10 µg/mL, 25 µg/mL, 50 µg/mL, 75 µg/mL and 100 µg/mL).*

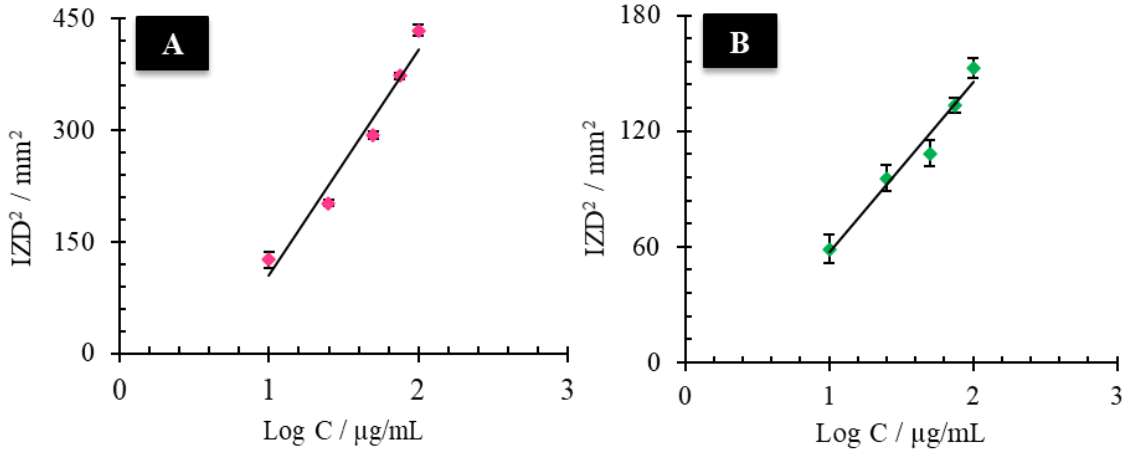

Figure 7: *Plots of IZD2 vs. Log C (A) AMX-Cu complex: y = 304,65x - 200,49 (R² = 0,964), (B) AMX-Fe complex: y = 88,151x - 30,72 (R² = 0,9664) for the determination of Minimum Inhibitory Concentrations (MIC).*

The minimum inhibitory concentration (MIC) of synthesized metal complexes against the selected organism were extrapolated from the graph and tabulated (Table 1), the result is as

follows: 25 µg/mL of AMX-Cu and AMX-Fe complex showed inhibitory effect on *E. coli*, while the AMX ligand and AMX-Zn complex were not effective up to 75 µg/mL (patient 2). It was also noticed that Fe-AMX complex exhibited the highest antibacterial activity.

Table 1: *Inhibition zone diameter and minimum inhibitory concentration (MIC).*

Concentration (µg/mL)	Inhibition zone diameter (in mm)			
	Ligand	AMX-Cu	AMX-Fe	AMX-Zn
10	-	11.2±0.5	10.9±0.4	-
25	-	14.2±0.15	14.8±0.3	-
50	-	17.1±0.15	15.5±0.2	-
75	12.4±0.48	19.3±0.12	17.3±0.1	12.9±0.5
100	16.7±0.37	20.8±0.18	18.1±0.14	13.85±0.3
MIC	-	2.23	1.52	-

Values shown is the average ± standard deviation of three readings performed three times

III.4. Time-kill Assay and biofilm formation

Time kill assay provide useful information to describe the pharmacodynamics of trial anti-bacterial compounds. According to the Clinical and Laboratory Standards Institute (CLSI) protocols, a 3 log10 CFU/mL or greater reduction in the viability of the bacterial colony relative to the initial inoculum is the point that differentiates between bactericidal and bacteriostatic activity. The bactericidal and bacteriostatic activities were expressed separately as the decrease of the colony count by< 3 log10 and ≥ 3 log10 after 24 hours relative to the initial inoculum [50-51]. Representative time courses of bacterial burden associated with various compounds are presented in Fig. 8. As shown in Fig. 8, in the absence of AMX, the bacterial population reached the maximal number of bacteria (about 3×10^8 CFU/ml) approximately 24 h after the start of the experiment. In the presence of 75 µg/mL of AMX, the bacterial count grew more slowly than with the control. Little antimicrobial effect was observed in the case of AMX-Zn complex, as the bacteria in the presence of this complex grew over time to a level similar to the AMX. The AMX-Cu complex showed a bacteriostatic effect, as the log CFU/mL over time remained lower than 3 log CFU/mL, a bactericidal effect was observed in the case of AMX-Fe complex, reducing the starting log CFU/mL by greater than 3 logs after 24 h preexposure to AMX-Fe complex.

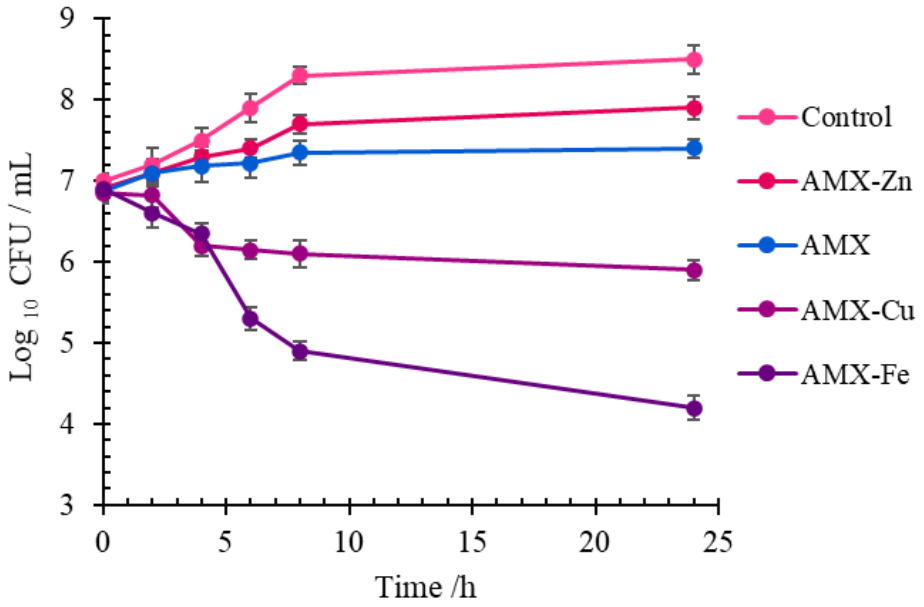

Figure 8: *Time-kill kinetics assay results for (A) control, (B) Amoxicillin, (C) AMX-Cu complex, (D) AMX-Zn complex and (E) AMX-Fe complex.*

Time-kill kinetics was also in complete agreement with the other data and showed no bacteria grew in the case of AMX-Cu and AMX-Fe complexes. The results of the bacterial population in the presence of 75 ug/L AMX and their metal complexes, after 24 hours of pre-exposure to antibiotics, are shown in Fig. 9.

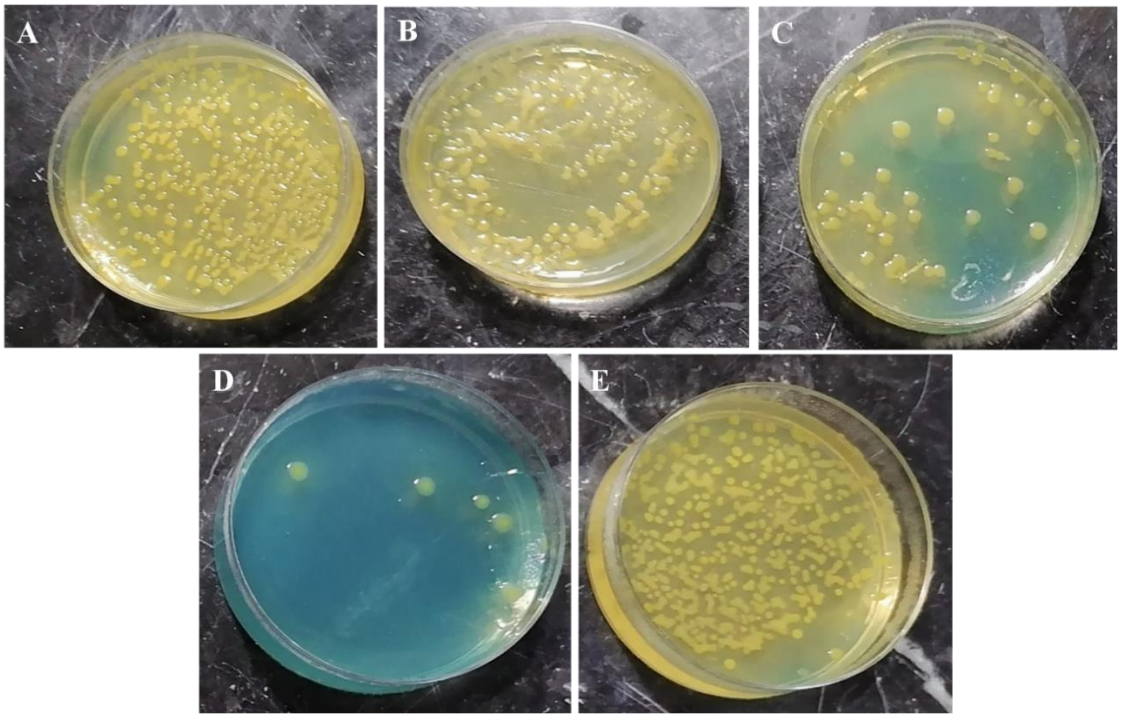

Figure 9: *Antibacterial activity of (A) control (B) Amoxicillin, (C) AMX-Cu complex, (D) AMX-Fe complex and (E) AMX-Zn complex after 24 h of preexposure to the antibiotics.*

In order to quantify the biofilm production capabilities of *E. coli* strains in the presence of M-AMX complexes, Strains were subjected to biofilm amount measurement, expressed as the absorbance of crystal violet (CV) at λ = 595 nm eluted from the biofilm. This method allows for the in vitro cultivation and quantification of bacterial biofilms. Strain-specific differences in biofilm formation were observed (Fig. 10A).

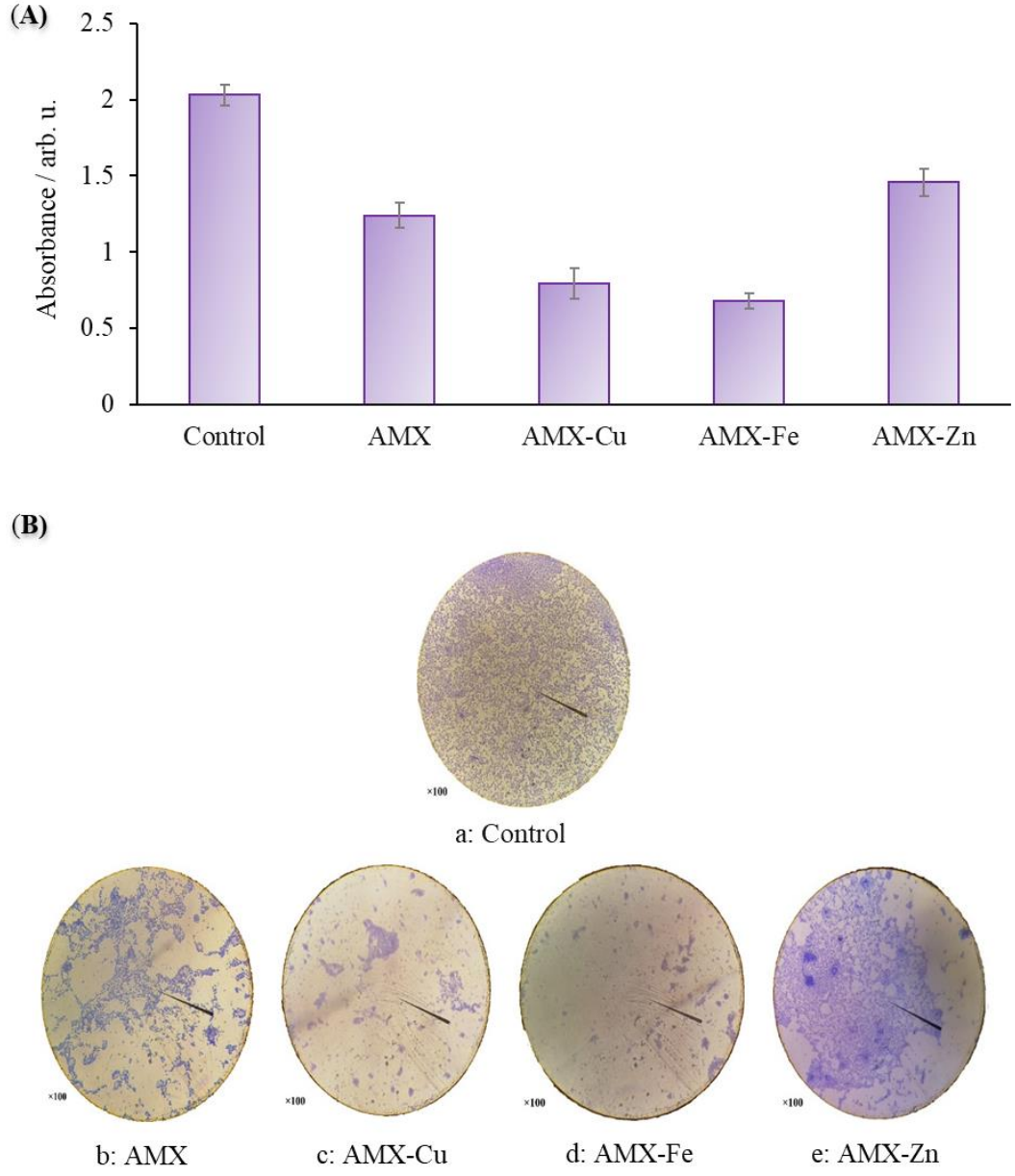

Figure 10: *(A) Biofilm formation by clinical strains of E. coli expressed as the absorbance of crystal violet at λ = 595 nm. (B) Images representing biofilm morphology and cell viability in the untreated control and after treatment with 75µg/mL of Amoxicillin and M-AMX complexes.*

In general, strains treated with AMX and AMX-Zn complexes exhibited high absorbances values (ABS = 1.24 ± 0.085 and 1.46± 0.09, respectively), that were closer to that seen in the

control (ABS = 2.03 ± 0.07), indicating that the *E. coli* strain may form biofilms under these treatment, while the AMX-Cu and AMX-Fe complexes treated strains, were significantly reduced biofilm formation by *E. Coli* compared to the control, the difference is statically significant as expressed by the CV absorbance values (ABS (AMX-Cu) = 0.79 ± 0.1 and ABS (AMX-Fe) = 0.68 ± 0.05). AMX-Cu and AMX-Fe complexes were able to inhibit biofilm formation, reducing the biomass by 61% and 66.5%, respectively relative to control, and by 36.3% and 45.16%, respectively relative to AMX, after 48 h of cell incubation.

Microscopic imaging of CV stained bacterial cells also confirmed the reduction in the viability of cells in biofilms in presence of this complexes in the culture (Fig. 10B). Moreover, the presence of AMX-Fe complex in the culture resulted in the death of most of the bacterial cells. These results proved that the novel compounds are promising antimicrobial and anti-biofilm agents, especially those based on cooper and iron ions. Such increased activity of metal complexes may be considered due to chelation of metal ions with AMX. During chelation, the polarity of the metal ion is considerably reduced to a greater extent due to the partial sharing of the positive charge of the metal ion with the donor groups in the ligand [52]. In addition, it increases the π-electron delocalization over the whole chelate ring and improves the lipophilicity of the complex [53]. The increased lipophilicity of complexes allows easy penetration into the lipid membranes of organisms and facilitates the blocking of metal binding sites in enzymes [54-55]. In addition, these complexes deactivate various cellular enzymes, which play a vital role in several metabolic pathways of these microorganisms. It has also been suggested that the ultimate action of the toxin is the denaturation of one or more proteins of the cell, resulting in the hindering of normal cellular processes [56]. However, the reduced bactericidal activity of AMX upon coordination with Zn(II) ion is most probably arises from the hydrolytic cleavage of the β-lactam ring after the complexation process with Zn(II). Factors that can contribute to activity other than this are nature of the metal ion, nature of the ligand, coordinating sites and geometry of the complex, concentration, hydrophilicity, lipophilicity, and the presence of co-ligands [55]. The mechanisms of inhibition of bacterial activity incorporated by Artificial metalloantibiotics mimics antibiotics. Biological macromolecules present in living organisms, like proteins, DNA, have many metal-binding sites. Therefore, coordination compounds can react with such cellular components, displaying possible toxic effects [57]. Further, the production of enzyme β-lactamase (BL) is the most common mechanism of bacterial resistance [58], which is a bacterial enzyme that hydrolyzes b-lactam-containing compounds and breaks open the β-lactam ring of the antibiotic, rendering the β-lactam antibiotic ineffective, which can confer bacteria with nearly complete resistance to all

b-lactams except monobactams [59]. The most widespread strategy used by BL inhibitors is the metal binding inhibition mechanism. Metal binding inhibitors function within two limiting mechanisms: 1) metal ion stripping, where the inhibitor either actively removes the active-site metal ions from the enzyme or sequesters metal ions that exited the active site; or 2) ternary complex formation, where the inhibitor binds to the metal ions and the surrounding protein residues, preventing antibiotics from binding [60].

Table 2: *Antibacterial activity of metals and complexes containing Amoxicillin antibiotic.*

Compound	Disk Content (µg/mL)	Inhibition zone diameter (mm)	MIC (µg/mL)	Ref
AMX	1000	30	-	[44]
AMX-La		12	-	
AMX-Ce		8	-	
AMX-Sm		9	-	
AMX-Y		11	-	
AMX	500	33	12.5	[23]
AMX-Fe		0	0	
AMX	-	-	62.5	[45]
AMX-Cu		-	1000	
AMX	-	10-15		[41]
AMX-Cu		15-20		
AMX-Ag		20-25		
AMX-Zn		10-15		
AMX-Ni		15-20		
AMX-Co		15-20		
AMX	50	15-20		[46]
AMX-Cu		20-25		
AMX-Zn		20-25		
Ag-NPs	-	7	-	[7]
Ag-NPs	50µL	4.6	-	[8]
Au-NPs		4	-	
Ag-NPs	0.78	16	2.10	[11]
	1.57	19		
	2.35	21		
AMX	25	-	-	present work
AMX-Cu		18	2.23	
AMX-Fe		25	1.52	
AMX-Zn		13	-	

Table 2 summarizes the Inhibition zone diameter (in mm) and minimum inhibitory concentration (MIC) of previously reported works and this study [7-8,11,61-63]. The found values are comparable with the results reported by other authors. In addition, compared with

other papers, a synergistic bactericidal activity between ligand and metal has been remarked. The results showed that the complexes exhibited an excellent impact on the antibacterial property. In this study, we hypothesis that physical and chemical factors impacted the antibacterial activity.

IV. Conclusion

In summary, the present study focuses on synthesis, characterization of the metal amoxicillin complexes and their application as antimicrobial agents. The synthesized complexes were characterized by UV-Visible spectrophotometry, IR spectroscopy and electrochemical methods. The binding constant/association constant (K) of the AMX with Cu(II), Fe(III) and Zn(II) were found to be 7.17×10^2, 7.65×10^2 and 4.46×10^4 L mol^{-1}, respectively. The results obtained by square wave voltammetry show that the bond formation between the metal ions and AMX leads to a decrease in AMX anodic peak intensity with the shift in oxidation potential, generally becoming more positive in the presence of Cu(II), Zn(II) and Fe(III). This result revealed that metal ions are able to change the electrochemical behavior of AMX, that can prevent AMX oxidation.

The antibacterial efficacy of the synthesized metal complexes against pathogenic bacteria (*E. coli*) was evaluated by measuring the zone of inhibition diameter. The complexes as AMX−Cu and AMX−Fe had higher bactericidal activity than the AMX−Zn and the control drug, showing that they had a good activity as bactericides. The Time-kill kinetics and biofilm formation also showed similar results to the growth curves corresponded to the MICs. The AMX interactions with metal ions should be taken into account, especially regarding the problem of antibiotic resistance and the selection of the most efficient antimicrobial therapy for patients with altered trace elements homeostasis. The result shows that the AMX protection against oxidation increase its antibacterial activity.

References

[1] J. D. Lutgring, C. A. D. Granados, J. E. McGowan, Antimicrobial Resistance: An International Public Health Problem. In Antimicrobial Drug Resistance: Clinical and Epidemiological Aspects. J. Springer. Cham. 2 (2017) 1519-1528. https://doi.org/10.1007/978-3-319-47266-9_39

[2] S. R. Partridge, S. M. Kwong, N. Firth, S. O. Jensen, Mobile genetic elements associated with antimicrobial resistance. J. Clin. Microbiol. Rev. 31 (2018) e00088-17. https://doi.org/10.1128/CMR.00088-17

[3] World Health Organization. Global antimicrobial resistance surveillance system (GLASS) report: early implementation 2020. (2020) 112. ISBN 978-92-4-000558-7 (electronic version).

[4] P. Yang, M. Bam, P. Pageni, T. Zhu, Y. P. Chen, M. Nagarkatti, A.W. Decho, C. Tang, Trio act of boronolectin with antibiotic-metal complexed macromolecules toward broad-spectrum antimicrobial efficacy. J. ACS. Infect. Dis. 3 (2017) 845-853. https://doi.org/10.1021/acsinfecdis.7b00132

[5] J. S. Möhler, T. Kolmar, K. Synnatschke, M. Hergert, L. A. Wilson, S. Ramu, A. G. Elliott, M. A. Blaskovich, H. E. Sidjabat, D. L. Paterson, G. Schenk, Enhancement of antibiotic-activity through complexation with metal ions-Combined ITC, NMR, enzymatic and biological studies. J. Inorg. Biochem. 167 (2017) 134-141. https://doi.org/10.1016/j.jinorgbio.2016.11.028

[6] Y. H. Liu, S. C. Kuo, B. Y. Yao, Z. S. Fang, Y. T. Lee, Y. C. Chang, T. L. Chen, C. M. J Hu, Colistin nanoparticle assembly by coacervate complexation with polyanionic peptides for treating drug-resistant gram-negative bacteria. J. Acta. Biomater. 82 (2018) 133-142. https://doi.org/10.1016/j.actbio.2018.10.013

[7] U. T. Khatoon, G. V. S. N. Rao, M. K. Mohan, A. Ramanaviciene, A. Ramanavicius, Antibacterial and antifungal activity of silver nanospheres synthesized by tri-sodium citrate assisted chemical approach. Vacuum. 146 (2017) 259-265. https://doi.org/10.1016/j.vacuum.2017.10.003

[8] U. T. Khatoon, G. V. S. N. Rao, M. K. Mohan, A. Ramanaviciene, A. Ramanavicius, Comparative study of Antifungal Activity of Silver and Gold Nanoparticles Synthesized by Facile Chemical Approach. J. Environ. Chem. Eng. 6 (2018) 5837-5844. https://doi.org/10.1016/j.jece.2018.08.009

[9] K. K. Y. Wong, X. Liu, Silver nanoparticles—The real “silver bullet” in clinical medicine? Med. Chem. Commun. 1 (2010) 125–131. https://doi.org/10.1039/C0MD00069H

[10] T. C. Dakal, A. Kumar, R. S. Majumdar, V. Yadav, Mechanistic Basis of Antimicrobial Actions of Silver Nanoparticles. Front. Microbiol. 7 (2016) 1831. https://doi.org/10.3389/fmicb.2016.01831

[11] N. Zafar, S. Shamaila, J. Nazir, R. Sharif, M. Shahid Rafique, J. Ul-Hasan, S. Ammara, H. Khalid, Antibacterial Action of Chemically Synthesized and Laser Generated Silver Nanoparticles against Human Pathogenic Bacteria. J. Mater. Sci. Technol. 32 (2016) 721–728. https://doi.org/10.1016/j.jmst.2016.05.009

[12] M. Kumar, K. K. Sodhi, P. Singh, P. K. Agrawal, D. K. Singh, Synthesis and characterization of antibiotic-metal complexes [$FeCl_3$ (L1) $2H_2O$ and Ni (NO_3) 2 (L_2) $2H_2O$] and enhanced antibacterial activity. J. Environ. Nanotechnol. Monit. Manag. 11 (2019) 100209. https://doi.org/10.1016/j.enmm.2019.100209

[13] L. H. Abdel-Rahman, A. A. Abdelhamid, A. M. Abu-Dief, M. R. Shehata, M. A. Bakheet, Facile synthesis, X-Ray structure of new multi-substituted aryl imidazole ligand, biological screening and DNA binding of its Cr (III), Fe (III) and Cu (II) coordination compounds as potential antibiotic and anticancer drugs. J. Mol. Struct. 1200 (2020) 127034. https://doi.org/10.1016/j.molstruc.2019.127034

[14] M. Swart, M. Costas, Spin states in biochemistry and inorganic chemistry: influence on structure and reactivity. John Wiley & Sons, Ltd, (2015). ISBN 987-1-118-89831-4

[15] D. H. Nies, The biological chemistry of the transition metal “transportome” of Cupriavidus metallidurans. J. Metallomics. 8 (2016) 481-507. https://doi.org/10.1039/c5mt00320b

[16] D. C. Coraça-Huber, S. Dichtl, S. Steixner, M. Nogler, G. Weiss, Iron chelation destabilizes bacterial biofilms and potentiates the antimicrobial activity of antibiotics against coagulase-negative Staphylococci. J. Pathog. Dis. 76 (2018) fty052. https://doi.org/10.1093/femspd/fty052

[17] W. Guerra, P. P. Silva-Caldeira, H. Terenzi, E. C. Pereira-Maia, Impact of metal coordination on the antibiotic and non-antibiotic activities of tetracycline-based drugs. J. Coord. Chem. Rev. 327 (2016) 188-199. https://doi.org/10.1016/j.ccr.2016.04.009

[18] K. Poole, At the nexus of antibiotics and metals: the impact of Cu and Zn on antibiotic activity and resistance. J. Trends. Microbiol. 25 (2017) 820-832. https://doi.org/10.1016/j.tim.2017.04.010

[19] Z. Ude, K. Kavanagh, B. Twamley, M. Pour, N. Gathergood, A. Kellett, C. J. Marmion, A new class of prophylactic metallo-antibiotic possessing potent anti-cancer and anti-microbial properties. J. Chem. Soc., Dalton Trans. 48 (2019) 8578-8593. https://doi.org/10.1039/C9DT00250B

[20] M. S. Pillai, S. P. Latha, Designing of some novel metallo antibiotics tuning biochemical behaviour towards therapeutics: synthesis, characterisation and pharmacological studies of metal complexes of cefixime, J. Saudi. Chem. Soc. 20 (2016) S60-S66. https://doi.org/10.1016/j.jscs.2012.09.004

[21] M. Claudel, J. V Schwarte, K. M Fromm, New Antimicrobial Strategies Based on Metal Complexes. J. Chemistry. 2 (2020) 849-899. https://doi.org/10.3390/chemistry2040056

[22] A. Hrioua, A. Loudiki, A. Farahi, S. Lahrich, M. Bakasse, S. Saqrane, M. A. El Mhammedi, Recent advances in electrochemical sensors for amoxicillin detection in biological and environmental samples, Bioelectrochemistry. (2020) 107687. https://doi.org/10.1016/j.bioelechem.2020.107687

[23] A. Hrioua, S. Aghris, N. Ajermoun, F. Ettadili, A. Farahi, S. Lahrich, M. Bakasse, S. Saqrane, M. A. El Mhammedi, Electrochemical Investigation of Amoxicillin Interaction with Some Metal Ions Related to Complexation Process, J. Electrochem. Soc. 167 (2020) 126501. https://orcid.org/0000-0001-6354-1785

[24] A. Hrioua, A. Farahi, S. Lahrich, M. Bakasse, S. Saqrane, M. A. El Mhammedi, Chronoamperometric Detection of Amoxicillin at Graphite Electrode using Chelate Effect of Copper(II) Ions: Application in Human Blood and Pharmaceutical Tablets, J. ChemistrySelect. 4 (2019) 8350 –8357. https://doi.org/10.1002/slct.201901689

[25] G. S. Al-Jebouri, A. M. noorikhaleel, Synthesis of new boron compounds with amoxicillin and some of its metal complexes with use them in antibacterial, assessment of hepatoprotictive and kidneyactivity, anticancer and antioxidant applications. J. Synthesis. 12 (2019) 0974-2441.

[26] N. K. Chaudhary, P. Mishra. In vitro antimicrobial screening of metal complexes of schiff base derived from streptomycin and amoxicillin: synthesis, characterization and molecular modelling. Am. J. Appl. Chem. 2 (2014) 19-26. 10.11648/j.ajac.20140201.15

[27] B. Božić, J. Korać, D. M. Stanković, M. Stanićović, M. Dalibor, Coordination and redox interactions of β-lactam antibiotics with Cu2+ in physiological settings and the impact on antibacterial activity. J. Free Radic. Biol. Med. 129 (2018) 279-285. https://doi.org/10.1016/j.freeradbiomed.2018.09.038

[28] F. I. Eze, U. Ajali, P. O Ukoha, Synthesis, physicochemical properties, and antimicrobial studies of iron (III) complexes of ciprofloxacin, cloxacillin, and amoxicillin. Int. J. Med. Chem. 2014 (2014) 735602. https://doi.org/10.1155/2014/735602

[29] S. Ashraf, U. Chaudhry, A. Raza, D. Ghosh, X. Zhao, In vitro activity of ivermectin against Staphylococcus aureus clinical isolates. Antimicrob. Resist. Infect. Control. 7 (2018) 1-6. https://doi.org/10.1186/s13756-018-0314-4

[30] G. Czerwonka, D. Gmiter, A. Guzy, P. Rogala, A. Jabłońska-Wawrzycka, A. Borkowski, T. Cłapa, D. Narożna, P. Kowalczyk, M. Syczewski, M. Drabik, A benzimidazole-based ruthenium (IV) complex inhibits Pseudomonas aeruginosa biofilm formation by interacting with siderophores and the cell envelope and inducing oxidative stress. Biofouling, 35 (2019) 59-74. https://doi.org/10.1080/08927014.2018.1564818

[31] D. B. Boyd, C. Y. Yeh, F. S. Richardson, Electronic structures of cephalosporins and penicillins. 5. Optical activity of the penicillin nucleus chromophores. J. Am. Chem. Soc. 98 (1976) 6100-6106. https://doi.org/10.1021/ja00436a004

[32] L. Szabó, T. Tóth, G. Rácz, E. Takács, L. Wojnárovits, ·OH and e- aq are yet good candidates for demolishing the β-lactam system of apenicillin eliminating the antimicrobial activity, J. Radiat. Phys. Chem. 124 (2016) 84–90. https://doi.org/10.1016/j.radphyschem.2015.10.012

[33] K. Hanson, L. Roskop, P. I. Djurovich, F. Zahariev, M. S. Gordon, M. E. Thompson, A Paradigm for Blue- or Red-Shifted Absorption of Small Molecules Depending on the Site of π-Extension, J. Am. Chem. Soc. 132 (2010) 16247–16255. https://doi.org/10.1021/ja1075162

[34] G. Liu, X. Zhang, Theoretical acquirement of the red shift of ν(F H) upon complexation with Ne, J. Spectrochim. Acta. Part A. 69 (2008) 917–920. https://doi.org/10.1016/j.saa.2007.05.055

[35] A.Y. Li, Chemical origin of blue- and redshifted hydrogen bonds: Intramolecular hyperconjugation and its coupling with intermolecular hyperconjugation, J. Chem. Phys. 126 (2007) 154102. https://doi.org/10.1063/1.2715561

[36] N. P. Gensmantel, P. Proctor, M. I. Page, Metal-ion Catalysed Hydrolysis of Some β-Lactam Antibiotics, J. Chem. Soc. 2 (1980) 1725-1732. https://doi.org/10.1039/P29800001725

[37] C. Y. Huang, "Determination of binding stoichiometry by the continuous variation method: the job plot,". Meth. Enzymol. 87 (1982) 509–525. https://doi.org/10.1016/S0076-6879(82)87029-8

[38] C. Y. Huang, Determination of binding stoichiometry by the continuous variation method: the job plot, J. Methods. Enzymol. 87 (1982) 509–525. https://doi.org/10.1016/S0076-6879(82)87029-8

[39] H. A. Benesi, J. H. Hildebrand, Spectrophotometric investigation of the interaction of iodine with aromatic hydrocarbons, J. Am. Chem. Soc. 71 (1949) 2703–2707. https://doi.org/10.1021/ja01176a030

[40] A. S. Orabi, Physicochemical Properties of Ampicillin and Amoxicillin as Biologically Active Ligands with Some Alkali Earth, Transition Metal, and Lanthanide Ions in Aqueous and

Mixed Solvents at 20, 30, and 40 ◦C, J. Solution. Chem. 34 (2005) 95-111. https://doi.org/10.1007/s10953-005-2075-y

[41] E. S. Ibrahim, S. A. Sallam, A. S. Orabi, B. A. El-Shetary, A. Lentz, Schiff bases of acetone derivatives: spectroscopic properties and physical constants, J. Monatsh. Chem. 129 (1998) 159. https://doi.org/10.1007/PL00010152

[42] N. Kanooco, R.V. Singh, J. P. Tandon, Synthesis and Structural Studies of Cxovanadium (V) Complexes of Semicarbazones, J. Syn. React. Inorg. Met. Org. Chem. 17 (1987) 837. https://doi.org/10.1080/00945718708059479

[43] A. L. Ram, M. N. Singh, S. Das, Complexes of Uranyl Nitrate, Uranyl Acetate, Uranyl Thiocyanate and Uranyl Chloride with Benzoyl, Salicyloyl and Isonicotinoyl Hydrazines, J. Synth. React. Inorg. Met.-Org. Chem. 16 (1986) 513. https://doi.org/10.1080/00945718608055925

[44] A. Bravo, J. R. Anacona, Synthesis and characterization of metal complexes with ampicillin, J. Coord. Chem. 44 (1998) 173. https://doi.org/10.1080/00958979808022891

[45] R. D. Stefano, M. Scopelliti, C. Pellerito, T. Fiore, R. Vitturi, M. S. Colomba, P. Gianguzza, G. C. Stocco, M. Consiglio, L. Pellerito, Organometallic complexes with biological molecules. XVIII. Alkyltin (IV) cephalexinate complexes: synthesis, solid state and solution phase investigations, J. Inorg. Biochem. 89 (2002) 279. https://doi.org/10.1016/j.jinorgbio.2003.12.013

[46] M. Imran, J. Iqbal, T. Mehmood, S. Latif, Synthesis, characterization and in vitro screening of amoxicillin and its complexes with Ag (I), Cu (II), Co (II), Zn (II) and Ni (II), J. Biol. Sci. 6 (2006) 946.

[47] B. Bonev, J. Hooper, J. Parisot, Principles of assessing bacterial susceptibility to antibiotics using the agar diffusion method, J. Antimicrob. Chemother. 61 (2008) 1295-1301. https://doi.org/10.1093/jac/dkn090

[48] CA-SFM/ EUCAST. Antibiogram Committee of the French Society of Microbiology, Recommendations 2018. (2018) 1–134.

[49] M. A. Islam, M. M. Alam, M. E. Choudhury, N. Kobayashi, M. U. A. Bangl, determination of minimum inhibitory concentration (mic) of cloxacillin for selected isolates of methicillin-resistant staphylococcus aureus (mrsa) with their antibiogram, J. Vet. Med. 6 (2008) 121–126. https://doi.org/10.3329/bjvm.v6i1.1350

[50] V. H. Tam, A. N. Schilling, M. Nikolaou, Modelling time–kill studies to discern the pharmacodynamics of meropenem, J. Antimicrob. Chemother. 55 (2005) 699–706. https://doi.org/10.1093/jac/dki086

[51] S. K. Pillai, R. C. Moellering, G. M. Eliopoulos, Antimicrobial Combinations. In Antibiotics in Laboratory Medicine. 5th edn (ed Lorian V. L.) 365–424 (Lippincott Williams & Wilkins, Philadelphia, 2005).

[52] P. Mishra, biocoordination, computational modeling and antibacterial sensitivities of cobalt (ii), nickel (ii), copper (ii) and bismuth (v) with gentamicin and amoxicillin antibiotics mixed ligands, Int. J. Pharm. Sci. Rev. Res. 3 (2010) 145-156.

[53] H. L. Singh, J. Singh, A. Mukherjee, Synthesis, Spectral and in-vitro Antibacterial studies of Organosilicon(IV) Complexes with Schiff bases derived from amino acids, J. Bioinorg. Chem. Appl. 2013 (2013) 425832. https://doi.org/10.1155/2013/425832

[54] N. Raman, J. Joseph, A. Sakthivel, R. Jeyamurugan, Synthesis, Structural Characterization and Antimicrobial Studies of Novel Schiff Base Copper (II) Complexes, J. Chil. Chem. Soc. 54 (2009) 354-357. http://dx.doi.org/10.4067/S0717-97072009000400006

[55] N. P. Ndahi, Y. P. Nasiru, U. K. Sandabe, Synthesis, Characterization & Antibacterial Studies of Some Schiff Base Complexes of Cobalt(II), Nickel(II) And Zinc(II). Asian J. biomed. pharm. sci. 2 (2012) 5116.

[56] N. Dharmaraj, P. Viswanathamurthi, K. Natarajan, Ruthenium (II) complexes containing bidentate Schiff bases and their antifungal activity, J. Transition Met. Chem. 26 (2001) 105. https://doi.org/10.1023/A:1007132408648

[57] B. S. Sekhon, Metalloantibiotics and antibiotic mimics-an overview. Indian. J. Pharm. Educ. 1 (2010) 1.

[58] J. N. Samaha-Kfoury, F. George, G. F Araj, Recent developments in ß-lactamases and extended spectrum ß-lactamases. BMJ. 327 (2003) 1209-1213. https://doi.org/10.1136/bmj.327.7425.1209

[59] K. Bush, Past and present perspectives on β-lactamases. Antimicrob. Agents. CH. 62 (2018) e01076-18. https://doi.org/10.1128/AAC.01076-18

[60] L. C. Ju, Z. Cheng, W. Fast, R.A. Bonomo, M.W. Crowder, The continuing challenge of metallo-β-lactamase inhibition: mechanism matters. Trends. Pharmacol. Sci. 39 (2018) 635-647. https://doi.org/10.1016/j.tips.2018.03.007

[61] M. S. Refat, H. M. A. Al-Maydama, F. M. Al-Azab, R. R. Amin, Y. M. S. Jamil, Synthesis, thermal and spectroscopic behaviors of metal–drug complexes: La(III), Ce(III), Sm(III) and Y(III) amoxicillin trihydrate antibiotic drug complexes, J. Spectrochim. Acta. A Mol. Biomol. Spectrosc. 128 (2014) 427-446. https://doi.org/10.1016/j.saa.2014.02.160

[62] B. Božić, J. Korać, D. M. Stanković, M. Stanić, M. Romanović, J. B. Pristov, S. Spasić, A. P. Bijelić, I. Spasojević, M. Bajčetić, Coordination and redox interactions of β-lactam

antibiotics with Cu2+ in physiological settings and the impact on antibacterial activity, J. Free Radic. Biol. Med. 129 (2018) 279-285. https://doi.org/10.1016/j.freeradbiomed.2018.09.038

[63] E. A. N. El-Gamel, Metal chelates of ampicillin versus amoxicillin: synthesis, structural investigation, and biological studies, J. coord. chem. 63 (2010) 534-543. https://doi.org/10.1080/00958970903494157

Conclusion

Antibiotics are among the most successful drugs used for human therapy. Despite the considerable number of newer antibacterials made available over the past decades, β-lactam antibiotics are still the most used antibacterials all over the world. Amoxicillin, in particular, still remains the most commonly utilised drug in this class because its oral absorption is better when compared with other β -lactam antibiotics. Besides being used for human therapy, AMX is extensively used for animal farming and for agricultural purposes. Residues from human environments and from farms may contain antibiotics and antibiotic resistance genes that can contaminate natural environments. The accumulation of antibiotic resistant bacteria and antibiotics in the environment can have severe consequences for both human health and for the evolution of environmental microbial populations. In order to overcome this problem, it is essential to develop simple, fast, and practical methodologies for the control and even the detection of these antibiotics in different matrices. Moreover, care must be taken to develop new strategies to combat bacterial resistance.

The objective of the thesis work focused on the indirect analysis of amoxicillin via its complexation with metal ions, as well as on the study of the synergy between the electrochemical behaviour of the organometallic complexes obtained and their activities against the bacterial resistance.

Indeed, the amoxicillin analysis is carried out indirectly by monitoring the variation of the intensity of the oxidation current of amoxicillin in the presence of copper (II) ions. The decrease of current intensity, recorded on the graphite electrode, was explained by the complexation of amoxicillin by copper (II) ions. Complex formation was confirmed by cyclic voltammetry as well as UV-visible and infrared spectroscopy. This methodology has been successfully used for the determination of amoxicillin in human blood and in pharmaceutical products containing the active ingredient of amoxicillin.

In addition, the complexation of amoxicillin has been extended to other transitional metals, in particular zinc (II) and iron (III). The formation of Metal-AMX complexes was examined by square wave voltammetry and UV-visible and infrared spectroscopy. Thus, the electrochemical oxidation of amoxicillin was significantly affected after complexation. Indeed, the oxidation was carried out at higher potentials that make the amoxicillin molecule more effective in resistant media. This electrochemical approach proved that the oxidation process of amoxicillin could be delayed by the presence of the transition metal.

In other hand, after studying their electrochemical behaviour, the antibacterial activity of these synthesized complexes was evaluated by the antibiogram method against the bacterium *Escherichia. Coli.* The results showed, on the one hand, that Metal-Amoxicillin complexes (Metal: Cu(II), Zn(II) and Fe(III)) showed a relatively interesting antibacterial activity compared to that of uncomplexed amoxicillin, and on the other hand, suggested the reinforcement of the antibacterial efficacy of amoxicillin after its complexation with the metal ions studied.